ISSN 1694-7398
e-ISSN
journals.manas.edu.kg

December 2018
Volume 6, Issue 2

MJEN

MANAS JOURNAL OF ENGINEERING

BISHKEK

KYRGYZ TURKISH MANAS UNIVERSITY
MANAS JOURNAL OF ENGINEERING (MJEN)

ISSN / e-ISSN: 1694- 7398
Year: 2018
Volume: 6
Issue: 2
http://journals.manas.edu.kg
journals@manas.edu.kg

PUBLICATION PERIOD

Manas Journal of Engineering (MJEN) is published twice year, MJEN is a peer reviewed online journal.

CORRESPONDENCE ADDRESS
Kyrgyz Turkish Manas University
Mira Avenue 56 Bishkek, KYRGYZSTAN
URL: http://journals.manas.edu.kg
e-mail: journals@manas.edu.kg
Tel : +996 312 492763- Fax: +996 312 541935

KYRGYZ TURKISH MANAS UNIVERSITY
MANAS JOURNAL OF ENGINEERING (MJEN)

CONTENT

İlknur Üstündağ *Aslı Erkal* *Zafer Üstündağ* *Ali Osman Solak*	*Electrochemical Detection of Cadmium and Lead in Rice on Manganese dioxide Reinforced Carboxylated Graphene Oxide Nanofilm*	*96-109*
Duygu Alpaslan *Tuba Erşen Dudu* *Nahit Aktaş*	*Synthesis, Characterization and Modification of Novel Food Packaging Material from Dimethyl acrylamide/Gelatin and Purple Cabbage Extract*	*110-128*
Duygu Balpetek Külcü *Ümit Gürbüz*	*Use of Ohmic Heating System in Meat Thawing and Its Effects on Microbiological Quality*	*129-142*
Omer Akın *Selami Bayeğ*	*The concept of Hukuhara Derivative and Aumann Integrals for Intuitionistic Fuzzy Number Valued Functions*	*143-163*
Okan Yakıt *Rita Ismaılova*	*Learning Management System Implementation. Case Study on User Interface Configurations.*	*164-176*
Dağıstan Şimşek *Peil Esengul kyzy*	*Solutions of the Rational Difference Equations*	*177-192*
Asan Omuraliev *Ella Abylaeva*	*Asymptotics of the Solution of the Parabolic Problem with a Stationary Phase and an Additive Free Member*	*193-202*

MANAS Journal of Engineering
ISSN 1694-7398 | e-ISSN 1694-7398

Volume 6 (Issue 2) (2018) Pages 96-109

Electrochemical Detection of Cadmium and Lead in Rice on Manganese Dioxide Reinforced Carboxylated Graphene Oxide Nanofilm.

İlknur Üstündağ[1], Aslı Erkal[2], Zafer Üstündağ[3*] Ali Osman Solak[4]

[1] Dumlupınar University, Faculty of Arts and Science, Department of Chemistry, Kütahya, Turkey
[2] Alanya Alaaddin Keykubat University, Rafet Kayış Eng. Faculty, Alanya, Antalya, Turkey
[3] Dumlupınar University, Faculty of Arts and Science, Department of Chemistry, Kütahya, Turkey
zustundag@gmail.com
[4] Kyrgyz-Turkish Manas University, Faculty of Eng., Chem Eng Department, Bishkek, Kyrgyzstan

Received: 13.12.2018; Accepted: 24.12.2018

Abstract: *Manganese dioxide decorated carboxylated graphene oxide (Mn-GO-COOH) attached onto the glassy carbon (GC) electrode to develop a new method for the simultaneous determination of Cd^{2+} and Pb^{2+} ions in rice samples. Graphene oxide (GO) was attached on 4-aminophenyl covalently modified glassy carbon surface via amide reaction. As-prepared modified material was characterized with XPS, SEM and electrochemical methods. A novel differential pulse anodic stripping voltammetric (DPASV) method was developed for the simultaneous determination of Cd^{2+} and Pb^{2+} on the GC/Mn-GO-COOH nanoplatform electrode. A linear response was found for the heavy metals in the range from 5 to 100 µg/L. The limit of detections (LODs) of Cd^{2+} and Pb^{2+} were 0.04 µg/L and 0.08 µg/L respectively. Manganese dioxide decorated carboxylated graphene oxide electrode was applied to the detection of Cd^{2+} and Pb^{2+} present in different rice samples by developed voltammetric method, and the accessed results were found to be in accordance with that of ICP-OES.*

Keywords: *Heavy metals, food analysis, differential pulse anodic stripping voltammetry, manganese decorated graphene oxide.*

1. INTRODUCTION

Rice, an Asian origin cereal grain, is a very important food with regard to human nutrition and one of the much consumed nutrient all over the world [1]. As in all foods, level of the toxic heavy metals contamination such as Pb and Cd is important in rice due to the environmental pollution. Since these metals have been extensively used in metal industry and in batteries besides many other areas, they can easily be adsorbed from contaminated soil by plants [2]. Both metals cause poisoning, and exhibit adverse effects on kidney, liver, heart, vascular and immune system of a person. In addition, exposure to these metals causes DNA aberration, cancer and birth disease [3]. Therefore, determination of these heavy metal concentrations is important especially in rice, because heavy metals exist in surface waters in colloidal, particulate, and dissolved phases in a substantial watery planting of rice.

Two-dimensional Graphene as a single layer is an allotrope of carbon in an hexagonal lattice [4]. Graphene oxide derivative modified electrodes for determination of Pb^{2+} and Cd^{2+} have begun to be used as electrode materials in literature over the last decade. Among the different electrochemical techniques for the determination of these ions in food samples on graphene oxide based electrode, the most preferred technique is the anodic stripping voltammetry using differential pulse or square wave voltammetry [5-8]. Graphene oxide (GO), which is a graphene derivative, contains a range of oxygen bearing functionalities such as hydroxyl, carbonyl, epoxide, and carboxyl groups [9]. When functionalized with some molecules such as –OH, -COOH, etc., graphene is likely to gain new materials having the different properties [10]. When activated with the chloroacetic acid, most of the epoxide, ester and hydroxyl groups on GO are converted to carboxylic acid groups [11, 12]. The carboxylated graphene oxide (GO-COOH) has begun to be widely used in recent years [11, 12].

There are several analytical methods used in the determination of metals in samples containing trace amounts. These are X-ray fluorescence spectroscopy [13-15], atomic absorption spectroscopy [16], inductively coupled plasma (ICP) spectroscopy [17, 18], and electrochemical methods such as amperometry [19], impedimetry [20] and voltammetry [21-23]. Recently, stripping voltammetry with differential pulse [24] and square wave [25] techniques are mostly preferred to determine trace elements in food.

Present investigation is focused on the preparation of manganese dioxide decorated carboxylated graphene oxide electrode (GC/Mn-GO-COOH) and its applicability for monitoring of Cd^{2+} and Pb^{2+} metals in various kinds of rice samples.

2. EXPERIMENTAL

2.1. Chemicals and Reagents

All chemicals and reagents were purchased from Merck, Fluka, Sigma-Aldrich and Riedel chemical company. GO and its derivatives were synthesized in our laboratory. The glassy carbon (GC) working electrode (MF-2012) was purchased from Bioanalytical Systems Company (USA). Bare GC electrodes were cleaned and polished in an aluminum oxide slurries with 0.1 and 0.05 micron sized particles (Baikowski, USA) on microfiber cloth pad (Buehler microfiber cloth, , USA). The

polished electrodes were sonicated with an ultrasonic bath cleaner (Bandelin-Sonorex, Germany) for approximately 5 min in ultrapure water (UPW, Human Power 1^+, S. Korea) and mixture of 1:1 (v/v) isopropyl alcohol/acetonitrile (MeCN) solutions.

2.1. Preparation of Manganese Dioxide Reinforced Carboxylated Graphene Oxide Electrode

GO was synthesized from graphite by electrochemical exfoliation method, as described elsewhere [4]. Pristine graphite was used as anode, in a mixture of 2.5 g H_2SO_4 and 10 mL of 30% KOH in 100 mL ultrapure water (UPW, 18.3 MΩ cm). A platinum stick was used as cathode electrode. The electrochemical exfoliation was performed under the constant DC potential of +20 V by direct current (DC) power source (Yıldırım Electronics, Turkey). The exfoliated materials were precipitated with a Hermle (Z36HK, Germany) ultracentrifuge under 15.000 rpm for 10 min. The raw GO was washed with UPW for three times. The GO was dried at 70 °C under vacuum for 12 h.

The GO-COOH was prepared according to the "Hongjie Dai and coworkers" method [11]. 1.2 g of NaOH and 1.0 g of chloroacetic acid were added into a GO suspension (4 mg GO/10 mL UPW). The suspension was sonicated for 1 h. The –OH terminated groups on GO was converted to carboxylic acid (-COOH) moieties. The functionalized GO-COOH in suspension solution was precipitated with an ultracentrifuge under 12.000 rpm for 10 min and washed with UPW for three times. The GO-COOH was dried at 70 °C under vacuum oven for 12 h.

12 mg GO and 0.5 g $MnCl_2.4H_2O$ were sonicated in isopropyl alcohol (100 mL) with an ultrasonic bath for 1 h [22]. The solution was heated to 85ºC. 0.3 g $KMnO_4$ involved 10 mL UPW was poured in the solution. The suspension solution was held at 85°C for 30 min on the magnetic stirring. Manganese oxide included carboxylated graphene oxide was centrifuged at 5000 rpm for 10 min and washed with UPW three times. The material was dried at 70°C under vacuum oven for 12 h. The nanomaterial was denoted as Mn-GO-COOH.

10 mg of Mn-GO-COOH was diluted with 10 mL UPW. The bare GC electrode was covered with 5 µL to 25 µL of Mn-GO-COOH suspension by microsyringe, and then dried under an infrared lamp (75 W) for 10 min for optimization study of Cd^{2+} and Pb^{2+} analysis by DPV. The electrode was denoted as GC/Mn-GO-COOH. Similarly, the GO-COOH and GO modified GC electrodes (GC/GO-COOH and GC/GO) were prepared for comparison.

2.2. Characterizations of Materials

All electrochemical measurements were performed under a highly purified Ar (99.999 %) atmosphere by Ivium CompactStat, (US) electroanalyzer at room temperature (25 ± 1°C) with triple electrode system. Ag/AgCl/KCl(sat) and platinum wire were used as reference electrode and counter electrodes, respectively. Cyclic voltammetry (CV) and electrochemical impedance spectroscopy (EIS) were used for electrochemical characterization of the modified electrodes. XPS measurement was carried out with an X-ray photoelectron spectrometer (PHI 5000, Versa Probe, ULVAC-PHI. Inc., Japan/USA). SEM images were recorded using a scanning electron microscopy (SEM, Zeiss-Evo, Germany). Infrared (IR) data was observed with a FT-IR spectrometer (Bruker, Tensor 27).

2.2. Sample Preparation and DPASV Procedure

Two commercial rice samples (Baldo and Jasmine) were purchased from a local supermarket and analyzed. The samples were digested as described elsewhere [26]. The rice samples were ground into fine powder in a planetary ball mill (Retsch, PM100, Germany). The samples were dried in oven at 105 °C for 12 h. 0.5 g of the rice flour was treated with 1.5 mL of concentrated $HClO_4$ and 1.5 mL of concentrated HNO_3. The suspension was heated to boiling on a hot plate until white fumes appeared. The evaporated mixture was diluted with 5 mL of 0.5 M HCl. The mixture was heated until a clear solution was obtained. The solution was filtered via a 400 nm syringe filter. The filtrate solution was diluted to 10 mL at 25 °C with 0.5 M HCl.

Differential pulse anodic stripping voltammetric method for the simultaneous determination of Cd^{2+} and Pb^{2+} was developed. Current-concentration linear response was found for the heavy metals in the range from 5 μg/L to 100 μg/L. Some optimization parameters, the limit of detections (LODs), precision and accuracy results of the developed method were investigated. The modified electrode was used for determination of Cd^{2+} and Pb^{2+} in two different rice samples. DPV results were recorded by positive scanning at a rate of 20 mV /s, a pulse amplitude of 25 mV, a pulse rate of 0.5 s, and a pulse width of 60 ms for a holding time of 2 s.

3. RESULTS AND DISCUSSIONS

3.1. Characterization of Materials

Electrochemical characterization of GC/Mn-GO-COOH electrodes were performed using 2 mM $K_4Fe(CN)_6/K_3Fe(CN)_6$ redox probe by CV and EIS. Cyclic voltammograms (CVs) of the redox probe on GC, GC/GO, GC/GO-COOH and GC/Mn-GO-COOH are given in Fig. 1.

Anodic peak current of the redox probe on GC, GC/GO, GC/GO-COOH GC/Mn-GO-COOH was calculated as 3.2 μA 108.9 μA 93.2 μA, and 180.8 μA. Anodic and cathodic peak current of the redox probe on GC/Mn-GO-COOH surface was significantly increased as is seen in Fig. 1. Electron transfer rate of the redox couple was probably accelerated with tunneling effect of the Mn-GO-COOH due to the high porosity and high surface area of the film on GC.

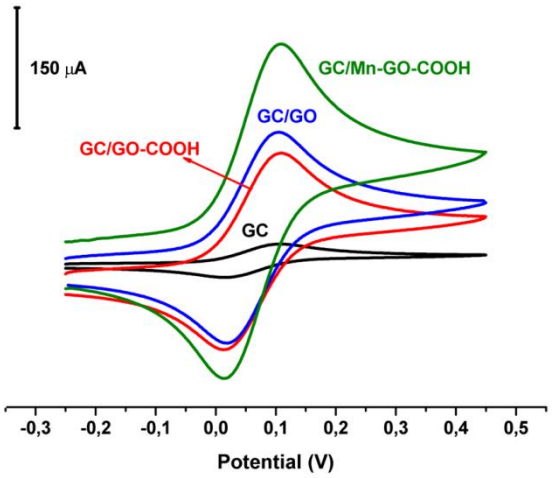

Figure 1. *CVs of 2 mM $K_4Fe(CN)_6$/ $K_3Fe(CN)_6$ redox probe on GC, GC/GO, GC/GO-COOH and GC/Mn-GO-COOH vs. Ag/AgCl (scan rate 200 mV/s).*

Nyquist plots of the redox probe on GC, GC/GO, GC/GO-COOH and GC/Mn-GO-COOH are given in Fig. 2. Charge transfer resistant (Rct) of the redox couple on the electrodes was determined with fit of Nyquist plots. All the plots were fitted as Warburg effected diffusion controlled CPE equivalent electrical circuit (inset in Fig. 2). Rct values of the redox couple on GC, GC/GO, GC/GO-COOH and GC/Mn-GO-COOH were determined as 0.87 kΩ, 0.53 kΩ, 0.77 kΩ, and 0.36 kΩ. Rct of the redox probe was dramatically decreased with GC/Mn-GO-COOH. This result is consistent with the currents measured in CV experiments. Electron transfer rate of the redox probe increased while charge transfer resistant decreased, as expected on GC/Mn-GO-COOH electrode.

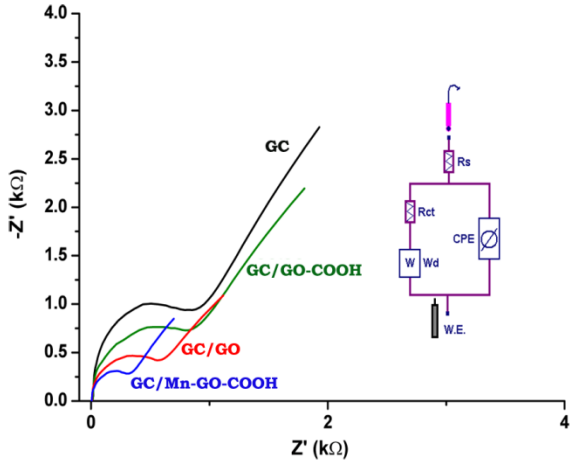

Figure 2. *Nyquist plots of 2 mM $K_4Fe(CN)_6$/$K_3Fe(CN)_6$ redox probe on GC, GC/GO, GC/GO-COOH and GC/Mn-GO-COOH vs. Ag/AgCl (0,1 Hz-100 kHz, DC potential is 0.13 V) and their equivalent electrical circuit (inset).*

GO and GO-COOH were characterized with XPS. C_{1s} spectra of GO and carboxylated graphene oxide (GO-COOH) are given in Fig. 3a. Mn2p XPS core spectrum of Mn-GO-COOH is given in Fig. 3b. In Fig. 3a, the weak C_{1s} core spectrum of GO is assigned to carboxyl group included carbon. The C_{1s} spectrum of carboxylated graphene oxide (GO-COOH) increased significantly [27]. In Fig. 3b, a Mn_{2p} core spectrum apparently indicates the presence of manganese in Mn-GO-COOH film at the surface [22].

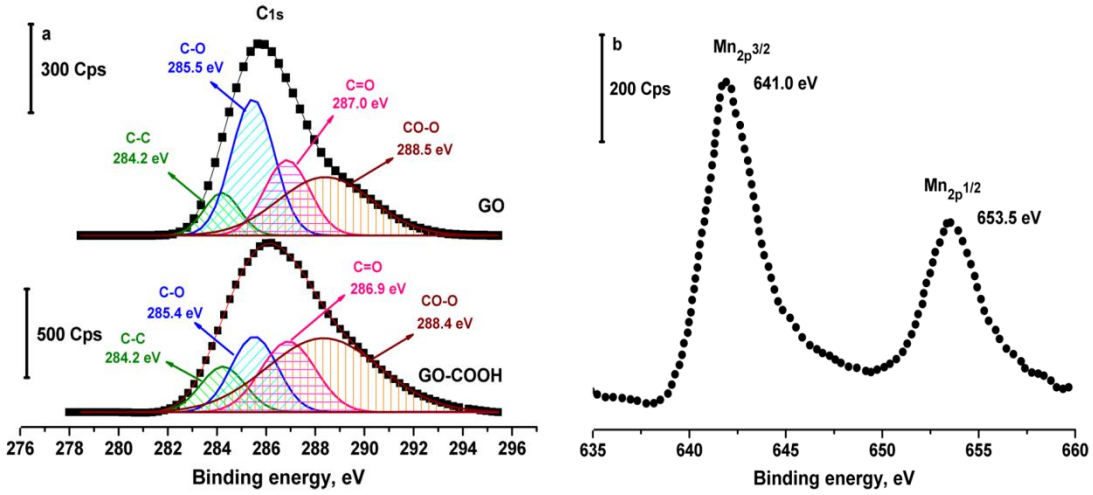

Figure 3. *C1s XPS core spectra of GO and GO-COOH, and Mn2p core spectrum of Mn-GO-COOH.*

SEM image of manganese dioxide reinforced carboxylated graphene oxide (Mn-GO-COOH) and its EDX spectrum are given in Fig. 4. In Fig. 4a, manganese dioxide clusters on the carboxylated graphene oxide can apparently be seen. Principal elements of C, O, Mn and residual amount of K (trace amount of K from $KMnO_4$) are seen in Fig. 4b [28].

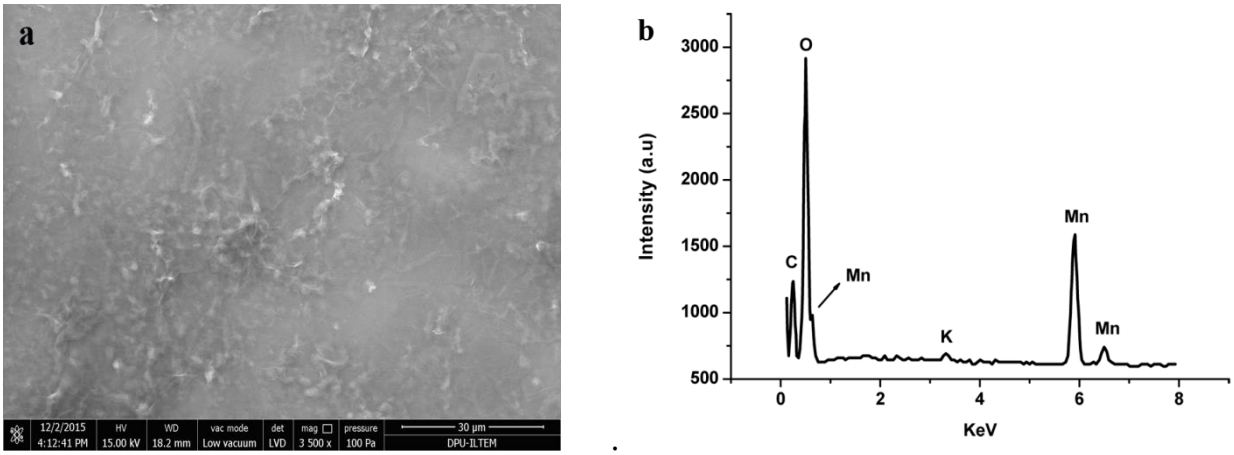

Figure 4. *SEM image (a) and EDX spectrum (b) of Mn-GO-COOH*

3.2. Simultaneous Determination of Cd^{2+} and Pb^{2+} Using DPASV

Analytical parameters of the method developed, such as pH of the aqueous media, deposition potential, deposition time, and volume of Mn-GO-COOH suspension were determined with 25 µg/L of Cd^{2+} and Pb^{2+} in 0.1 M sodium acetate/acetic acid buffer solution using DPASV technique to acquire the highest current response of both ions, i.e. of Cd^{2+} and Pb^{2+} simultaneously. The optimization results as anodic peak current vs. optimization parameter are given in Fig. 5. Different

pHs of 0.1 M solution were tested in the range of 3.0 - 5.5. It was found that a pH of 4.5 proved the highest anodic peak currents (Fig. 5a). Thence, calibration studies, 0.1 M sodium acetate/acetic acid buffer solution at 4.5 of pH with 120 s for deposition time (Fig. 5b) with 15 µL of Mn-GO-COOH suspension (Fig. 5c) dropped GC were chosen as the optimum parameters. The deposition potential was studied in the potential range of -0.8 to -1.4 V vs. Ag/AgCl. Deposition potential was selected as -1.2 V (Fig. 5d). Lower current values observed at the more negative potentials beyond -1.2 V may be due to the hydrogen gas evolution on the electrode surface -1.2 V [1, 29, 30].

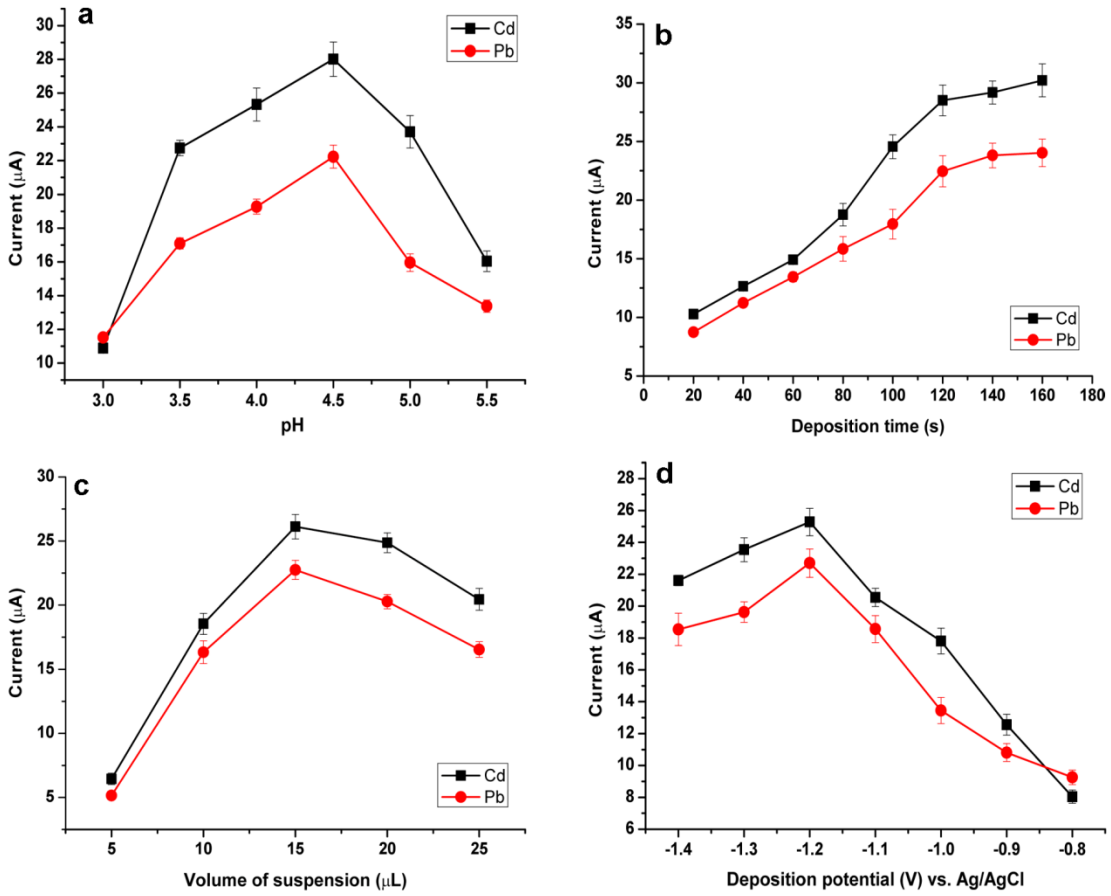

Figure 5. *Optimization study for 25 µg/L Cd^{2+} and Pb^{2+}. Effects of pH (a), deposition time (b), volume of Mn-GO-COOH suspension on GC (c), and deposition potential (d) on the anodic stripping peaks current.*

Differential pulse anodic stripping voltammograms for different concentrations of Cd^{2+} and Pb^{2+} between 5 µg/L - 100 µg/L under the optimized conditions were illustrated in Fig. 6. The linear calibration plots for the ions at different concentrations in the range of 5 to 100 µg/L are shown in Fig. 7. The linear equations for Cd^{2+} and Pb^{2+} were $Ip(Cd^{2+})=0.9494[Cd^{2+}]+5.0334$ (R^2: 0,9988) and $Ip(Pb^{2+})=0.7250[Pb^{2+}]+4.0398$ (R^2: 0,9968), respectively. LODs are 0.04 µg/L for Cd^{2+} and 0.08 µg/L for Pb^{2+} (S/N=3) with sensitivity of 0.9494 µA.L/µg and 0.725 µA.L/µg, respectively.

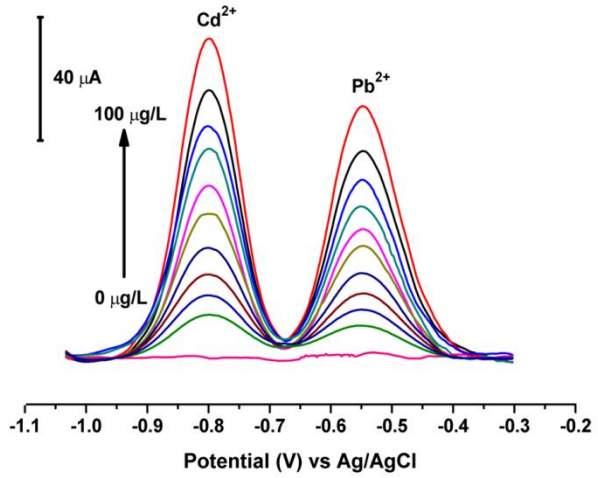

Figure 6. *Differential pulse anodic stripping voltammograms for different concentrations (0, 5, 10, 20, 30, 40, 50, 60, 70, 80, 100 μg/L) of Cd^{2+} and Pb^{2+}.*

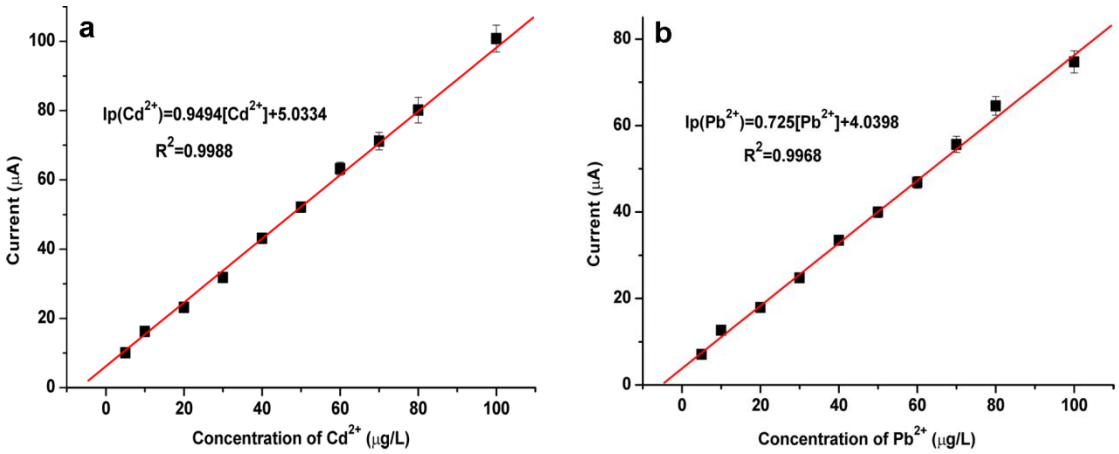

Figure 7. *Calibration curves for addition of 0, 5, 10, 20, 30, 40, 50, 60, 70, 80, 100 μg/L Cd^{2+} (a) and Pb^{2+} (b).*

Comparison of the sensor performance of DPASV and square wave anodic stripping voltammetry (SWASV) for the determination of Cd^{2+} and Pb^{2+} between different works in literature is given in Table 1.

The possible influence caused by interfering some ion species such as Na^{+}, K^{+}, Ca^{2+}, Mg^{2+}, Al^{3+}, Fe^{2+}, Zn^{2+}, Cu^{2+}, Cr^{3+}, Mn^{2+} on the stripping current of 10 μg/L Cd^{2+} and Pb^{2+} under the optimized conditions are given in Table 2. The changes of peak current results of Cd^{2+} and Pb^{2+} in the presence of Na^{+}, K^{+}, Ca^{2+}, Mg^{2+}, Al^{3+}, Cr^{3+}, Mn^{2+} (max: 100-fold) are within tolerable limits, i.e. lower than 5%. The tolerable limit for Fe^{2+} and Zn^{2}+ was 50-fold and 30-fold, respectively. The interference effect of copper was found to be very high. The tolerable limits of Cu^{2+} with 3-fold was determined as -4.77% for Cd^{2+} and -4.33 for Pb^{2+}. When 4-fold of copper ions was added, current responses of Cd^{2+} and Pb^{2+} were dramatically decreased by about 18.2% and 11.7%, respectively.

Table 1. *Sensor performance of DPVASV and square wave anodic stripping voltammetry (SWASV) for the determination of Cd^{2+} and Pb^{2+}.*

Electrode	Technique	Calibration range		LOD		Ref.
		Cd^{2+}	Pb^{2+}	Cd^{2+}	Pb^{2+}	
Bi-D24C8/Nafion SPCE	SWASV	0.5 ppb – 60 ppb	0.5 ppb - 60 ppb	0.27 ppb	0.11 ppb	[1]
Pt/MWCNT/P1,5-DAN	SWASV	4 ppb – 150 ppb	4 ppb – 150 ppb	3.2 ppb	2.1 ppb	[31]
GO/ κ-Car/L-cys/GC	SWASV	5 nM – 50 nM	5 nM – 50 nM	0.58 nM	1.08 nM	[29]
Bi/GR/IL-SPE	SWASV	1 ppb – 80 ppb	1 ppb – 80 ppb	0.08 ppb	0.10 ppb	[30]
PolyL-GCE	DPASV	40 nM – 1000 nM	1 nM – 100 nM	10 nM	0.7 nM	[32]
MWCNT-RGO	DPASV	0.5 ppb – 30 ppb	0.5 ppb - 30 ppb	0.1 ppb	0.2 ppb	[33]
GO-MnO2	DPASV	0.01 nM – 100 nM	0.01 nM – 100 nM	0.14 nM	1.24 nM	[22]
Bi/MGF-Nafion/GCE	DPASV	2 ppb – 70 ppb	0.5 ppb – 110 ppb	0.437 ppb	0.210 ppb	[34]
GC/Mn-GO-COOH	DPASV	5 ppb – 100 ppb	5 ppb – 100 ppb	0.04 ppb	0.08 ppb	this study

Table 2. *Interferences of different ions on the simultaneous detection of 10 μg/L for both Cd^{2+} and Pb^{2+} as peak current signal percentage change.*

Interfering ions	Concentration, μg/L	Signal change (%)	
		Cd^{2+}	Pb^{2+}
Na^{+}	1000	+0.22	+0.17
K^{+}	1000	-0.71	-0.83
Ca^{2+}	1000	+1.29	+2.35
Mg^{2+}	1000	+1.78	+0.33
Al^{3+}	1000	-1.33	+2.27
Fe^{2+}	400	-4.86	+3.71
Zn^{2+}	300	+3.89	-4.98
Cu^{2+}	30	-4.77	-4.33
Cr^{3+}	1000	-2.48	-1.79
Mn^{2+}	1000	-2.2	-1.25

Reproducibility of GC/Mn-GO-COOH electrode was investigated under the optimum conditions for 25 μg/L each of Cd^{2+} and Pb^{2+} solution, on the as-prepared five different electrodes.

Precision and accuracy of the developed methods, for intra-day and inter-day, were studied with standard samples. Three different concentrations of 2.0 μg/L, 5.0 μg/L and 10 μg/L for both Cd^{2+} and Pb^{2+} in the linear range were determined in five independent series on the same day for intra-

day precision and seven consecutive days for inter-day precision. The results for intra-day and inter-day experiments are given in Table 3.

3.3. Real Sample Analysis

The developed method was applied to determine of Cd^{2+} and Pb^{2+} on GC/Mn-GO-COOH electrode in rice samples by DPASV. The results from the method in the rice analysis were validated using ICP-OES method. Analytical recovery values of Cd^{2+} and Pb^{2+} in market rice samples are given in Table 4. The recovery rates for spiked ranged from 96.5 to 102.6% for Cd^{2+} and 97.5 to 103.1% for Pb^{2+}.

Table 3. *Five independent series on the same day for intra-day precision and seven consecutive days for inter-day precision of the method.*

Added, µg/L	Intra-day						Inter-day					
	Found Value, µg/L		Precision * %		Accuracy %		Found Value, µg/L		Precision * %		Accuracy %	
	Cd^{2+}	Pb^{2+}	Cd^{2+}	Pb^{2+}	Cd^{2+}	Pb^{2+}	Cd^{2+}	Pb^{2+}	Cd^{2+}	Pb^{2+}	Cd^{2+}	Pb^{2+}
2	2.02±0.04	1.97±0.03	1.98	1.52	1.0	-1.5	1.98±0.05	2.03±0.02	2.53	0.99	-1.0	1.5
5	5.15±0.15	4.91±0.14	2.91	2.85	3.0	-1.8	10.25±0.25	10.20±0.17	2.44	1.67	2.5	2.0
10	9.88±0.33	10.17±0.26	3.34	2.56	-1.2	1.7	50.27±1.33	49.75±1.55	2.65	3.12	0.5	-0.5

*RSD

Table 4. *Concentration of Pb^{2+} and Cd^{2+} in rice samples found by DPASV and ICP-OES (n=3, Degree of confidence 95%).*

Samples	Added, µg/L	DPASV, µg/L		ICP-OES, µg/L		Recovery %	
		Cd^{2+}	Pb^{2+}	Cd^{2+}	Pb^{2+}	Cd^{2+}	Pb^{2+}
Jasmine-1	0	ND*	3.63±0.06	ND*	3.57±0.06	-	-
	2	1.98±0.04	5.80±0.11			99.0	103.0
	4	3.88±0.27	7.87±0.46			97.0	103.1
Jasmine-2	0	1.28±0.05	4.68±0.12	1.21±0.08	4.79±0.13	-	-
	5	6.33±0.13	9.50±0.48			100.8	98.1
	10	10.88±0.36	14.81±0.09			96.5	100.9
Baldo-1	0	2.17±0.05	5.33±0.17	2.20±0.11	5.43±0.17	-	-
	2	4.10±0.08	7.15±0.49			98.3	97.5
	4	6.33±0.21	9.20±0.65			102.6	98.6
Baldo-2	0	ND*	2.74±0.10	ND*	2.83±0.42	-	-
	5	4.88±0.40	7.85±0.31			97.6	101.4
	10	9.83±0.65	12.57±0.76			98.3	98.7

*ND: Not detectable

4. CONCLUSION

A novel Mn-GO-COOH electrode was prepared for the simultaneous determination of trace amount of Cd^{2+} and Pb^{2+} in rice samples by DPASV. Carboxylic acids terminated GO became more functional when reinforced with MnO_2 for the simultaneous determination of Cd^{2+} and Pb^{2+}. Probable enhanced synergic effects of MnO_2 on GO-COOH were evaluated due to more porous structure, higher specific surface area and hence larger amounts of the adsorption of ions. The

electrode material was characterized using electrochemical methods such as CV and EIS. Spectroscopic and microscopic characterization of the surface materials was carried out by XPS and SEM. A novel analytical method was developed with the modified electrode for simultaneous determination of Cd^{2+} and Pb^{2+} in aqueous media. Calibration curves were linear within the range of 5 to 100 μg/L for both metals under the optimized conditions. The limit of detections were 0.04 μg/L for Cd^{2+} and 0.08 μg/L for Pb^{2+} (S/N=3). The possible interference effects of different ions were investigated for the simultaneous determination of Cd^{2+} and Pb^{2+}. Especially, Fe^{2+}, Zn^{2} and Cu^{2+} were found to be effective even at low concentrations. Reproducibility of the electrode was investigated under the optimum conditions. Precision and accuracy of the method were determined as intra-day and inter-day. The precision % values varied from 1.52 to 3.34 for intra-day and from 0.99 to 3.12 for inter-day precision for Cd^{2+} and Pb^{2+}. Accuracy of the developed method was calculated between -1.8 to 3.0 for intra-day and inter-day. The percent recovery values for Cd^{2+} and Pb^{2+} in real samples were calculated between 96.5 and 103.1.

REFERENCES

[1]. Keawkim, K., et al., Determination of lead and cadmium in rice samples by sequential injection/anodic stripping voltammetry using a bismuth film/crown ether/Nafion modified screen-printed carbon electrode. *Food Control*, 31, (2013), 14-21.

[2]. Qiao J., et al., EDTA-assisted leaching of Pb and Cd from contaminated soil. *Chemosphere*, 167, (2017), 422-428.

[3]. Koduru J.R. Lee K.D., Evaluation of thiosemicarbazone derivative as chelating agent for the simultaneous removal and trace determination of Cd(II) and Pb(II) in food and water samples. *Food Chemistry*, 150, (2014), 1-8.

[4]. Çelik G.K., et al., 3,8-Diaminobenzo[c]Cinnoline Derivatived Graphene Oxide Modified Graphene Oxide Sensor for the Voltammetric Determination of Cd^{2+} and Pb^{2+}. *Electrocatalysis*. 7, (2016), 207-214.

[5]. Wu Y., et al., The effective determination of Cd(II) and Pb(II) simultaneously based on an aluminum silicon carbide-reduced graphene oxide nanocomposite electrode. *Analyst*, 142, (2017), 2741-2747.

[6]. Guo Z., et al., Simultaneous determination of trace Cd(II), Pb(II) and Cu(II) by differential pulse anodic stripping voltammetry using a reduced graphene oxide-chitosan/poly-l-lysine nanocomposite modified glassy carbon electrode. *Journal of Colloid and Interface Science*. 190, (2017), 11-22.

[7]. Wei Y., et al., SnO2/Reduced Graphene Oxide Nanocomposite for the Simultaneous Electrochemical Detection of Cadmium(II), Lead(II), Copper(II), and Mercury(II): An Interesting Favorable Mutual Interference. *The Journal of Physical Chemistry* C. 116, (2012), 1034-1041.

[8]. Xuan X., M.F. Hossain J.Y. Park, A Fully Integrated and Miniaturized Heavy-metal-detection Sensor Based on Micro-patterned Reduced Graphene Oxide. *Sci Rep*. 6, (2016), 33125.

[9]. White R.L., et al., Comparative studies on copper adsorption by graphene oxide and functionalized graphene oxide nanoparticles. *Journal of the Taiwan Institute of Chemical Engineers*. 85, (2018), 18-28.

[10]. Meng N., et al., Carboxylated graphene oxide functionalized with β-cyclodextrin—Engineering of a novel nanohybrid drug carrier. *International Journal of Biological Macromolecules*. 93, (2016), 117-122.

[11]. Sun X., et al., Nano-Graphene Oxide for Cellular Imaging and Drug Delivery. *Nano Res*, 1, (2008), 203-212.

[12]. Yu L., et al., Graphene oxide and carboxylated graphene oxide: Viable two-dimensional nanolabels for lateral flow immunoassays. *Talanta*. 165, (2017), 167-175.

[13]. Kalfa O.M., et al., Analysis of tincal ore waste by energy dispersive X-ray fluorescence (EDXRF) Technique. *Journal of Quantitative Spectroscopy and Radiative Transfer* 103, (2007), 424-427.

[14]. Üstündağ Z., İ. Üstündağ, Y. Kağan Kadıoğlu, Multi-element analysis of pyrite ores using polarized energy-dispersive X-ray fluorescence spectrometry. *Applied Radiation and Isotopes*. 65, (2007), 809-813.

[15]. Üstündağ İ., et al., Geochemical compositions of trona samples by PEDXRF and their identification under confocal Raman spectroscopy: Beypazarı-Ankara, Turkey. Nuclear Instruments and Methods in Physics Research Section B: *Beam Interactions with Materials and Atoms*. 254, (2007), 153-159.

[16]. Paus P.E., Determination of some heavy metals in sea water by atomic absorption spectrophotometry. *Fresenius' Zeitschrift für analytische Chemie*. 264, (1973), 118-122.

[17]. Martinez–Lopez C., M. Sakayanagi, J.R. Almirall, Elemental analysis of packaging tapes by LA-ICP-MS and LIBS. *Forensic Chemistry*, (2018).

[18]. Xia J., et al., Lead speciation analysis in rice by reversed phase chromatography with inductively coupled plasma mass spectrometry. *Journal of Food Composition and Analysis*. 60, (2017), 74-80.

[19]. Silwana B., et al., Amperometric determination of cadmium, lead, and mercury metal ions using a novel polymer immobilised horseradish peroxidase biosensor system. *J Environ Sci Health A Tox Hazard Subst Environ Eng*. 13, (2014), 1501-11.

[20]. Wei J., et al., Ultrasensitive and Ultraselective Impedimetric Detection of Cr(VI) Using Crown Ethers as High-Affinity Targeting Receptors. *Analytical Chemistry*, 87(3), (2015), 1991-1998.

[21]. Üstündağ İ., et al., Gold nanoparticle included graphene oxide modified electrode: Picomole detection of metal ions in seawater by stripping voltammetry. *Journal of Analytical Chemistry*,. 71(7), (2016), 685-695.

[22]. Erkal A., et al., An Electrochemical Application of MnO2 Decorated Graphene Supported Glassy Carbon Ultrasensitive Electrode: Pb2+ and Cd2+ Analysis of Seawater Samples. *Journal of the Electrochemical Society*, 162(4), (2015), H213-H219.

[23]. Üstündağ İ., A. Erkal, Determination of Dopamine in the Presence of Ascorbic Acid on Digitonin-Doped Coal Tar Pitch Carbonaceous Electrode. *Sensors and Materials*. 29, (2017), 85-94.

[24]. Yavuz S., et al., Carbonaceous Materials-12: a Novel Highly Sensitive Graphene Oxide-Based Carbon Electrode: Preparation, Characterization, and Heavy Metal Analysis in Food Samples. *Food Analytical Methods*. 9, (2016), 322-331.

[25]. Erkal A., et al., Electrografting and Surface Properties of Some Substituted Nitrophenols on Glassy Carbon Electrode and Simultaneous Pb2+ - Cd2+ Analysis via Assist of Graphene Oxide Terminated Surface. *Journal of the Electrochemical Society*. 161, (2014), H696-H704.

[26]. Ye Q.-Y., et al., Determination of Trace Cadmium in Rice by Flow Injection On-Line Filterless Precipitation-Dissolution Preconcentration Coupled with Flame Atomic Absorption Spectrometry. *J. Agric. Food Chem*. 51, (2003), 2111-2114.

[27]. Muthoosamy K., et al., Exceedingly biocompatible and thin-layered reduced graphene oxide nanosheets using an eco-friendly mushroom extract strategy. *International Journal of Nanomedicine*. 10 (2015), 1505-1519.

[28]. Bocchetta P., et al., Accurate Assessment of the Oxygen Reduction Electrocatalytic Activity of Mn/Polypyrrole Nanocomposites Based on Rotating Disk Electrode Measurements, Complemented with Multitechnique Structural Characterizations. *Journal of Analytical Methods in Chemistry*. 203, (2016), 1-16.

[29]. Priya T., et al., A novel voltammetric sensor for the simultaneous detection of Cd2+ and Pb2+ using graphene oxide/κ-carrageenan/l-cysteine nanocomposite. *Carbohydrate Polymers*. 182, (2018), 199-206.

[30]. Wang Z., et al., Electrochemical determination of lead and cadmium in rice by a disposable bismuth/electrochemically reduced graphene/ionic liquid composite modified screen-printed electrode. *Sensors and Actuators B: Chemical*. 199, (2014), 7-14.

[31]. Vu H.D., et al., Anodic stripping voltammetric determination of Cd2+ and Pb2+ using interpenetrated MWCNT/P1,5-DAN as an enhanced sensing interface. *Ionics*. 21, (2014), 571-578.

[32]. Buica G.-O., et al., Voltammetric sensing of lead and cadmium using poly(4-azulen-1-yl-2,6-bis(2-thienyl)pyridine) complexing films. *Journal of Electroanalytical Chemistry*. 693, (2013), 67-72.

[33]. Huang H., et al., Ultrasensitive and simultaneous detection of heavy metal ions based on three-dimensional graphene-carbon nanotubes hybrid electrode materials. *Analytica Chimica Acta*. 852,(2014), 45-54.

[34]. Xiao L., et al., An efficient electrochemical sensor based on three-dimensionally interconnected mesoporous graphene framework for simultaneous determination of Cd(II) and Pb(II). *Electrochimica Acta*. 222, (2016), 1371-1377.

MANAS Journal of Engineering
ISSN 1694-7398 | e-ISSN 1694-7398

Volume 6 (Issue 2) (2018) Pages 129-142

Use of Ohmic Heating System in Meat Thawing and Its Effects on Microbiological Quality

Duygu Balpetek Külcü[1], Ümit Gürbüz[*2,3]

[1.]Giresun University, Engineering Faculty, Food Engineering Department, Giresun, Turkey
[2.]Selçuk University, Faculty of Veterinary Medicine, Department of Food Hygiene and Technology, Konya,Turkey.
[3.]Kyrgyz Turkish Manas University, Faculty of Veterinary Medicine, Department of Food Hygiene and Technology, Bishkek, Kyrgyzstan, ugurbuz@selcuk.edu.tr

Received: 09.11.2018; Accepted: 05.12.2018

Abstract: *This study was conducted to determine the application of the ohmic heating system in meat thawing process and its effects on the microbiological quality of the meat. For this purpose, traditional thawing methods (room temperature and refrigerator) were compared with the ohmic system. Beef loin (Longissimus lumborum, LL) was used as the material in the experiments by cutting into 5x10cm pieces. The samples were divided into three groups by taking the thawing methods into consideration. The grouped meat samples were frozen at -35±1°C for 24 hours and stored at -18°C for 6 months. During the storage period, changes in color (L*, a*, b*) and microbiological condition of the samples were determined periodically throughout the storage period. In all experimental meat samples thawed by different methods, considering the period of frozen storage; There were statistically significant differences in total microorganism, Pseudomonas spp. and coliform numbers after the second month ($p<0.05$). It was also observed that decreases observed in the number of yeast-mold during storage period were not significant ($p>0.05$). When the thawing methods applied in this study evaluated in terms of L*, a*, b* values, there was no statistically difference between the groups ($p> 0.05$). As a result, it has been concluded that the ohmic heating system can be used as an alternative method for thawing frozen meat.*

Keywords: *Thawing, meat, storage, microbiology, ohmic heating*

1. INTRODUCTION

Ohmic heating is an effective method for thawing of frozen foods, but there are only a few studies in the literature describing the Electrical Conductivity (EC) values of foods. Liu et al. [1] examined ohmic heating thawing in three different tuna muscles experimentally over a range of temperatures. The EC values of tuna muscles were measured at several frequencies and temperatures, from 50Hz to 20 kHz and from −30°C to +20°C, respectively. The effect of the electric current direction and the presence or absence of the membrane in the muscle were analyzed. It was shown that EC values are influenced by frequency, temperature, moisture content, and fat content. Also, EC values were changed rapidly above −7°C. Their results also showed that the parallel current direction gives higher EC values than series. Furthermore, the membranes in the muscle and the fat distribution are important factors that affect EC values.

Meat taken into frozen storage must be properly thawed before consumption. Many methods are used to thawing frozen meats. It is stated that the dissolution of frozen meat and meat products is more important than the quality of the product, freezing and frozen preservation. As a result of inadequate thawing methods, excessive weight loss, a decrease in meat nutrient value due to increase of leach water rate and an increase of microbial flora are considered as the most important problems. Freezing process means that the storage of frozen meat at -10°C or lower temperatures while deep freezing process at from -20°C to -35°C. It has been reported that frozen meat should be stored at -18°C [2].

In freezing process, the meat starts to freeze at -0.6°C and water in meat starts to crystallize at -1.50°C. It is stated that the freezing and thawing process should pass the -3°C boundary quickly and the water should be crystallized in small size. Generally, it is assumed that the development of bacteria at -10°C, yeasts at -12°C and molds at -18°C stops [2]. Frozen food becomes liquid or soft due to the rising of temperature above the freezing point in thawing heating. Thawing is a critical procedure for controlling the microbial and physicochemical properties of a food product [3].

Total viable bacteria, yeast and mould counts are commonly used microbiological methods in determining the microbiological quality of foods. Total viable bacteria, yeast and mould counts have high importance for the demonstration of whether food is stored at suitable temperatures during processing, transport and storage phases and the adequacy of sanitation in food premises. These counts also help to take necessary precautions by informing about the beginning of the deterioration, the possible shelf life of food, uncontrolled dissolution of frozen foods, inadequate cooling, contamination and level of contamination at the production phase [4].

Inactivation of microorganisms is very important in many industrial food applications. Microbial inactivation is an important parameter that must be addressed in food production processes regarding product safety and quality management. The presence of undesirable or high amounts of certain microorganisms can lead to product spoiling (e.g. material spoiling) and the quality loss

(e.g. changes in appearance, unwanted odor, undesirable taste, discoloration, etc.) and/or health problems.

Cho et al. [5] observed that ohmic heating leads to lower thermal inactivation time when compared to conventional method in their research on the *B. subtilis* and *B. atrophaeus* inactivation kinetics. It is thought that this difference is probably due to the electric field in the environment.

For this reason, it is emphasized that ohmic heating is caused by a thermal effect and non-thermal killing effect on the microorganisms analyzed. According to Sun et al. [6], the effect of electrical inactivation is more important than heat. It has been shown that this effect is related to the electric voltage and frequency.

Tian et al. [7] compared long term ohmic and water bath cooking in their study. Water bath cooking takes 2 times more than long term ohmic to achieve equal cooking level. The bacterial diversity decreased weekly similar between the two methods and the bacterial community structure in samples were similar at the end of storage and were mainly composed of *Carnobacterium*, *Pseudomonas*, *Kluyvera*, and *Bacillus*. But, the TVB-N (Total volatile basic nitrogen) value was higher in water bath cooked samples. As a result, long term ohmic cooking has the potential to produce safe and high-quality meat products with a shorter cooking time.

Ohmic heating is also promising new technology for the fruit juice industry. Park and Kang [8] demonstrate that the electric effect of ohmic heating is a very important factor for reducing process times and temperatures for inactivation of *E. coli* O157:H7, *S. typhimurium*, and *L. monocytogenes*. Especially, ohmic heating is an effective technology for processing acidic fruit juices, because it has a dramatic pasteurization effect on food-borne pathogens due to low pH, thermal treatment, and the electric effect.

Aguilar-Machado et al., [9] showed that ohmic heating has a higher effect on the pigments than conventional heating treatment. However, this effect is less noticed than microbial inactivation. Degradation can be negligible depending on the target microorganism with ohmic heating at optimum microbial inactivation conditions.

The microbial inactivation associated with ohmic heating is more widespread in nature, such as conventional heating. Cho et al. [10] showed that electrical pretreatment of ohmic heating can reduce the severity of additional thermal applications for subsequent microbial inactivation. The similarity of microbial inactivation curves of ohmic heating to the traditional heating curves, except for differences in curves, is probably more likely to be explained by the electrical field.

Zell et al. [11] applied ohmic heating to the meat samples (*M.semitendinosus*) inoculated *L. innocua*. They specified that ohmic heating method is significantly effective on *L. innocua* and results of their study can be used at the microbial safety point.

İçier et al. [3] investigated the effect of ohmic thawing on the structural changes of shredded beef samples and showed that the samples thawing with conventional method were more flexible than the samples thawing with ohmic heating.

Bozkurt and İçier [12] compared ohmic and traditional methods in their study, and they found that there was no difference between liquid loss, solubilization homogeneity and some color parameters (*L**, *a**, *b**) in thawing frozen beef samples but there are differences in thawing time, level, and energy use. Researchers also indicate that the size of the meat is an important factor in thawing process.

Li and Sun, [12] declared that freezing and thawing are complex processes including chemical transfer and heat transfer which greatly affect the product quality. Researchers have indicated that new thawing methods, such as microwave, ohmic heating, high pressure thawing, and sound thawing, shorten the thawing time, thereby reducing water loss and improving product quality.

The thawing of frozen foods is known to be a very critical process, especially in terms of the microbial safety of the thawing food. For this reason, thawing of the food must be carried out as rapidly as possible at low temperatures. This method is particularly thought to be used as an alternative method of thawing the meat.

In this work, the effects of traditional thawing methods, as well as the use of ohmic heating, and the effects on the microbiological quality of the food have been investigated.

2. MATERIALS AND METHODS

In this study, beef loin samples (*Longissimus lumborum, LL*) were used as material. Experimental meat samples were prepared in a size of 5x10cm and weighing 200-250g. Experimental meat samples were subjected to color (*L**, *a**, *b**) and microbiological (total mesophilic aerobic microorganism, *Pseudomonas* spp., coliform and yeast-mold) analysis before freezing. The prepared meat praperats were coded and divided into 3 groups that have 18 samples in each group. Group I samples were thawed at the room temperature; group II samples were thawed by ohmic heating and group III samples were thawed in the refrigerator environment. The samples were frozen at -35°C for 24 hours in a special freezer (UCF 20SF, Uğur Deep Freezer, Turkey) by rapid freezing method. After freezing process, the experimental samples were stored in the same freezer at -18°C for 6 months.

The frozen conserved meats were thawed in different ways every month from the 1st month to the 6th month of the conservation. For each group, 3 samples were dissolved by different thawing method in each month. group I samples were dissolved at room temperature (20 ± 2°C), group II samples were subjected to an ohmic heating system applied with 50volt electric current in the same environment, group III samples were dissolved in a refrigerator set at +30°C. The dissolution process was continued until the internal heat of the meat was 0 ± 1°C, and the dissolution was terminated when this value was reached. The internal temperature was measured throughout the

dissolution of frozen meat by a data logger (TESTO 175 Data Logger, TESTO AG, Germany). Color (*L*, a*, b**) and microbiological (total mesophilic aerobic microorganism, *Pseudomonas* spp., coliform and yeast-mold counts) analysis of samples were conducted at each month from the 1st to the 6th in terms of quality qualifications. All analysis were carried out in 2 parallel lines.

1.1. Reflectance Color Analysis

Reflectance color analysis was performed by using a Minolta-brand colorimeter (CR-400 model, Konica Minolta, Osaka, Japan) having D65 illuminant, 2° observers, 8mm illumination range in Diffuse/O mode. *L** represents the value of brightness, *a** represents the value of redness and *b** represents the value of yellowness. For each samples, three color readings were taken from the surface of the samples[14].

1.2. Microbiological Analyses

Microbiological enumerations were performed by the reference cultural methods [15, 16,17] on Plate Count Agar (PCA, CM-0325, Oxoid), Dichloran Rose Bengal Chloramphenicol Agar(DRBC, Merck 1.00466), Violet Red Bile Agar (VRBA CM-0107,Oxoid) and Pseudomonas Selective Agar (CFC Agar Base, Merck 1.07620) for total viable count (TVC), yeast and mould (YM), coliform, *Pseudomonas*, respectively. Initial suspensions were prepared by adding 225 mL maximum recovery diluent (MRD, Merck 1.12535) into stomacher bags containing 25 g sample. Inoculated PCA and VRBA plates were incubated at 35°C for 48h for TVC and coliform, while DRBC agar and CFC agar plates were incubated at 25°C for 5 and 2 days for YM and *Pseudomonas* counts, respectively.

After incubation, all colonies grown on PCA and DRBC agar plates were counted and microorganism counts were calculated as log CFU/g. Characteristic coliform colonies with a red center on VRBGA (CM 1082, Oxoid) plates were confirmed on glucose agar. Pigmented or fluorescent colonies on CFC agar plates, considered as presumptively *Pseudomonas*, were firstly subjected to oxidase test (Merck 1.133000). Oxidase positive colonies were transferred to Kligler agar (Merck 1.03913) in order to check aerobic growth. Colonies verified as *Pseudomonas* were identified at species level using a biochemically-based identification system [18].

1.3. Statistical Analyses

SPSS 16.0 package program was used for statistical evaluations. The Kruskal-Wallis test was employed for microbiological data, the General Linear Model was used in color analyses, the Duncan test and Paired t-test were employed in paired comparisons of the parametric data, the Mann-Whitney test and Wilcoxon test, were used for nonparametric data.

3. RESULTS AND DISCUSSION

Thawing times of experimental samples taken into frozen storage were determined by thawing with different methods each month periodically. The internal temperature values of the frozen meat have

been determined between -14.4±1.6°C and -15.7±0.7. The internal temperature of frozen meats reached these temperature values in 83.3-86.7 minutes by ohmic method98.0-106.7 minutes at room temperature, and 500-606.7 minutes in the refrigerator environment. (Thawing criterion was set at 0±1°C). According to the obtained results, it was observed that the thawing process was performed in the shortest time by using ohmic method. Similar results have been observed by Bozkurt and İçier [12]. Bozkurt and İçer [12] compared ohmic and traditional methods in their research and found that differences in thawing time, rate and energy use in dissolving frozen beef samples, and specified that the meat size is an important factor in thawing process.

It is thought that ohmic heating system can be used as an alternative method, especially in meat thawing. As a matter of fact, Li and Sun[13]stated that ohmic heating could be used in order to thaw frozen food, therefore it was possible to thaw frozen tuna fish from -3^0C to 3^0C in a very short time. In the research, shorter time was needed to thaw frozen meat through ohmic heating system, so this point confirms the opinions of Li and Sun [13].

As the experimental modeling, the total viable bacterial counts, *Pseudomonas* spp., coliform, and yeast-mould counts were investigated periodically in the thawed samples by using the three separate methods. The mirobial differences among the methods are displayed in Table 1.

Table 1. *Microflora of the experimental samples thawed by using different thawing methods during storage period (log_{10} cfu/g).*

		Thawing Method			
		Conventional	Ohmic	Refrigerator	
Storage Time (Month)	Microorganism	X± Sx	X± Sx	X± Sx	*p-value*
0	TVC	4.23±4.13	4.22±3.51	4.30±3.19	0.778
	Pseudomonas spp.	2.18±1.58	2.16±1.57	2.54±2.24	0.144
	Coliform	2.17±1.54	2.19±1.35	2.29±1.45	0.166
	Yeast-Mould	2.52±2.25	3.10±2.46	2.81±2.73	0.809
1	TVC	3.76±3.19	4.11±3.12	4.12±3.36	0.304
	Pseudomonas spp.	2.46±1.89	2.37±1.66	2.67±2.13	0.138
	Coliform	ND	ND	1.72±1.46	0.161
	Yeast-Mould	2.41±2.19	2.36±2.12	2.69±2.48	0.724
2	TVC	4.37±3.50[a]	4.24±3.31[b]	3.67±3.35[c]	0.001
	Pseudomonas spp.	3.88±3.12[a]	3.41±3.31[ab]	2.93±1.45[c]	0.039
	Coliform	2.15±1.99	1.41±1.32	1.15±0.4	0.235
	Yeast-Mould	2.59±2.20	2.69±2.38	2.38±2.19	0.719
3	TVC	4.64±4.51	3.60±3.16	4.28±3.77	0.400
	Pseudomonas spp.	2.90±1.96	2.34±1.70	3.35±3.20	0.171
	Coliform	1.83±1.51[a]	<10	2.10±1.61[a]	0.294
	Yeast-Mould	2.47±2.15	2.70±2.24	2.66±2.49	0.879
4	TVC	4.37±3.76[a]	3.78±3.16[b]	4.17±3.19[b]	0.012
	Pseudomonas spp.	1.57±1.40	ND	ND	0.261
	Coliform	1.42±1.31	ND	ND	0.302
	Yeast-Mould	2.66±2.23	2.35±2.13	2.66±2.35	0.627

5	TVC	2.35±1.68[b]	2.86±2.18[a]	2.88±2.21[a]	0.004
	Pseudomonas spp.	ND	ND	ND	-
	Coliform	ND	ND	ND	-
	Yeast-Mould	2.76±2.12	2.49±2.12	2.58±2.35	0.688
6	TVC	2.90±2.34[a]	2.30±2.17[b]	3.10±2.24[a]	0.001
	Pseudomonas spp.	1.32±0.91	1.36±0.42	1.47±1.10	0.508
	Coliform	ND	ND	ND	-
	Yeast-Mould	2.45±2.12	2.22±1.25	2.42±2.28	0.949

TVC: Total viable count. ND: Not Date.a,b,c:The valueswith different letters in the same row are significantly different ($p<0.05$)

Ferna´ndez et al.[19]determined the total viable bacterial counts in raw meat (*M.longissimus dorsi*) as 3.53±0.23$\log_{10}$/g. The researchers stated that the microorganisms which belong to *Enterobacteriaceae* family were below the detectable number.

When thawing methods are taken into consideration, no differences were found in the microbiological analyses conducted on fresh meat samples which would be subjected to freezing operation between groups in terms of all investigated parameters (*P>0.05*).

In consequence of thawing operation carried out on the experimental samples, which were taken to frozen storage and kept there for 6 months, periodically at the end of each month by using different methods, differences in the total number of viable microorganisms were observed among groups in thawing at the end of 2nd, 4th, 5th and 6th months (*p<0.05*).

When thawing methods are considered and the number of *Pseudomonas* spp.in the experimental samples is evaluated, it is seen that there were significant differences in thawing at the end of 2nd month and 3rd month among groups (*p<0.05*). No differences were found among groups in other periods (*P>0. 05*). No reproduction of microorganisms from the mentioned group was detected in the 4th month and 5th month in the samples which were thawed in the refrigerator and by using ohmic heating system and in the 5th month in the samples which were thawed at room temperature.

The yeast-mold values of the experimental samples followed a fluctuating course in all thawing methods applied. The determined differences were not statistically significant (*p>0.05*).

When the number of coliform microorganisms of the experimental samples was considered, no coliform microorganism reproduction was detected in the samples which were thawed by using ohmic heating system at the end of 1st, 3rd, 4th, 5th and 6th month, in the samples which were thawed at refrigerator temperature at the end of 4th, 5th and 6th month and in the samples which were thawed at room temperature at the end of 1st, 5th and 6th month. The differences among groups in terms of number of microorganisms in the mentioned group were determined only in the 3rd month (*p<0.05*).

In general, a reduction with changing rates in microflora is provided by freezing meat. The great variance that the reduction in the microflora exhibits may result from the operations which are carried out while obtaining meat and the reproduction occurring during thawing.

The microbiological data obtained in consequence of the research support the opinions and thoughts given above. The general number of viable microorganisms which was found as 4.22-4.30$\log_{10}$cfu/g at the beginning was determined as 2.30-3.10 $\log_{10}$cfu/g in the 6th month thawing after frozen storage and a considerable reduction was observed in the microflora. A similar situation was determined for coliform microorganisms and the reproduction of microorganisms in this group completely stopped depending on the progress of the storage period. The reproduction of coliform microorganisms, which is also considered as the hygiene indicator, revealed the security of frozen storage in the sense of food security.

When *Pseudomonas* microorganisms are taken into consideration in general, it is emphasized that they would dominate meat microflora over time in cold environments. When research findings are evaluated, it is seen that the microorganisms in this group reached the highest level after 2nd month thawing (2.93-3.88 $\log_{10}$cfu/g), but they lost their activity in the following periods. This situation can be explained with the number of *Pseudomonas* at the beginning of the preservation. On the other hand, yeasts and molds followed a fluctuated course and continued their liveliness. This can be explained by the capacity of yeasts and molds to reproduce in low water activity values and at low temperatures (-10……-15^{0}C).

With the purpose of identification of *Pseudomonas* spp., in consequence of identification of different colonies which reproduced in Pseudomonas Agar Base medium, it was observed that the colonies reproducing in all groups included a considerable amount of *Pseudomonas aeruginosa*. In addition, *Pseudomonas stutzeri* was also identified in one of the samples which were coded in order to thaw in the refrigerator. In microorganism identification conducted on fresh meat samples before starting freezing operation, the bacteria of *E.coli, Stenotrophomonas maltophilia, Pantoea agglomerans, Sphingomonas paucimobilis* were identified.

The reflectance values for colors (*L**, *a**, *b**) of the meat samples which were kept in frozen storage were determined after thawing in each month with a different method at the beginning and during the storage period. *L**, *a**, *b** values of the samples which were thawed at room temperature are given in Table 2, *L**, *a**, *b** values of the samples which were thawed by using ohmic heating system are given in Table 3 and *L**, *a**, *b** values of the samples which were thawed in the refrigerator are given in Table 4.

Table 2. *L*, a*, b* values of the experimental samples which were thawed at room temperature*

			Before Freezing	After Thawing	
Checking Property	Storage Time(Month)	N	X± Sx	X± Sx	*p-value*
*L**	1	6	42.41±3.88	37.55±1.25	0.261
	2	6	38.02±2.86	34.41±0.40	0.266
	3	6	39.86±5.18	35.62±1.08	0.457
	4	6	40.48±3.61	39.38±1.72	0.790
	5	6	44.13±3.64	38.11±1.10	0.166
	6	6	41.24±3.36	36.97±1.01	0.271
	P		**0.907**	**0.067**	

*a**	1	6	20.08±0.79 [ab]	18.94±0.64	0.292
	2	6	21.86±0.57 [a]	20.04±0.36	**0.024****
	3	6	22.51±1.23 [a]	18.62±0.42	**0.024****
	4	6	20.50±1.17 [a]	17.86±0.95	0.112
	5	6	16.29±1.94 [b]	17.46±0.44	0.582
	6	6	18.92±1.58 [ab]	19.11±1.22	0.925
	P		**0.028**	**0.208**	
*b**	1	6	10.48±1.89	4.29±0.99	**0.016****
	2	6	9.52±1.49	5.90±0.33	**0.039****
	3	6	10.74±2.48	3.93±1.01	**0.030****
	4	6	9.79±2.42	4.83±0.90	0.084
	5	6	8.30±1.85	4.95±0.39	0.131
	6	6	10.69±2.52	5.19±1.10	0.087
	P		**0.965**	**0.657**	

a,b: The values with different letters in the same column are significantly different ($p<0.05$).
: represents the difference in terms of *L,*a**,*b** values before freezing and after thawing. ($p<0.05$).
*L**: Brightness *a**: Redness *b**: Yellowness

Table 3. *L*, a*, b* values of the samples which were thawed by using ohmic heating system*

			Before Freezing	After Thawing	
Checking Property	Storage Time(Month)	N	X± Sx	X± Sx	*p-value*
*L**	1	6	40.26±5.505	36.73±0.812	0.553
	2	6	37.25±0.978	37.42±0.792	0.900
	3	6	45.29±4.051	36.44±1.402	0.066
	4	6	41.05±4.402	36.81±0.880	0.385
	5	6	38.86±2.814	36.84±0.512	0.497
	6	6	43.29±4.525	36.21±0.912	0.181
	P		**0.745**	**0.961**	
*a**	1	6	18.75±2.100	19.43±0.613	0.762
	2	6	18.45±1.821	17.04±0.673	0.494
	3	6	15.27±1.419	18.24±0.936	0.112
	4	6	18.38±1.254	17.64±0.282	0.589
	5	6	16.88±1.636	17.33±0.561	0.807
	6	6	19.63±1.472	18.17±0.564	0.377
	P		**0.492**	**0.143**	
*b**	1	6	8.44±1.636	5.05±0.750	0.302
	2	6	7.69±0.692	3.23±0.808	**0.002****
	3	6	7.54±2.565	3.33±1.091	0.176
	4	6	7.40±2.049	4.81±0.322	0.266
	5	6	8.11±2.304	4.41±0.390	0.172
	6	6	11.58±1.527	4.37±0.438	**0.004****
	P		**0.739**	**0.330**	

: represents the difference in terms of *L,*a**,*b** values before freezing and after thawing. ($P<0.05$).
*L**: Brightness *a**: Redness *b**: Yellowness

Table 4. *L*, a*, b* values of the samples which were thawed in the refrigerator*

Checking Property	Storage Time(Month)	N	Before Freezing X± Sx	After Thawing X± Sx	*p-value*
*L**	1	6	41.37±2.84	36.29±0.60	0.136
	2	6	35.58±2.22	37.74±0.64	0.156
	3	6	43.89±5.62	35.37±0.85	0.192
	4	6	42.82±4.57	37.02±0.26	0.262
	5	6	43.32±3.33	37.40±0.85	0.116
	6	6	42.57±4.90	36.77±0.62	0.293
	P		**0.716**	**0.191**	
*a**	1	6	20.34±2.76[a]	18.38±0.82	0.523
	2	6	18.99±0.58[a]	19.50±0.46	0.507
	3	6	19.83±0.65[a]	19.80±0.27	0.966
	4	6	20.93±0.69[a]	18.61±0.57	**0.028****
	5	6	14.67±1.21[b]	17.60±0.63	**0.057****
	6	6	18.48±0.57[ab]	18.81±1.20	0.810
	P		**0.033**	**0.335**	
*b**	1	6	10.76±2.95	3.83±1.04	0.067
	2	6	8.58±0.95	5.86±0.74	**0.048****
	3	6	9.32±2.54	5.84±0.29	0.231
	4	6	11.07±2.38	5.11±0.58	0.054
	5	6	7.92±2.22	4.48±0.45	0.159
	6	6	9.55±3.02	6.16±0.40	0.314
	P		**0.937**	**0.100**	

a,b: The values with different letters in the same column are significantly different ($p<0.05$).
: represents the difference in terms of *L*,a*,b values before freezing and afterthawing. ($P<0.05$).

No statistical differences were detected between *L** values of the experimental samples which were thawed at room temperature and the values which were measured before freezing the meat and the values measured in the experimental samples which were thawed at the end of preservation (*p>0.05*). In terms of *a** values, differences were determined in the 1st, 2nd and 3rd months between the meat thawed at the end of storage and the values measured in the fresh meat before preservation (*p*<0,05). It was also observed that there were meaningful differences in the values measured in fresh meat before preservation (*p<0.05*). In the context of *b** values, it was observed that there were differences in the values measured after thawing at the beginning in the 1st, 2nd and 3rd months (*p<0.05*).

No statistical differences were determined between *L*, a*, b** values of the samples which were thawed by using the ohmic heating system and the values measured in fresh meat before preservation (*P<0.05*). After thawing, significant differences were observed only in *b** values in the 2nd and 6th months in comparison to fresh meat before preservation (Table 3; *p<0.05*).

In terms of *L** values of the experimental samples which were thawed at refrigerator temperature, there were no statistical differences between the values measured in fresh meat and the values measured in the experimental values after storage time. Differences were determined in terms of *a** values between the values measured in the 4th month of meat samples which were thawed at the

end of storage period and the values measured in fresh meat before storage. In addition to this, meaningful differences were also observed in values measured in fresh meat before the preservation. When b^* values are considered, it has been determined that there are statistical differences between the values measured in the 2nd month just at the beginning after thawing ($p<0.05$).

When L^* values of the samples are considered in general, it is seen that the mentioned values in the samples which were thawed at room temperature were between 38.02-44.13 before freezing, between 34.41-39.38 after thawing (Table 2), in the samples which were thawed using ohmic heating system were between 37.25-43.29 at the beginning, between 36.21-37.42 after thawing (Table 3), in those samples which were classified in order to thaw in the refrigerator were between 35.58-43.89 at the beginning and between 35.37-37.74 after thawing (Table 4). Based on these determined values, it was observed that there were decreases in L^* values of fresh meat and the same values in frozen and thawed meat. This situation was also detected by Boles and Swanb [20]. The researchers determined L^* values which were kept at -1.5^{0}C for 8 weeks and measured periodically every week as 33.8 at the beginning and as 34.1 after 8-week preservation. L^* values were determined by many researchers. Hernández et al.[21] established the L^* value in animals which were slaughtered under stress as 28.9; and in animals which were slaughtered under normal conditions as 37.94.

Apple et al., [22] determined that L^* value of *M.gluteus medius* muscle in an animal belonging to USDA eminent classes 36.8. The researchers reported that there were differences between inner, central and outer surfaces of the same meat preparation in terms of color measurement.

Farouk and Swan, [23] found L^* values in beef as 49.7; Liu et al., [24] determined L^* values belonging to steak as38.07; Fernández et al.,[19]found this value in raw meat (*M.longissimus dorsi*) as 26.35, and 26.98 in frozen meat and they claimed that there were no differences in these values before and after freezing.

When L^* values are interpreted in general terms, it is seen that there are differences among researchers. It is possible to explain this situation with the meat preparation, slaughter, storage and preservation conditions applied. In fact, Apple et al., [22]suggested that there were differences between inner, central and outer surfaces of the same meat preparation in terms of color measurement. This suggestion seems to support the idea.

In general, no differences were detected among the groups in terms of a^* values obtained from the experimental samples. It was determined that a^* values of the samples before freezing were between 14.67 - 22.51, a^* values of the samples after thawing were between 17.04 - 20.04 . In the conducted researches, Hernández et al.,[21]found a^* value as 22.3 in animals slaughtered under stress, as 15.68 in animals slaughtered under normal conditions; Apple et al., [22]determined the same value in *M. gluteus medius* muscle of an animal belonging to eminent class as 14.8; Farouk and Swan, [22] determined it as 13.1 in beef; Boles and Swan, [20] determined the same value in

meat that they preserved at -1.5^{0}C for 8 weeks and measured periodically every week as 17.6 at the beginning, as 16.5 after preservation; Liu et al., [23] detected the value as 17.27 in steak; Fernández et al., [19] detected *a** value in fresh meat (*M.longissimus dorsi*) as 8.86 and as 7.43 in frozen meat. In general, the obtained findings in regard to *a** value and the finding of the researchers show a partial similarity. The observed differences probably result from different samples used by researchers, conditions of slaughter, conditions of storage and preservation. A similar situation is also valid for *b** values.

Consequently, color is the most important criterion for the visual quality and consumption of meat. Particularly, the transition of myoglobin, which is known as the color pigment in muscles, into oksi, deoksi and metmiyoglobine is significant.

4. CONCLUSION

As a result, frozen storage still maintains its importance in terms of reliability for the preservation of the meat, if it is carried out under suitable conditions. However, it is also important occurred physical, chemical and microbiological activities in thawing process of the meat as well as the preservation. In conventional thawing methods, there are some negativities such as long thawing time, weight loss due to the high amount of leakage, nutritional losses with leaking liquid and microbial activities occurred at unexpected rate especially during thawing, so it is necessary to develop and apply new and more reliable dissolution methods. When the results are taken into account, it has been concluded that the ohmic heating system can be a useful method for thawing frozen meat and studies should be continued in this regard.

Acknowledgments

The authors are grateful for financial support provided for the project entitled “Application of Ohmic Heating System in Meat Thawing and Its Effects on Quality” under project no.12102023 by The Selçuk University, Scientific Research Projects Coordination Unit.

REFERENCES

[1]. Liu L., Llave Y., Jin Y., Zheng D. Fukuoka M., Sakai N. Electrical conductivity and ohmic thawing of frozen tuna at high frequencies. *J of Food Eng*. 197, **(**2017), 68-77.

[2]. Öztan A. Et Bilimi ve Teknolojisi. TMMOB Gıda Mühendisleri Odası Yayınları, Kitaplar Serisi. 6. Baskı. Yayın No:1, Filiz Matbaacılık Sanayi, Ankara, (2008), 182-191.

[3]. İçier F., Izzetoğlu G.T., Bozkurt H., Ober A. Effects of ohmic thawing on histological and textural properties of beef cuts. *J of Food Eng*, 99, (2010), 360–365.

[4]. Ünlütürk A., Turantaş F. Gıda Mikrobiyolojisi. Meta Basım Matbaacılık Hizmetleri, 3th ed., İzmir, Turkey, (2003). 261-276.

[5]. Cho H.Y., Yousef A.E., Sastry S.K. Kinetics of inactivation of *Basillus subtilis* spores by contionuous or intermittent ohmic and conventional heating. *Biotechnology and Bioeng.* 62(3), (1999), 368-372.

[6]. Sun H., Kwamura S., Himoto J.I., Itoh K., Wada T., Kimura T. Effects of ohmic heating on microbial counts and denaturation of proteins in milk. *Food Sci. Technol Res.* 14(2), (2008), 117-123.

[7]. Tian X., Wu.W, Yu Q., Hou M., Gao F., Li X., Dai R. Bacterial diversity analysis of pork *Longissimus lumborum* following long term ohmic cooking and water bath cooking by amplicon sequencing of 16S rRNA gene. *Meat Sci.*123, (2017), 97–104.

[8]. Park I.K., Kang D.H., Effect of electropermeabilization by ohmic heating for inactivation of *Escherichia coli O157:H7*, *Salmonella enterica* Serovar *Typhimurium*, and *Listeria monocytogenes* in buffered peptone water and apple Juice. *Applied and Environmental Micro*, 79(23): (2013), 7122–7129.

[9]. Aguilar-Machado D., Morales-Oyervides L., Contreras-Esquivel J.C., Aguilar C., Me´ndez-Zavala A., Raso J., Montan˜ez J. Effect of ohmic heating processing conditions on color stability of fungal pigments. *Food Sci. Technol*. Inter, (2016), 1-11.

[10]. Cho P.P., Yousef A.E, Sastry S.K. Growth kinetics of *Lactobacillus acidophilus* under ohmic heating. *Biotechnology and Bioeng*, 49, (1996). 334-340.

[11]. Zell M., Lyng J.G., Cronin D.A, Morgan D.J. Ohmic cooking of whole turkey meat- effect of rapid ohmic heating on selected product parameters. *Food Chemistry*. 120, (2010), 724-729.

[12]. Bozkurt H., Icier F. Ohmic thawing of frozen beef cuts. *Journal of Food Process Eng*, 35(1), (2012), 16-36.

[13]. Li B., Sun D.W. Novel methods for rapid freezing and thawing of foods- a review. *J of Food Eng*. 54, (2002), 175-182.

[14]. Rohrle F.T., Moloney A.P., Osorio M.T., Luciano G., Priolo A., Caplan P., Monahan F.J. Carotenoid, colour and reflectance measurements in bovine adipose tissue to discriminate between beef from different feeding systems. *Meat Sci*.88(3), (2011), 347-353.

[15]. Food and Drug Administration (FDA). Center for Food Safety and Applied Nutrition Bacteriological Analytical Manuel. USA. (2001).

[16]. Food and Drug Administration (FDA). Center for Food Safety&Aplied Nutrition, Bacteriological Analytical Manual. USA. (2002).

[17]. Türk Standartları Enstitüsü (TSE). Türk Standardı, Et ve et ürünleri-*Pseudomonas* spp. sayımı, TS ISO 13720. Ankara. (1997).

[18]. bioMerieux. Marcy L'Etoile.VITEK 2 Compact GN Card, Product Number:21341. (2007).

[19]. Fernández P.P., Sanz P.D., Molina-Garcı´a A.D., Otero L., Guignon B., Vaudagna S.R. Conventional freezing plus high pressure–low temperature treatment: Physical properties, microbial quality and storage stability of beef meat. *Meat Sci.* 77, (2007), 616–625.

[20]. Boles J.A., Swanb J.E. Meat and storage effects on processing characteristics of beef roasts. *Meat Sci*, 62, (2002), 121–127.

[21]. Hernández B., Lizaso G., Horcada A., Beriain M.J., Purroy A. Meat colour of fighting bulls. *Arch. Latinoam. Prod. Anim*, 14(3), (2006), 90-94.

[22]. Apple J.K., Machete J.B., Stackhouse R.J., Johnson T.M., Cari A.K., Yancey J.W.S. Color stability and tenderness variations within the gluteus medius from beef top sirloin butts. *Meat Sci*, 96, (2014), 56–64.

[23]. Farouk M.M., Swan J,E. Effect of muscle condition before freezing and simulated chemical changes during frozen storage on the pH and colour of beef. *Meat Sci.* 50(2), (1998), 245-256.

[24]. Liu Y., Lyon B.G., Windham W.R., Realini C.E., Pringle D.T.D., Duckett S. Prediction of color, texture, and sensory characteristics of beef steaks by visible and near infrared reflectance spectroscopy. A feasibility study. *Meat Sci.*65, (2003), 1107–1115.

MANAS Journal of Engineering
ISSN 1694-7398 | e-ISSN 1694-7398

Volume 6 (Issue 2) (2018) Pages 110-128

Synthesis, Characterization and Modification of Novel Food Packaging Material from Dimethyl acrylamide/Gelatin and Purple Cabbage Extract

Duygu Alpaslan[1], Tuba Erşen Dudu[1], Nahit Aktaş*[1,2]

[1]Van Yüzüncü Yıl University, Engineering Faculty, Department of Chemical Engineering, Campus, Van 65080, Turkey, naktas@yyu.edu.tr
[2]Kyrgyz-Turkish Manas University, Faculty of Engineering, Department of Chemical Engineering, Bishkek, Kyrgyz Republic.

Received: 28.11.2018; Accepted: 13.12.2018

Abstract: *A novel and functional Multi-Responsive Hydrogel (MRH) was synthesized from N, N dimethyl acrylamide (DMAAm), gelatin, citric acid (CA) and purple cabbage extract (PCE) to be utilized as smart food packaging material. The MRH, which was p(Gelatin-co-DMAAm)/CA-PCE, was synthesized through redox polymerization technique as film form in petri dishes. Mechanical and water resistances of the MRH was improved by addition of citric acid and N, N, methylenebisacrylamide (MBA) as cross linker. PCE was added to the reaction mixture to obtain antimicrobial, antioxidant and anthocyanin properties. Dynamic and Mechanical Analyzer (DMA), Thermo Gravimetric Analyzer (TGA), Fourier Transform Infrared Spectroscopy (FT-IR) and Scanning Electron Microscopy (SEM) were used for the characterizations. FT-IR revealed the existence of bonding between the functional group of PCE and Gelatin, carbonyl groups of DMAAm and carboxylic acid groups of CA. TGA result represented that MRH was stable up to 527°C. SEM results were proved that PCE improved the thermal stability, flexibility and durability as well as pH sensibility of the MRH. Antimicrobial activity of MRH was observed when it tested against Escherichia coli (ATCC 8739), Bacillus subtilis (ATCC 6633) and Staphylococcus aureus (ATCC 6538). Additionally, total antioxidant and anthocyanin activities of MRH were studied at different pH values for monitoring the color change. Furthermore, MRH was applied to the real samples such as whole pasteurized milk and chicken. It exhibited good color indication and antimicrobial activity on pasteurized whole milk and chicken. It was concluded that MRH was a significant candidate to be used in food packaging.*

Keywords: *Functional hydrogel, multi response polymers, p(gelatin-co-DMAAm)/CA-PCE, smart food packaging, antimicrobial effect, antioxidant activity, anthocyanin activity.*

1. INTRODUCTION

Marked-bench or instant monitoring of the food quality is one of the most important issues for costumers, producers and public health care institutions as well [1-2]. Traditional food packaging methods are still commonly utilized for protection, security, convenience, containment, informative transmission, agglomeration and tamper indication in food industry. The package itself is tasked with protection of the food from the deteriorative effects of external environmental circumstances like light, heat, pressure, moisture, microorganisms, vibration, gaseous emissions and so on. The food packaging materials are generally manufactured from glass, metals, plastics [3], papers, paperboards [4], polymers and fabric. Many natural materials such as gelatin, starch and cellulose are also used in food packaging for their biocompatibility, low toxicity and decomposability [5]. For the improving of the packaging quality additional natural compounds such as citric acid [6], pigments from purple cabbage are added to the main materials to the packaging material to gain mechanical strength, antioxidant properties, antimicrobial and anthocyanin properties [7,8]. Furthermore, addition of pigments enables the color change, which is related to the pH shifts, during the food deteriorations [9,10].

Anthocyanins are water-soluble, naturally-colored substances that provide a variety of colors like pink, red, violet, blue and purple to many fruits, vegetables and flowers. They act as natural pH indicator as well [11]. Anthocyanin with red color is called flavylium that occurs at pH 1[12], while colorless carbinol form predominantly occurs around pH 4.5 and blue-green quinoidal anhydrous form can be observed between pH 7 and 8 [13].

Recently, being as a polymeric material, hydrogels are becoming one of the most utilized materials for the food packaging purposes due to their biocompatible, flexible, easy modifiable properties as well as high water absorption capacity and low cost [14]. Furthermore, modifiable hydrogels/multi responsive polymers rapidly and reversibly respond to various physical and chemical conditions and stimuli, such as water, pH, heat, UV light, daylight, electrostatic field, magnetic field and changes in physicochemical and microbiological properties. In recent decades, multi response polymers are being used as catalysts, adsorbents, modification agents of electrodes, wound dressings [15], drug-delivery systems, enriched mediums for microorganisms [16], cell culture substrates and regenerative medicines [17].

The objective of this study is to synthesize, characterize and apply a Multi Responsive Hydrogel (MRH) with addition of natural compounds, which are gelatin, citric acid and purple cabbage extract, being a novel instant food quality monitoring device while used as a food packaging material. MRH, which is p(Gelatin-co-DMAAm)/CA-PCE, was synthesized via redox polymerization as film from in petri dishes from N, N dimethyl acrylamide (DMAAm), gelatin, citric acid (CA) and purple cabbage extract (PCE). PCE was added as the pigment source in which the pigments' colors were changed by medium pH, which is a result of food decomposition. Morphological, surface, thermal and structural characterizations of the MRH were studied by SEM, TGA and FT-IR. The swelling behavior and pH sensitivity of the synthesized MRH was studied. Furthermore, the antimicrobial, antioxidant and color-specific activities of MRH were investigated. Escherichia coli, Bacillus subtilis, Staphylococcus aureus microorganisms were used to investigate the antimicrobial activities of MRH. It was concluded that MRH was exhibited good color indication and antimicrobial activity on pasteurized whole milk and chicken.

2. MATERIAL AND METHOD

2.1. Materials

N, N dimethyl acrylamide (DMAAm), Gelatin (99%), N, N, methylenebisacrylamide (MBA) (99%), ethanol, sodium hydroxide (NaOH) and HCl (36.5-38% v/v) were purchased from Sigma; ammonium per sulfate (APS) (98%) and N, N, N, N-tetramethylenediamine (TEMED) were purchased from Merck. All reagents were of analytical grade of highest purity available and they were used without further purification. Purple cabbage, pasteurized whole milk and chicken were obtained from local suppliers. Distilled water (DI, 18.2 MΩ cm; Millipore Direct-Q3UV) was also used throughout this study.
For antibacterial activity assays, three bacterial strains obtained from the Biology Department at Van Yüzüncü Yıl University and were used. Bacillus subtilis (ATCC 6633), Staphylococcus aureus (ATCC 6538) were utilized as gram-positive bacteria, while Escherichia coli (ATCC 8739) was used as gram-negative bacteria.

2.2. Solvent Extraction from Purple Cabbage (Brassica oleracea var. capitata f. Rubra)

For each type of hydrogel, 200 g purple cabbage was grounded and extracted with DI water and then concentrated by rotary evaporator (30% vv-1 of PCE). The PCE was stored at 4°C for further analysis like antioxidant, antimicrobial activity and anthocyanin tests [10].

2.3 Synthesis and Preparations of the Hydrogels and MRHs

Redox polymerization technique was utilized for preparation of p(Gelatin-co-DMAAm)/CA-PCE based hydrogels. In order to achieve this synthesis, 2 mL of DMAAm was mixed with 2 g of Gelatin in 5 mL DI water and 5 mL of PCE was added to the reaction mixture. Afterwards, MBA (0.25 mol% with respect to total monomer amount) was mixed through vortex followed by addition of 60 µL TEMED to PCE hydrogel mixture and finally the initiator solution APS (1 mol% with respect to total monomer amount) in 100 µL DI water was added. Then the solution was placed in plastic petri with a 10 mm diameter and was allowed to polymerize and to complete crosslinking at ambient conditions for 24 h. These preparation steps are schematically given in Fig. 1. The synthesized hydrogels were kept in DI water and renewed every 8 h for 24 h to eliminate unreacted monomers. Finally, hydrogels in film form were dried in oven at 40ºC till their weights were stabilized and stored 4ºC for characterization and utilization.

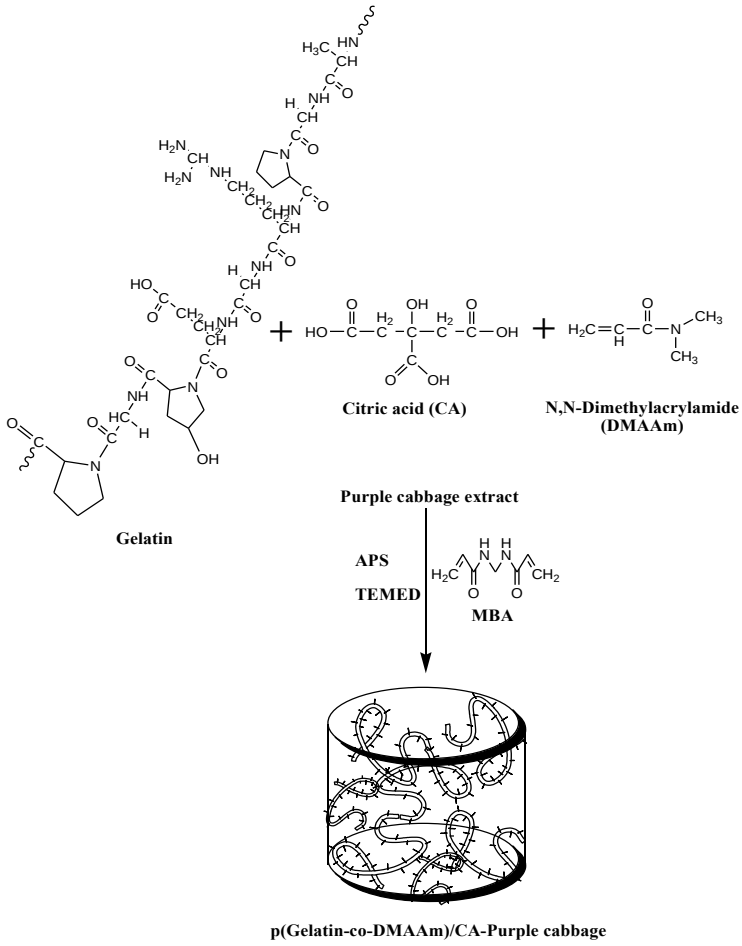

Figure 1. *The hydrogels preparation.*

2.4. Swelling Behavior of the Hydrogels

Swelling properties of hydrogels were carried out in three runs at room temperature by placing certain amounts of dried hydrogels and MRH in DI water. The increase in mass was periodically measured by weighting of the hydrogels and MRH after blot drying with filter paper to remove the superficial water and returned into the same swelling media. The hydrogels and MRH were kept in swelling medium for 24 h to determine the maximum swelling values, Smax%.

The percent swelling degree (S%) as the function time was calculated as:

$$S\% = \frac{M_t - M_0}{M_0} \times 100 \quad (1)$$

Where, Mo and Mt are the initial mass and the mass of hydrogels at time t, respectively [16].

2.5. TGA, FT-IR and SEM Analysis of Hydrogels

Thermal behaviors of the hydrogels and MRH were investigated by a Gravimetric Analyzer (TG/DSC, Setaram Labsys Evo 1600 model, France). Approximately 4-6 mg of samples were

placed in ceramic crucibles and analyzed during heating up to 50-1000°C under Argon atmosphere with 100 mL min-1 flow rate at 10°C min-1 heating rate.

The FT-IR analysis of DMAAm and Gelatin based the hydrogels were investigated using Fourier Transform Infrared Spectroscopy (FT-IR, Thermo Nicolet iS10 FT-IR Spectrometer, USA) using ATR apparatus with 4 cm-1 resolution between 4000 and 650 cm-1.

The surface morphologies of the synthesized materials, which were p(Gelatin-co-DMAAm)/CA and MRH, were monitored by Scanning Electron Microscopy (SEM) (Zeiss Ultra Field emission (FESEM-EDX), Germany).

2.6. Liquid Chromatograph Mass Spectrometer (LC-MS/MS, Q Exactive) Analysis

Liquid Chromatography Mass Spectrometer (Hybrid Quadrupole-Orbitrap Mass Spectrometer, Thermo, USA) was used to determine the PCE composition. The extract samples were renovated by capillary column Hypersil Gold (50 x 2.1 mm) while Helium was used as a carrier gas, at a flow rate of 0.3 mL min-1. Determinations of individual components were identified by analytical standards (antimicrobial, antioxidant and anthocyanin).

2.7. Mechanical Strength Test

Dynamic and mechanical behaviors of the synthesized and modified materials were carried out by DMA (Mettler Tolledo Tritone Technology, UK) device. The samples were prepared in approximately 1 mm height and 4 mm diameter. DMA measurements were recorded at 1 Hz frequency and at a heating rate of 5ºC min-1while the temperature ranged from 30 to 80ºC. The modulus properties such as storage modulus and loss modulus were recorded as a function of temperature.

2.8. Antimicrobial Properties of the Hydrogels

The agar diffusion method was used to evaluate the antimicrobial activity as explained in the literature [18]. Escherichia coli (ATCC 8739), Bacillus subtilis (ATCC 6633), Staphylococcus aureus (ATCC 6538) bacteria were used for the test. The test was run for three different media, which are PCE, p(Gelatin-co-DMAAm)/CA and MRH monitored for 24 h. The numbers of bacteria were counted in CFU.

2.9. Antioxidant Properties of the Hydrogels

Total phenolic substances were determined according to ABTS method [19]. The absorbances of samples in phosphate buffered saline (PBS) at 734 nm were recorded against the blank. The observed absorbance values indicated of the reduction in the ABTS radicals in the media. The impact of PCE against the ABTS radicals in the media was calculated using the following equation:

$$ABTS\ Activity\% = \frac{A_0 - A_1}{A_0} \times 100 \quad (2)$$

Where, A0 is absorbance of control sample and A1 is absorbance of the sample.
In Folin-Ciocalteu method, phenolic compounds oxidize Folin-Ciocalteu reagent in an alkaline media while the color of the media changes. Gallic acid equivalent of the phenolic compounds

according to this concentration were then calculated from linear regression equations derived from standard curves that were prepared with gallic acid. Total amounts of phenolic compounds in PCE were reported as mg gallic acid per litter. In this analysis, saturated sodium carbonate solution was prepared by dissolving 35 g Na2CO3.10H2O in 100 mL of DI water and left to stand overnight. Crystallization was initiated by addition of Na2CO3 solution and saturated carbonate solution was prepared by filtering through glass wool after crystallization ended. One mL of Folin-Ciocalteu agent was then added to 0.1 mL of each sample. The mixture was then allowed to rest for 4 min followed by addition of 1.25 mL of saturated sodium carbonate solution. Samples were then allowed to stand for 120 min and the absorbance was recorded at 720 nm wavelength using a Thermo UV-Vis spectrophotometer (Genesis 10S UV-Vis, USA) [20].

2.10. Anthocyanin Properties of the Hydrogels

Anthocyanin properties of hydrogels which are p(Gelatin-co-DMAAm), p(Gelatin-co-DMAAm)/CA and MRH, were measured as indicated in the literature [21]. The absorbance of each dilution was then determined at 516 nm and total absorbance of turbidity at 700 nm. Anthocyanin activity was obtained from maximum absorbance value by subtracting from the total value. This procedure was repeated for each MRH

Anthocyanins activity of extracts and hydrogels were calculated with the following equation;

$$Activity\% = \frac{\left|\left[(A_{516} - A_{700})pH_1 - (A_{516} - A_{700})pH_{4,5}\right] \times 1000 \times MW\right|}{[(l) \times \delta]} \quad (3)$$

where, cyaniding-3-glucoside (cyn-3-glue) MW is 449.2 g, ε (molar absorptivity coefficient) is 13000 and, l is 1 cm; pelergonidine-3-glucoside MW is 433.2 g, ε (molar absorptivity coefficient) is 22440 and, l is 1 cm, malvidine-3-glucoside MW is 493.2 g, ε (molar absorptivity coefficient) is 22440 and, l is 1 cm [22].

2.11. Colorimetric Properties of the Hydrogels

The effect of the medium pH on MRH and the hydrogels were studied according to literature [23]. Generally, the indicator is a weak acid (In H), which is in equilibrium with the surrounding pH according to below equation:

$$\text{In } H^{ki}_{k-I} = In^- + H^+ \quad (4)$$

Where Hkik-I is acidic color intensity and In- is alkali color intensity. The variation of the medium colors with variation of medium pH was measured within the visible region while p(Gelatin-co-DMAAm)/CA hydrogel was used as the blank sample.

The absorption spectra (380−770 nm) of all solutions were recorded at constant intervals (Δλ = 2 nm) with a (Analytikjena, Spercord S 600, Germany spectrophotometer), using 5 mm path length quartz cells and distilled water as a reference. The CIELab parameters were calculated from the absorption spectra by using the original software Croma Lab, following the recommendations of the Commission International de L'Eclariage: CIE 1976 and the Standard Illuminant D65, corresponding to natural daylight. The color identifications were made by CIE 1976 (L*a*b*) (CIELab) uniform color diagram. a* and b* are the axis of the 2D coordinate system, in which a* takes positive values for reddish colors and negative values for greenish ones while b* takes

positive values for yellowish colors and negative for the bluish ones and L* defines lightness, ranging from black to white according to the CIELab uniform diagram a psychometric index. Other color parameters were obtained by equations 5 and 6; hue angle (h) and (C), which stand for color and color intensity respectively [24,25].

The L* defines lightness, C* specifies chroma and h* denotes hue angle, an angular measurement.

$$C^* = (a^2 + b^2)^{1/2} \quad (5)$$

$$h = \arctan\left(\frac{b^*}{a^*}\right) \quad (6)$$

The CIELab parameters (L*, a*, b*, C*, h*) were determined for 5 mL solutions of each hydrogel at different pH values, ranging from 1 to 12. ΔE (Euclidean). The values were calculated from the initial pH value (pH 1) and after each increase of pH, considering the Euclidean distance between the two color points. Euclidean distance of hydrogels was calculated with the following equation;

$$\Delta E = ((\Delta L^*)^2 + (\Delta a^*)^2 + (\Delta b^*)^2)^{1/2} \quad (7)$$

2.12. Real Samples Applications

Whole milk and chicken breast were used as the real samples. Firstly, those real samples were infected by Staphylococcus aureus, Escherichia coli and Bacillus cereus than treated with MRH, which were cut into 10 mm in diameter, were placed on 50 mL of whole milk and to 100 g chicken. MRH exposed samples were kept in a temperature controlled incubator (Memmert UN 110, Germany) at different temperature, which were 4ºC, 10ºC, 20ºC, 30ºC and 40ºC, for 48 h. The color (CIELab) parameters (L*, a*, b*, C*, h*) were calculated for each sample while untreated whole milk and chicken were used as the blanks.

3. RESULTS AND DISCUSSION

3.1. Characterization of the Synthesized Hydrogels

The moisture content of a given food is one of the most important parameters for its shelf life and structural degradation. It is known that polymers prepared form gelatin and DMAAm have not water resistance, mechanical strength and dissolved easily in an aqueous media. Therefore, water resistance and mechanical strength of MRH were adjusted by addition of biocompatible MBA as cross linker and CA to the polymer mixture during the synthesis [26]. Water resistance of MRH, which was p(Gelatin-co-DMAAm)/CA-PCE, was observed higher than those of p(DMAAm), p(DMAAm)/CA, p(Gelatin-co-DMAAm), p(Gelatin-co-DMAAm)/CA in DI as shown in Fig. 2 and at different pH values ranging from 2-12. The films prepared form MRH were non-dissolved and stable in aqueous media more than five months. Relatively high water absorption of MRH to the conventional food packaging materials enables it to fast response to the pH change in the media.

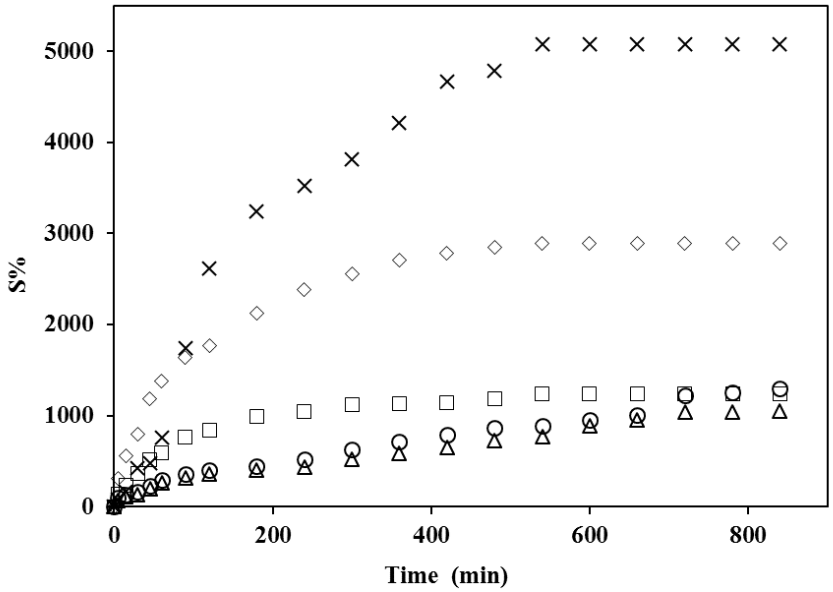

Figure 2. *Swelling behavior of prepared hydrogels; △ p(DMAAm), O p(DMAAm)/CA, X p(Gelatin-co-DMAAm), ◇ p(Gelatin-co-DMAAm)/CA and □ MRH.*

As given in Fig. 3, the FTIR spectra for p(DMAAm) showed the characteristic peak belonging to amide at 1616 cm-1 and the peaks between 1398 cm-1 and 1250 cm-1 were related to C–N stretching. Other peaks corresponding to p(Gelatin-co-DMAAm)/CA hydrogel were missing, which can be justified by the new bonds intervened during crosslinking process. When PCE was added, the broad peak between 3649 cm-1 and 3080 cm-1 was reduced and stress of the peaks at 2359 cm-1 and 2342 cm-1 wave numbers were decreased. In other words, those appeared new bonds and structural variances demonstrated the existence of a hydrogen-bonding interaction between p(DMAAm), p(Gelatin-co-DMAAm)/CA and MRH.

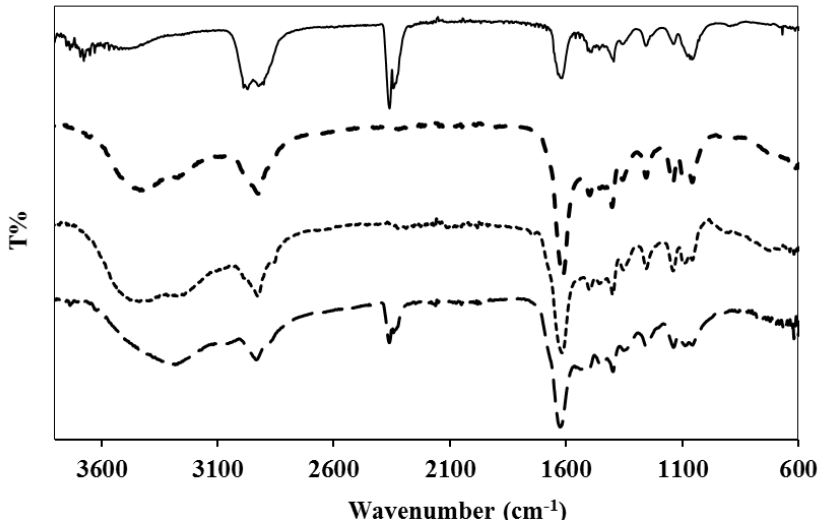

Figure 3. *FT-IR analysis of — p(DMAAm), - -p(Gelatin-co-DMAAm), -----p(Gelatin-co-DMAAm)/CA and — — MRH.*

Thermal stabilities of synthesized hydrogels were investigated using a TGA/DSC analyzer. In Fig. 4, the thermal degradation of p(DMAAm) hydrogel has one step and during this stage, the total mass loss was about 97% while temperature reached 500°C. This can be explained with accelerated mass loss of hydrogel due to the main chains and cross-linked networks in p(DMAAm) getting destroyed [27]. p(Gelatin-co-DMAAm)/CA hydrogel degradation has three steps. At the initial stage, the first mass loss around 15% (205°C) was due to evaporation of surface water and of the remaining small molecules. The second step began when the temperature was 250°C and at 359°C temperature, mass loss became approximately 57.8%. Third step began 359°C and the mass loss, which was about 19.8%, tended to be constant till the temperature of 465°C. Thermal degradation of MRH was observe in two steps as shown in Fig. 4. The mass loss of MRH at the first stage was approximately 12.8% because of the evaporation of the surface water while the temperature increased to 196°C. The second step began when the temperature was 196°C and average mass loss was approximately 75.3% from 196°C to 527°C. The total mass loss was reached to 88.1% during decomposition of MRH.

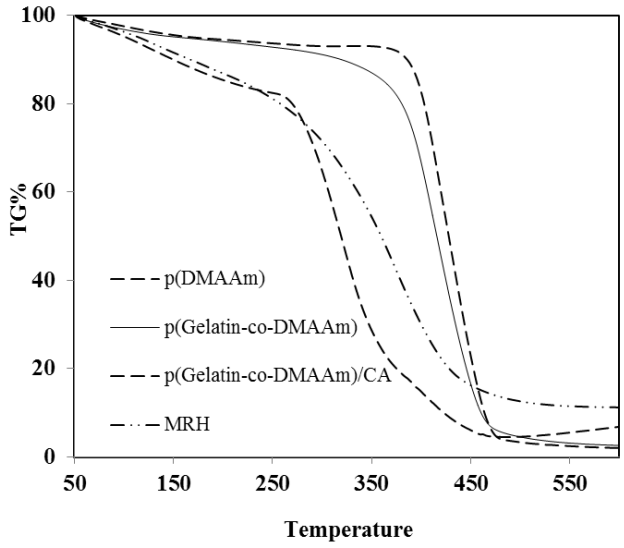

Figure 4. *Thermogravimetric analysis of p(DMAAm), p(Gelatin-co-DMAAm), p(Gelatin-co-DMAAm)/CA and MRH.*

Surface morphologies of synthesized materials were monitored using SEM and represented in Fig. 5a and b. Fig. 5a shows the surface image of p(Gelatin-co-DMAAm)/CA hydrogel prepared with gelatin, DMAAm and CA. As seen clearly, roughness, cracks and cracks were formed on the surface after the polymerization was completed. This image shows that the structure is not tunable and elastic. However, when PCE added the polymerization reaction to synthesized MRH the cracks and fragilities were lost and the structure became smoother and more elastic as shown in Fig. 5b. Furthermore, after the PCE is added, it was verified by DMA analyzes that MRH was more elastic than p(Gelatin-co-DMAAm)/CA. It was concluded that the homogeneously dispersed PCE in the hydrogel structure acted as a bond in the structure, removing cracks and brittleness, and made the structure more flexible and smooth.

a) b)

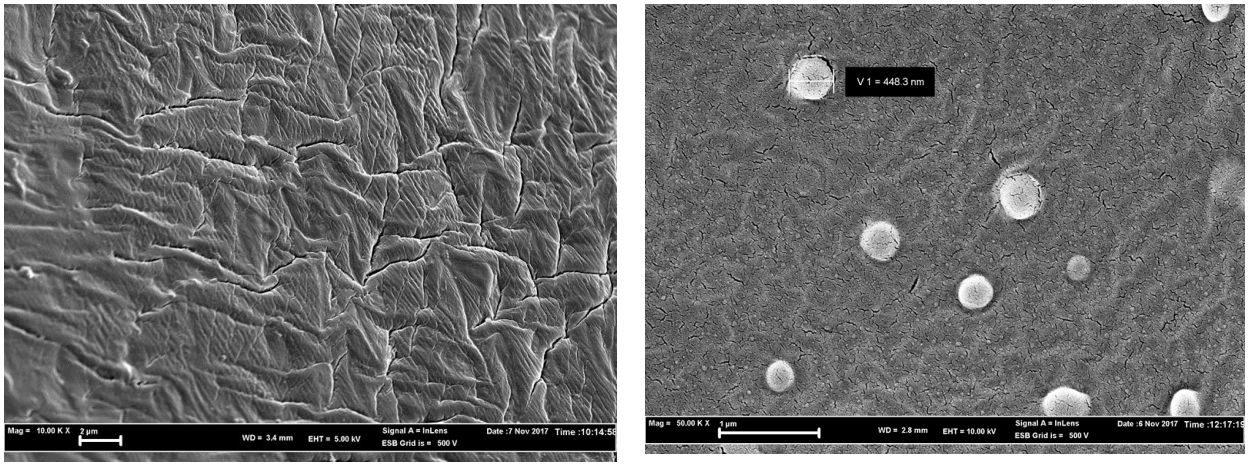

Figure 5. *SEM images of (a) p(Gelatin-co-DMAAm)/CA and (b) MRH.*

3.2. Liquid Chromatography Mass Spectrometer (LC-MS/MS, Q Exactive) analysis

Apparently, purple cabbage includes some compounds, which are act as indicators when medium pH changes. Purple cabbage extracts include quercetin, rutin, coumaric acid, caffeic acid, ferullic acid and naringenin substance, all having antioxidant, antimicrobial activities and copigments and pelargonidin substance with even higher anthocyanin activities [28]. Copigmentation cofactors (copigments) involves the anthocyanin glucosides, phenolic acids, flavonoids and in particular the derivatives of the flavonol and flavone subgroups [29,30]. To determine those substances, purple cabbage was extracted with water and analyzed by a Q Exactive. The detected compounds known for their antioxidant, antimicrobial and anthocyanin activities were as follows; digalloyl-glucose izomer-1, digalloyl-glucose izomer-2, digalloyl-glucose izomer-3, quercetin hexoside-isomer-1, quercetin hexoside-isomer-2,quercetin-3-o-galactoside, quercetin-3-o-glucoside, kaempferol-3-galactoside, kaempferol-3-glucoside, coumaric acid hexoside-isomer-1, coumaric acid hexoside-isomer-2, coumaric acid hexoside-isomer-3, 3-p-coumaroylquinic acid, 4-p-coumaroylquinic acid, caffeic acid, quercetin-3-o-rutinoside, isorhamnetin-3-o-rutinoside, naringenin, rutin, ferullic acid and pelargonidin [28].

3.3. Application of Mechanical Strength Test

The mechanical properties of hydrogels were studied by a Dynamic Mechanical Analysis (DMA) for their elasticity and given in Fig. 6. Decreasing storage modulus values at low temperatures, which are interpreted as molecules moving easily because of having more free volume [32]. It was obtained that p(Gelatin-co-DMAAm)/CA was more flexible and shapeable than the MRH according to decreasing storage modulus values. It was observed that the storage energy of p(Gelatin-co-DMAAm)/CA increased between 40°C and 60°C and molecules move with more difficultly between these temperature values (Fig. 6a). In Fig. 6b, the energy storage of MRH decreased between 30°C and 80°C as the cross-linking property of hydrogel was increased. The loss modulus was observed that MRH has reduced likelihood of losing energy. Because of the poor mechanical strength of gelatin, DMAAm, CA, MBA were added to the polymerization mixture to improve their mechanical strength and the flexibility. MRH possessed stronger mechanical properties than p(Gelatin-co-DMAAm)/CA. It was concluded that PCE worked as a bridge molecule, which interacted the DMAAm by hydrophilic interaction and promotes a better mixing with gelatin [32].

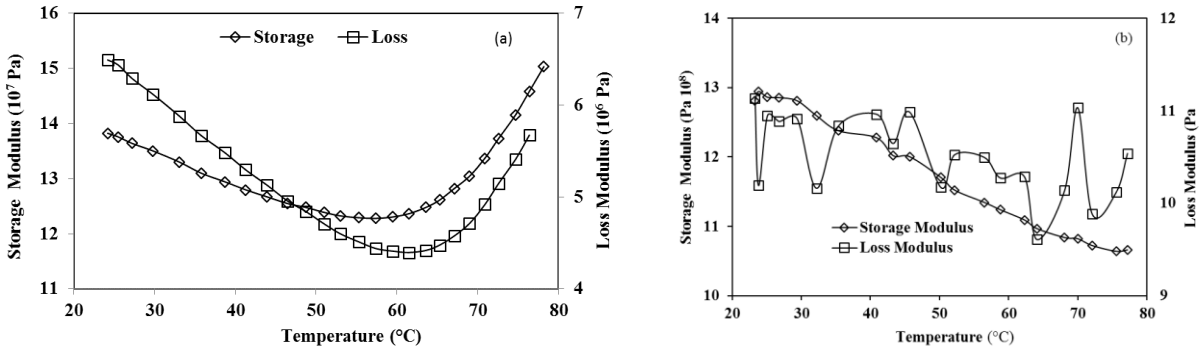

Figure 6. *DMA analysis (a) p(Gelatin-co-DMAAm)/CA and (b) MRH.*

3.4. Determination of Antimicrobial Properties of the Hydrogels

The antimicrobial activity is an important feature that includes the production of the antimicrobial substance and competitive dismissal of pathogens microorganisms. The antimicrobial activity for PCE and MRH were tested against three common bacteria and the obtained data were given in Table 1. MRH was treated with the bacteria for 72 h. and the MIC (Minimal Inhibition Concentration) values were determined as 100 mg mL-1 against Staphylococcus aureus and over 100 mg mL-1 against Escherichia coli and Bacillus cereus. MIB (Minimal Bactericidal Effect) values of PCE, p(Gelatin-co-DMAAm)/CA and MRH were observed over 200 mg mL-1 against Staphylococcus aureus, Escherichia coli and Bacillus cereus. As presented in Table 1, the antimicrobial effects of hydrogel are very well when compared to those of literature [7,33]. Antimicrobial activity of purple cabbage's extract is beneficial for food, agriculture and medicinal applications [33]. The antimicrobial effect of MRH will reduce and/or inhibit the microbial growth in the environment when utilized properly. Many important microbial and chemical deteriorative changes occur with the reactions within the food. In addition to temperature, other environmental factors such as water, color and pH induced deleterious changes in foods that are catalyzed by microbial growth [34,35]. And if microbial growth still occurs in the environment of MRH, the change in pH of the medium will be monitored by color change.

Table 1. *Comparison of the MIC and MIB values of PCE, p(Gelatin-co-DMAAm)/CA and MRH and PCE by diffusion method appeared in the literature (Agar Well Diffusiona (mm), Micro Dilutionb).*

Substance	*Escherichia coli*		*Bacillus cereus*		*Staphylococcus aureus*	
	MIC (mg mL^{-1}- mg g^{-1})	MIB	MIC (mg mL^{-1}- mg g^{-1})	MIB	MIC (mg mL^{-1}- mg g^{-1})	MIB
PCE	100	>200	100	>200	100	>200 [This study]
p(Gelatin-co-DMAAm)/CA	>100	>200	>100	>200	>100	>200 [This study]
MRH	>100	>200	100	>200	100	>200 [This study]
PC	<0.25[b]	------	<0.5[b]	------	<0.25[b]	------
	12.5[a]				14.2[a] [7]	
	14.4[a]		------		16.1[a] [33]	

3.5. Determination of Antioxidant Properties of the Hydrogels

Total antioxidant activities of PCE and MRH were measured by ABTS method and calculated according the following equation;

$$ABTS\ \ Activity\% = \frac{A_0 - A_1}{A_0} \times 100 \quad (8)$$

Troloks equivalent value (TEAC) of PCE, p(Gelatin-co-DMAAm), p(Gelatin-co-DMAAm)/CA and MRH were calculated by Equation 9 and given in Table 2.

$$TEAC = \frac{A}{3.4396} \times f \quad (9)$$

Where, A is slope of measurement, 3.4396 is the slope of standard and f is dilution factor.

Table 2. *Comparison of total phenol content (gallic acid equivalent phenol content) and TEAC (Trolox equivalent antioxidant capacity) values of PCE, p(Gelatin-co-DMAAm), p(Gelatin-co-DMAAm)/CA, MRH and PCE appeared in the literature.*

Substance	Antioxidant	
	Total phenol (mg g^{-1})	TEAC (µmol g^{-1})
PCE	3020	36 [This work]
p(Gelatin-co-DMAAm)	93	----- [This work]
p(Gelatin-co-DMAAm)/CA	310	1 [This work]
MRH	1297	16 [This work]
Brassica oleraceae L. var. acephala DC	0.0013	----- [36]
Brassica oleraceae	1.91	----- [37]
Brassica oleraceae	1.71	15 [38]

Total phenol amount of PCE and MRH were calculated using Folin-Ciocalteu method at 760 nm wavelength and inhibition % from the following equation;

$$Absorbance_{(760nm)} = 0.009[Gallic\ acid\ ] + 0.1034 \quad (10)$$

Gallic acid equivalent value of PCE, p(Gelatin-co-DMAAm), p(Gelatin-co-DMAAm)/CA and MRH were calculated as displayed in Table 2. It is indicated that total antioxidant activity of PCE and hydrogels are very well when compared to those of literature [36,38]. A significant proportion of the antioxidant activity originates from phenolic substances in extract and hydrogel structures were analyzed from Q Exactive analysis. Therefore, the antioxidant substance releasing of MRH minimize the negative effects of free radicals.

3.6. Determination of Anthocyanin Properties of the Hydrogels

As shown in Table 3, total anthocyanin activities of PCE and MRH were determined for cyaniding-3-glucoside, pelergonidine-3-glucoside and malvidin-3-glucoside. It is indicated that total anthocyanin activities of PCE and hydrogels are very promising when compared to those of literature [12,39,40]. There are numerous physical and chemical factors, which can have a negative impact on the stability of anthocyanin, the most important of which are increases or decreases in the temperature, light, oxygen concentration and pH, along with presence or absence of ascorbic acid and metal ions.

Table 3. *Comparison of anthocyanin values of PCE, MRH and Brassica oleraceae appeared in the literature.*

Substance	Anthocyanin (mg mL^{-1}- mg g^{-1})		
	Malvidin-3-glucoside	Cyanidin-3-glucoside	Pelergonidine-3-glucoside
PCE	1.9	6.67 [This study]	6.7
MRH	1.1	3.6	1.2
Brassica oleraceae	---	0.7 [39]	---
Brassica oleraceae	---	1.14 [40]	---
Brassica oleraceae	---	0.76 [19]	---

3.7. Determination of Colorimetric Properties of the Hydrogels.

The colorimetric interpretation of copigmentation based on the CIELab color diagram has demonstrated to be practical interest because both quantitative and qualitative color changes can be better understood. It has been demonstrated that pH, copigment structure and concentration have significant influences on the copigmentation process, which induced different absolute and relative color changes in anthocyanin solutions [41,42]. Table 4 represents the chromatic characteristics of MRH according to CIELab color diagram [37,38]. Each color has its own distinct appearance, based on three elements: hue (a), chroma (b) and value (lightness) (L) [8,9]. The color change of MRH was measured by immersing that into water for 5 min. in which pH values ranging from 1 to 12. A visible color change was detected instantly after contact of MRH and water. The colorimetric parameters ΔL^* Δa^* Δb^* for MRH were calculated by Equation 6 while pH varying from 1 to 12. ΔE^* was calculated to be 134.81. It is reported that about 3-unit change in ΔE^* can be easily detected by an average human eye [42]. According to the method, a* value of -12.83 indicates greener or less red while b*value of 21.85 indicates yellow or less blue. As clearly indicated in Table 4, when pH varying from 1 to 12, ΔL^*, ΔC^* and ΔH^* values calculated to be -88.88, 101.38 and 1.07 respectively. It means that MRH at pH 1 is lighter than MRH at pH 12. PCE was utilized by Chen and Gu, as absorption-type pH sensors to determine purple cabbage pigmentation in sol-gel film [12]. Walkowiak-Tomczak and Czapski, observed the color change in red cabbage extract by varying pH [25]. It was concluded that MRH easily responded pH changes caused by chemical and/or microbiological activities in the media.

Table 4. *Color Parameters (CIELab) L*, a*, b* measured for MRH in different pH solutions.*

pH intervals	L*	a*	b*	ΔE	ΔC	ΔH
1-2	67.03	-12.83	21.85	71.66	25.33	-1.04
2-3	3.89	13.60	4.69	14.90	14.38	0.33
3-4	18.16	5.43	-6.86	20.16	8.75	-0.90
4-5	-56.59	-3.32	-13.68	58.31	14.08	1.33
5-6	-18.97	0.11	7.55	20.41	7.55	1.56
6-7	-0.76	0.17	0.12	0.79	0.21	0.63
7-8	-2.41	0.61	-8.00	8.37	8.02	-1.49
8-9	15.76	-0.78	5.21	16.61	5.26	-1.42
9-10	-14.22	1.14	-1.16	14.31	1.63	-0.79
10-11	5.69	0.76	-3.94	6.96	4.01	-1.38
11-12	71.29	0.69	13.28	72.52	13.30	1.52
1-12	-88.88	-48.76	-88.86	134.81	101.36	1.07

3.8. Utilization of MRH for Real Samples.

It is difficult to verify pH changes and inhibition effect on microorganisms existing in a food. The MRH was applied to various foods such as chickens and dairy products, which are frequently consumed and known as perishable foods [43,44]. Fig. 7a shows the rate of change in color of MRH exposed to spoiling whole milk at room temperature. Color change of MRH was similar in spoiled milk containing Staphylococcus aureus, Escherichia coli and Bacillus cereus. Prior to the first 8 h, no color change was detected visibly. Thereafter, the color of MRH was steadily changed from red to green (8–24 h). However, after 24 h more intense color change was observed visibly allowing a better visualization of the occurrence of spoilage.

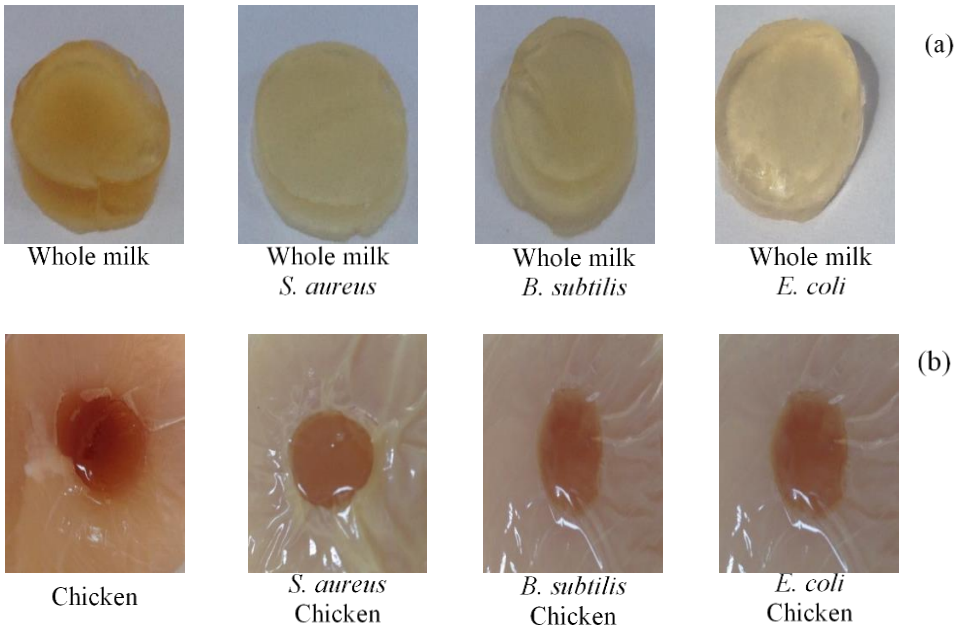

Figure 6. *MRH color response in contact with (a) Whole milk, Whole milk S. aureus, Whole milk B. Subtilis and Whole milk E. coli and (b) Chicken, Chicken S. aureus, Chicken B. Subtilis and Chicken E. coli at 20 ºC.*

When whole milk reaches to temperature above of 4-7ºC, it begins to decompose and the medium pH changes. The pH change in whole milk with microbial growth was monitored at room

temperature and the pH of whole milk changed from 6.81 to 4.8. (48 h). Many kinds of factors such as microbial contamination and subsequent accumulation of lactic acid due to microbial metabolism can cause to a decrease of pH of milk [43,44]. Thus, whole milk spoilage can be detected and monitored through a colorimetric monitoring system as in the MRH developed in the present work. Similar results were obtained in the whole milk treated with Staphylococcus aureus, Escherichia coli and Bacillus cereus (Fig. 7a). Color of MRH gradually changed from 10 h up to the 24 h after which no further color change was observed. The colorimetric measurements are given in Table 5, as indicated in literature [11].

Table 5. *Total color change (ΔE) parameters (CIELab) after from upon contact with whole milk and chicken of MRH.*

MRH	ΔE	ΔC	ΔH
Whole milk	570.8	221.29	1.51
Whole milk- *S. aureus*	143.15	135.95	1.38
Whole milk- *B. subtilis*	430.79	138.42	1.43
Whole milk- *E. coli*	408.63	147.14	1.40
Chicken	454.92	273.91	0.62
Chicken- *S. aureus*	141.27	20.75	-0.46
Chicken- *B. subtilis*	127.18	24.37	-1.11
Chicken- *E. coli*	182.81	131.47	1.07

Raw chicken is highly perishable. Under aerobic packaging conditions the shelf life of the refrigerated product is limited by the growth of microorganisms and changed the medium pH [43,44]. Fig. 7b displays the rate of change in color of MRH exposed to spoiling chicken at different temperatures like 4ºC, 10ºC, 20ºC, 30ºC and 40ºC and to different microorganisms like Staphylococcus aureus, Escherichia coli and Bacillus cereus. Prior to the first 8 h, slight color changes were detected by bare eye. The colorimetric measurement values of these results are tabulated in Table 5, as indicated in literature [11].

The board antimicrobials, antioxidants, anthocyanins and the distinguishable color change properties of PCE at different pH contributed to the MRH for whole milk and chicken. Moreover, the MRH should have wide application in kinds of food as meat, vegetable and fruits products. For example, many of microorganisms during spoilage of meat, vegetable and fruits products can be inhibited and the color changed can be recorded. This study results demonstrated that MRH may function as a quality indicator and preservative for various food products.

4. CONCLUSION

MRH, which was synthesized through redox polymerization technique from DMAAm, gelatin, CA and PCE, was a biocompatible polymer, which indicate non-toxic components and safe indicators for food coverage. MRH has a high potential to be used to increase the lifetime of foods on the markets. In the present study, developed MRH has excellent spectroscopic and physicochemical properties to be utilized as smart food packaging while it rapidly responds pH changes in the environment simultaneously reflect its color in a wide spectrum from green to red. It provides a cheap and simple way for directly detected if a food would face any physical and chemical decomposition and spoiled. MRH was tested on chicken, whole milk against three

microorganisms, which are Staphylococcus aureus, Escherichia coli and Bacillus cereus results were promising. It is claimed that MRH can be very effective in terms of anthocyanin, antimicrobial and antioxidant properties and safe as food packaging materials.

REFERENCES

[1]. De Jong AR, Boumans H, Slaghek T, Van Veen J, Rijk R, Van Zandvoort M. Active and intelligent packaging for food: Is it the future? *Food Additives and Contaminants* 22 (2005);975-979.

[2]. Yam KL, Takhistov PT, Miltz J. Intelligent packaging: concepts and applications. *Journal of Food Science*; 70, (2005), R1-10.

[3]. Marsh K, Bugusu B. Food packaging—roles, materials and environmental issues. *Journal of Food Science*; 72 (2007), 39-55.

[4]. Robertson GL. *Food Packaging and Shelf Life*. New York, CRC Press, (2010).

[5]. Bot A, van Amerongen IA, Groot RD, Hoekstra NL, Agterof WG. Large deformation rheology of gelatin gels. *Polymer Gels and Networks*; 4, (1996), 189-227.

[6]. Ghanbarzadeh B, Almasi H, Entezami AA. Entezami. Improving the barrier and mechanical properties of corn starch-based edible films: Effect of citric acid and carboxymethyl cellulose. *Industrial Crops and Products*; 33, (2011), 229-235.

[7]. Xiao C, Huimin Z, Chen Q. Study on antibacterial activity of purple cabbage extract. *Journal of Food Engineering and Technology*; 4, (2015), 13-16.

[8]. Heredia FJ, Francia-Aricha EM, Rivas-Gonzalo JC, Vicario IM, Santos-Buelga C. Chromatic characterization of anthocyanins from red grapes—I, pH effect. *Food Chemistry*; 63, (1998), 491-498.

[9]. Bobelyn E, Hertog ML, Nicolaï BM. Applicability of an enzymatic time temperature integrator as a quality indicator for mushrooms in the distribution chain. *Postharvest Biology and Technology*; 42, (2006), 104-114.

[10]. Abou-Arab AA, Abu-Salem FM, Abou-Arab EA. Physico-chemical properties of natural pigments (anthocyanin) extracted from *Roselle calyces* (*Hibiscus subdariffa*). *Journal of American Science*; 7, (2011), 445-456.

[11]. Hurtado NH, Morales AL, González-Miret ML, Escudero-Gilete ML, Heredia FJ. Color, pH stability and antioxidant activity of anthocyanin rutinosides isolated from tamarillo fruit (*Solanum betaceum Cav.). Food Chemistry*; 117, (2009), 88-93.

[12]. Giusti MM, Wrolstad RE. Characterization and measurement of anthocyanins by UV-visible spectroscopy, in R.E. Wrolstad (Eds) Current protocols in food analytical chemistry. *Current Protocols in Food Analytical Chemistry* New York, John Wiley, (2001), F1.2.1-F1.2.13

[13]. Chigurupati N, Saiki L, Gayser C, Dash AK. Evaluation of red cabbage dye as a potential natural color for pharmaceutical use. *International Journal of Pharmaceutics*; 241, (2002), 293-299.

[14]. Zhang Z, Tomlinson MR, Golestanian R, Geoghegan M. The interfacial behaviour of single poly (N, N-dimethylacrylamide) chains as a function of pH. *Nanotechnology*; 19, (2007), 35505-35515.

[15]. Sahiner M, Alpaslan D, Bitlisli BO. Collagen-based hydrogel films as drug-delivery devices with antimicrobial properties. *Polymer Bulletin*; 71, (2014), 3017-3033.

[16]. Sahiner N, Alpaslan D. Metal-ion-containing ionic liquid hydrogels and their application to hydrogen production. *Journal of Applied Polymer Science*; 131, (2014), 40183-84.

[17]. Alpaslan D, Sahiner M, Yuceer Y, Akcali A, Aktas N, Sahiner N. Milk hydrogels as nutrient media and survival rate enhancer under cryogenic conditions for different microorganisms. *Polymer Bulletin*; 12, (2016), 3351-3370.

[18]. I Galaev IY, Mattiasson B. Smart'polymers and what they could do in biotechnology and medicine. *Trends in Biotechnology*; 17, (1999), 335-340.

[19]. Yayintas OT, Alpaslan D, Karagul Yuceer Y, Yilmaz S, Sahiner N. Chemical composition, antimicrobial, antioxidant and anthocyanin activities of mosses (*Cinclidotus fontinaloides (Hedw.) P. Beauv.* and *Palustriella commutata (Hedw.) Ochyra*) gathered from Turkey. *Natural Product Research*, (2017), 1-5.

[20]. Childs RE, Bardsley WG. The steady-state kinetics of peroxidase with 2, 2′-azino di-(3-ethyl-benzthiazoline-6-sulphonic acid) as chromogen. *Biochemical Journal*;145, (1975), 93-103.

[21]. Singleton VL, Rossi JA. Colorimetry of total phenolic with phosphomolybdic-phosphotungstic acid reagents. *American journal of Enology and Viticulture*;19, (1965), 144-158.

[22]. Brouillard R, Delaporte B. Chemistry of anthocyanin pigments, 2. kinetic and thermodynamic study of proton transfer, hydration and tautomeric reactions of malvidin-3-glucoside. *Journal of the American Chemical Society*; 99, (1977), 8461-8468.

[23]. Ahmadiani N, Robbins RJ, Collins TM, Giusti MM. Giusti, Anthocyanins contents, profiles and color characteristics of red cabbage extracts from different cultivars and maturity stages. *Journal of Agricultural and Food Chemistry*; 62, (2014), 7524-7531.

[24]. Wrolstad RE, Durst RW, Lee J. Tracking color and pigment changes in anthocyanin products. *Trends in Food Science Technology*; 16, (2005), 423-428.

[25]. Torskangerpoll K, Andersen ØM. Color stability of anthocyanins in aqueous solutions at various pH values. *Food Chemistry*; 89, (2005), 427-440.

[26]. Walkowiak-Tomczak D, Czapski J. Color changes of a preparation from red cabbage during storage in a model system. *Food Chemistry*; 104, (2007), 709-714.

[27]. Lee KY, Rowley JA, Eiselt P, Moy EM, Bouhadir KH, Mooney DJ. Controlling mechanical and swelling properties of alginate hydrogels independently by cross-linker type and cross-linking density. *Macromolecules* ; 33, (2000), 4291-4294.

[28]. Caria G, Alzari V, Monticelli O, Nuvoli D, Kenny JM, Mariani A. Poly (N, N-dimethyl acrylamide) hydrogels obtained by frontal polymerization. *Journal of Polymer Science Part A: Polymer Chemistry* ; 47, (2009), 1422-1428.

[29]. Bylka W, Matlawska I. Pilewski NA. Natural flavonoids as antimicrobial agents. *Journal of the American Nutraceutical Association*; 7, (2004), 24-31.

[30]. Boulton R. The copigmentation of anthocyanins and its role in the color of red wine: a critical review. *American Journal of Enology and Viticulture* ; 52, (2001), 67-87.

[31]. Baranac JM, Petranović NA, Dimitrić-Marković JM. Spectrophotometric study of anthocyanin copigmentation reactions. *Journal of Agricultural and Food Chemistry* ; 44, (1996), 1333-1336

[32]. Menard KP. *Dynamic mechanical analysis: a practical introduction*, second ed., CRC press, New York, (2008).

[33]. Ayaz FA, Hayırlıoglu-Ayaz S, Alpay-Karaoglu S, Grúz J, Valentová K, Ulrichová J, Strnad M. Phenolic acid contents of kale (*Brassica oleraceae L. var. acephala* DC.) extracts and their antioxidant and antibacterial activities. *Food Chemistry*; 107, (2008), 19-25

[34]. Kilcast D, Subramaniam P. (Eds.*). The stability and shelf-life of food*. Cambridge CRC press; (2000), 1-22.

[35]. in't Veld JHH. Microbial and biochemical spoilage of foods: an overview. *International Journal of Food Microbiology*; 33, (1996), 1-18.

[36]. Nica D, Gergen I, Alda Liana MA, Alda S, Gogoasa I, Moigradean Diana BAB, Bordean DM. Comparative assessment of mineral content and antioxidant properties of some cabbage varieties available on Romanian market. *Journal of Horticulture, Forestry and Biotechnology*; 16, (2012), 18-21.

[37]. Sosnowska D, Redzynia M, Anders B. Antioxidant capacity and content of *Brassica oleracea* dietary antioxidants. *International Journal of Food Science Technology*; 41, (2006), 49-50.

[38]. Scalzo RL, Genna A, Branca F, Chedin M, Chassaigne H. Anthocyanin composition of cauliflower (*Brassica oleracea L. var. botrytis*) and cabbage (*B. oleracea L. var. capitata*) and its stability in relation to thermal treatments. *Food Chemistry*; 107, (2008), 136-144.

[39]. Volden J, Borge GIA, Bengtsson GB, Hansen M, Thygesen IE, Wicklund T. Effect of thermal treatment on glucosinolates and antioxidant-related parameters in red cabbage (*Brassica oleracea L. ssp. capitata f. rubra*). *Food Chemistry*; 109, (2008), 595-605.

[40]. Chen X, Gu Z. Absorption-type optical pH sensitive film based on immobilized purple cabbage pigment. *Sensors and Actuators B: Chemical*; 178, (2013), 207-211.

[41]. Martínez JA, Melgosa M, Pérez MM, Hita E, Negueruela AL. Note. Visual and instrumental color evaluation in red wines. *Revista de Agaroquimica y Tecnologia de Alimentos*; 7, (2001), 439-444.

[42]. Gordillo B, Rodríguez-Pulido FJ, Escudero-Gilete ML, González-Miret ML, Heredia FJ. Impact of adding white pomace to red grapes on the phenolic composition and color stability of Syrah wines from a warm climate. *Journal of Agricultural and Food Chemistry*; 62, (2014), 2663-2671.

[43]. Lee OH, Lee BY. Antioxidant and antimicrobial activities of individual and combined phenolics in *Olea europaea* leaf extract. *Bioresource Technology*; 101, (2010) 3751-3754.

[44]. Yoshida CM, Maciel VBV, Mendonça MED, Franco TT. Chitosan biobased and intelligent films: Monitoring pH variations. *LWT-Food Science and Technology*;55, (2014), 83-89.

MANAS Journal of Engineering
ISSN 1694-7398 | e-ISSN 1694-7398

Volume 6 (Issue 2) (2018) Pages 143-163

The concept of Hukuhara derivative and Aumann integral for intuitionistic fuzzy number valued functions

Ömer Akın[*1,2], Selami Bayeğ[1]

[1] Department of Mathematics, TOBB University of Economics and Technology, Ankara, Turkey
[2] Kyrgyz – Turkish Manas University, Faculty of Science, Department of Applied Mathematics and Informatics, Bishkek, Kyrgyzstan, omerakin@etu.edu.tr

Received: 14.10.2018; Accepted: 13.12.2018

Abstract: *In this paper we have rstly dened a metric based on the Hausdor metric in intuitionistic fuzzy environment and studied its properties. Then we have proved that the metric space of intuitionistic fuzzy number valued functions is complete under this metric. Besides, we have studied the concept of Aumann integral for intuitionistic fuzzy number valued functions in terms of α and β cuts. Finally, we have given the relation between the Hukuhara derivative and Aumann integral for intuitionistic fuzzy valued functions by using the fundamental theorem of calculus.*

Keywords: *Intuitionistic fuzzy sets, intuitionistic fuzzy number valued functions, hukuhara derivative, Aumann integral, intuitionistic Hausdor metric.*

1. INTRODUCTION

In science and technology, vagueness or ambiguity is an inevitable phenomena. Hence to understand and interpret the models containing elements of uncertainty, probabilistic (stochastic, random) or possibilistic approaches are developed. Generally, the possibilistic approaches are based on fuzzy set theory.

Fuzzy set theory was firstly introduced by L. A. Zadeh in 1965 [1]. In fuzzy sets, every element in the set is accompanied with a function $\mu : X \to [0, 1]$, called membership function. The membership function may have uncertainty in some applications because of the subjectivity of the expert or the missing information in the model, as well. Hence some extensions of fuzzy set theory were proposed [2-4]. One of these extensions is Atanassov's intuitionistic fuzzy set (IFS) theory [2].

In 1986, Atanassov [2] introduced the concept of intuitionistic fuzzy sets and carried out rigorous researches to develop the theory [5]. In this set concept, he introduced a new degree $\nu : X \to [0, 1]$, called non-membership function, such that the sum $\mu+\nu$ is less than or equal to 1. Hence the difference $1-(\mu+\nu)$ is regarded as degree of hesitation. Since intuitionistic fuzzy set theory contains membership function, non-membership function and the degree of hesitation, it can be regarded as a tool which is more flexible and closer to human reasoning in handling uncertainty due to imprecise knowledge or data.

Intuitionistic fuzzy set and fuzzy set theory have flourishing interesting applications in different fields of science and engineering such as population dynamics [6], decision-making problems [7, 8] image processing and pattern recognition [9], medicine [10, 11], fault analysis [12]. More detailed information about applicability of fuzzy sets and intuitionistic fuzzy sets can be found in [13-21].

The space of compact and convex sets has a linear structure with respect to Minkowski sum and scalar multiplication [22]. This linear structure is that of a cone rather than a vector space since the inverse element of a set with respect to Minkowski sum does not always exists. That is, if $A = \{a\}$ is not a singleton set, the Minkowski sum of A and $-A$ is not always the identity element $\{0\}$ i.e., $A + (-1)A \neq \{0\}$ [22]. This is a drawback not only in theory of compact and convex sets but also in theory of fuzzy sets and IFS. That is why Hukuhara tried to handle the inverse element problem. He defined a new difference called Hukuhara difference (H-difference) for compact and convex sets [23]. Later Hukuhara difference of fuzzy sets and Hukuhara derivative (H-derivative) of fuzzy number valued functions were introduced and studied [24–26].

The concept of fuzzy integral was firstly defined by Sugeno [27]. Later Ralescu and Adams defined the fuzzy integral of positive measurable functions [28]. They studied some properties such as monotone convergence theorem and Fatou's lemma. Later Dubois and Parade generalized the Riemann integral over compact and convex sets to fuzzy valued functions [29]. This approach is mainly related with the concept of Aumann integral. Aumann integral is defined for set valued functions by Aumann [30]. Since a fuzzy-valued function is essentially a family of set-valued functions, fuzzy Aumann integration concept is employed in the concept of fuzzy integral and fuzzy differential equations [22, 25].

In this paper we have firstly defined a new metric in intuitionistic fuzzy environment and study its properties. Then we have shown that the metric space of fuzzy number valued functions is complete under this metric. Moreover, we have studied the concepts of the Aumann integration for intuitionistic fuzzy number valued functions in terms of α and β cuts. And we have proved the relation between Hukuhara derivative and Aumann integral for intuitionistic fuzzy valued functions by using the fundamental theorem of calculus.

This paper is organized as follows. In Section 2 some preliminaries are given. In Section 3 we introduce a metric on the set of intuitionistic fuzzy numbers and study its properties. In Section 4, we study some fundamental theorems on Aumann integration and Hukuhara differentiability for intuitionistic fuzzy valued functions. Finally we give summary and conclusions in Section 5.

2. PRELIMINARIES

Definition 2.0.1 *[5] Let $\mu_A, \nu_A : \mathbb{R}^n \to [0,1]$ be two functions such that for each $x \in \mathbb{R}^n$, $0 \leq \mu_A(x) + \nu_A(x) \leq 1$ holds. The set*

$$\tilde{A}^i = \{(x, \mu_A(x), \nu_A(x)) : x \in \mathbb{R}^n; \mu_A, \nu_A : \mathbb{R}^n \to [0,1]\}$$

is called an intuitionistic fuzzy set in $\mathbb{R}^n$. Here μ_A and ν_A are called membership and non-membership functions, respectively.

We will denote set of all intuitionistic fuzzy sets in $\mathbb{R}^n$ by $IF(\mathbb{R}^n)$.

Definition 2.0.2 *[5] Let $\tilde{A}^i \in IF(\mathbb{R}^n)$. The α-cut of $\tilde{A}^i$ is defined as follows:*

For $\alpha \in (0,1]$

$$A(\alpha) = \{x \in \mathbb{R}^n : \mu_A(x) \geq \alpha\},$$

and for $\alpha = 0$

$$A(0) = cl\left(\bigcup_{\alpha \in (0,1]} A(\alpha)\right).$$

Definition 2.0.3 *[5] Let $\tilde{A}^i \in IF(\mathbb{R}^n)$. The β-cut of $\tilde{A}^i$ is defined as follows:*

For $\beta \in [0,1)$

$$A^*(\beta) = \{x \in \mathbb{R}^n : \nu_A(x) \leq \beta\},$$

and for $\beta = 1$

$$A^*(1) = cl\left(\bigcup_{\beta \in [0,1)} A^*(\beta)\right).$$

Definition 2.0.4 *[5] Let $\tilde{A}^i \in IF(\mathbb{R}^n)$. For α and $\beta \in [0,1]$ with $0 \leq \alpha + \beta \leq 1$, the set*

$$A(\alpha, \beta) = \{x \in \mathbb{R}^n : \mu_A(x) \geq \alpha, \nu_A(x) \leq \beta\}$$

is called (α, β)-cut of $\tilde{A}^i$

Theorem 2.0.1 *[5] Let $\tilde{A}^i \in IF(\mathbb{R}^n)$. Then*

$$A(\alpha, \beta) = A(\alpha) \cap A^*(\beta)$$

holds.

We will denote the set of all intuitionistic fuzzy numbers in $\mathbb{R}^n$ by $IF_N(\mathbb{R}^n)$.

Definition 2.0.5 *[31] Let X be a topological space. Let f be a function from X to $\mathbb{R} \cup \{-\infty, \infty\}$.*

1. f is called an upper semi-continuous function if for all $k \in \mathbb{R}\{x \in X : f(x) < k\}$ is an open set.
2. f is called an lower semi-continuous function if for all $k \in \mathbb{R}\{x \in X : f(x) > k\}$ is an open set.

Definition 2.0.6 *[32] Let f be a function defined on a convex subset K of $\mathbb{R}^n$.*

1. f is called a quasi-concave function on K if for all $x, y \in K$ and $t \in [0, 1]$,

   $$f(tx + (1 - ty)) \geq \min\{f(x), f(y)\}$$

   holds.
2. f is called a quasi-convex function on K if for all x, $y \in K$ and $t \in [0, 1]$,

   $$f(tx + (1 - ty)) \leq \max\{f(x), f(y)\}$$

   holds.

Definition 2.0.7 *An intuitionistic fuzzy set $\tilde{A}^i \in IF(\mathbb{R}^n)$ satisfying the following properties is called an intuitionistic fuzzy number in $\mathbb{R}^n$:*

1. $\tilde{A}^i$ is a normal set, i.e., $A(1) \neq \varnothing$ and $A^*(0) \neq \varnothing$.
2. $A(0)$ and $A^*(1)$ are bounded sets in $\mathbb{R}^n$.
3. $\mu_A : \mathbb{R}^n \to [0, 1]$ is an upper semi-continuous function; i.e., $\forall k \in \mathbb{R}^+ \cup \{0\}$, $\{x \in A : \mu_A(x) < k\}$ is an open set.
4. $\nu_A : \mathbb{R}^n \to [0, 1]$ is a lower semi-continuous function; i.e., $\forall k \in \mathbb{R}\{x \in A : \nu_A(x) > k\}$ is an open set.
5. The membership function μ_A is quasi-concave; i.e., $\forall \lambda \in [0, 1], \forall x,\ y \in \mathbb{R}^n$

   $$\mu_A(\lambda x + (1 - \lambda)y) \geq \min(\mu_A(x), \mu_A(y))$$

6. The non-membership function ν_A is quasi-convex; i.e.,$\forall\lambda \in [0,1], \forall x,\ y \in \mathbb{R}^n$

$$\nu_A(\lambda x + (1-\lambda)y) \leq \max(\nu_A(x), \nu_A(y)); \forall\lambda \in [0,1],$$

Definition 2.0.8 *[22] Let $x \in \mathbb{R}^n$ and A be a non-empty subset of $\mathbb{R}^n$. The distance from x to A is determined by*

$$d(x, A) = \inf\{\|x - a\| : a \in A\}$$

Definition 2.0.9 *[22] Let A and B be non-empty subsets of $\mathbb{R}^n$. Let S_1^n denote the closed unit ball in $\mathbb{R}^n$.*

1. The Hausdorff separation of A to B is defined by

$$\rho(A, B) = \sup\{d(a, B) : a \in A\}$$

or, equivalently,

$$\rho(A, B) = \inf\{r > 0 : A \subseteq B + rS_1^n\}$$

2. The Hausdorff separation of A to B is defined by

$$\rho(B, A) = \sup\{d(b, A) : b \in B\}$$

or, equivalently,

$$\rho(B, A) = \inf\{r > 0 : B \subseteq A + rS_1^n\}$$

Note that $\rho(A, B) \neq \rho(B, A)$ in general.

Definition 2.0.10 *[22] Let A and B be non-empty subsets of $\mathbb{R}^n$. The Hausdorff distance of A and B is defined as*

$$d_H(A, B) = \max\{\rho(A, B), \rho(B, A)\}$$

Note that the Hausdorff distance function is a metric on the family of non-empty compact subsets of $\mathbb{R}^n$.

Theorem 2.0.2 *[22] Let A, B, C and D be compact sets in $\mathbb{R}^n$ and $\lambda \in \mathbb{R}$. Then the followings hold:*

1.

$$d_H(A + C, B + C) = d_H(A, B)$$

2.

$$d_H(\lambda A, \lambda B) = |\lambda|\, d_H(A, B)$$

3.

$$d_H(A + B, C + D) \leq d_H(A, C) + d_H(B, D)$$

We will denote set of all compact and convex subsets of $\mathbb{R}^n$ by $K_C(\mathbb{R}^n)$.

Theorem 2.0.3 *[22]$(K_C(\mathbb{R}^n), d_H)$ is a complete metric space.*

Theorem 2.0.4 *Let $\{C_\beta : \beta \in [0,1]\}$ be a family of subsets of $\mathbb{R}^n$ satisfying the followings:*

1. C_β is a non-empty compact and convex subset of $\mathbb{R}^n$
2. If $0 \leq \beta_1 \leq \beta_2 \leq 1$ then $C_{\beta_1} \subseteq C_{\beta_2}$
3. If (β_n) is a non-increasing converging sequence to β then $C_\beta = \bigcap_{n=1}^{\infty} C_{\beta_n}$

Then $\{\beta \in [0,1] : x \in C_\beta\}$ is a closed and bounded interval.

Proof For $x \in C_1$, define $I_x = \{\beta \in [0,1] : x \in C_\beta\}$. Since I_x is bounded, its infimum exists, say $\beta^* = \inf I_x$. If we show $I_x = [\beta^*, 1]$ then the proof is done.

If $\beta^* = 1$ then $I_x = \{1\}$ is and there is nothing to prove..

Assume that $\beta^* < 1$ and $\beta \in (\beta^*, 1)$. By the definition of infimum there exists a real number $\beta_1 \in I_x$ such that $\beta^* < \beta_1 \leq \beta$. Hence by (2) we can write that $C_{\beta_1} \subseteq C_\beta$. Since $\beta_1 \in I_x$ we get $x \in C_{\beta_1} \Rightarrow x \in C_\beta \Rightarrow \beta \in I_x$. And this means that every β larger than β^* is an element of I_x. Hence $(\beta^*, 1] \subseteq I_x$.

Assume (β_n) is a non-increasing sequence converging to β^*. Since $\beta^* \leq \beta_n$ and $C_{\beta^*} \subseteq C_{\beta_n}$ we have

$$C_{\beta^*} = \bigcap_{n=1}^{\infty} C_{\beta_n}$$

And since $(\beta_n) \subset I_x$, for every $n \in \mathbb{N}$, $x \in C_{\beta_n} \Rightarrow x \in C_{\beta^*} \Rightarrow \beta^* \in I_x$. Hence $[\beta^*, 1] \subseteq I_x$.

Now let us show that $I_x \subseteq [\beta^*, 1]$.

Let $\beta \in I_x$. Then $\beta^* \leq \beta \Rightarrow \beta \in [\beta^*, 1] \Rightarrow I_x \subseteq [\beta^*, 1]$.

Therefore we obtain that $I_x = [\beta^*, 1]$. Namely, I_x is a closed and bounded interval. □

Theorem 2.0.5 *[34] Let $\tilde{A}^i \in IF_N(\mathbb{R}^n)$ and $\alpha, \beta \in [0,1]$ such that its α and β cuts given by $A(\alpha) = \{x \in \mathbb{R}^n : \mu_A(x) \geq \alpha\}$ and $A^*(\beta) = \{x \in \mathbb{R}^n : \nu_A(x) \leq \beta\}$. Then the followings hold:*

1. For every $\alpha \in [0,1]$, $A(\alpha)$ are non-empty compact and convex sets in $\mathbb{R}^n$.
2. If $0 \leq \alpha_1 \leq \alpha_2 \leq 1$ then $A(\alpha_2) \subseteq A(\alpha_1)$.

3. If (α_n) is a non-decreasing sequence in $[0,1]$ converging to α then

$$\bigcap_{n=1}^{\infty} A(\alpha_n) = A(\alpha).$$

4. If (α_n) is a non-increasing sequence in $[0,1]$ converging to 0 then

$$cl\left(\bigcup_{n=1}^{\infty} A(\alpha_n)\right) = A(0).$$

5. For every $\beta \in [0,1]$, $A^*(\beta)$ are non-empty compact and convex sets in $\mathbb{R}^n$.

6. If $0 \leq \beta_1 \leq \beta_2 \leq 1$ then $A^*(\beta_1) \subseteq A^*(\beta_2)$.

7. If (β_n) is a non-increasing sequence in $[0,1]$ converging to β then

$$\bigcap_{n=1}^{\infty} A^*(\beta_n) = A^*(\beta).$$

8. If (β_n) is a non-decreasing sequence in $[0,1]$ converging to 1 then

$$cl\left(\bigcup_{n=1}^{\infty} A^*(\beta_n)\right) = A^*(1).$$

Theorem 2.0.6 *[33] Let $\{C_\alpha \subseteq \mathbb{R}^n : \alpha \in [0,1]\}$ be a family of sets in $\mathbb{R}^n$ satisfying (1.)-(4.) in Theorem 2.0.5 and $\{C_\beta \subseteq \mathbb{R}^n : \beta \in [0,1]\}$ be a family of set in $\mathbb{R}^n$ satisfying (5.)-(8.) in Theorem 2.0.5 Let us define the functions $\mu : \mathbb{R}^n \to [0,1]$ and $\nu : \mathbb{R}^n \to [0,1]$ by*

$$\mu(x) = \begin{cases} \sup\{\alpha \in [0,1] : x \in M_\alpha\}, & x \in C_0 \\ 0, & x \notin C_0 \end{cases}$$

$$\nu(x) = \begin{cases} \inf\{\beta \in [0,1] : x \in M_\beta\}, & x \in C_1 \\ 1, & x \notin C_1 \end{cases}$$

Then there exists an intuitionistic fuzzy number $\tilde{A}^i \in IF_N(\mathbb{R}^n)$ with its α and β cuts $A(\alpha)$ and $A^*(\beta)$ satisfying the followings:

1. For all $\alpha \in [0,1]$, $A(\alpha) = C_\alpha$.

2. For all $\beta \in [0,1]$, $A^*(\beta) = C_\beta$.

Definition 2.0.11 *[22] Let A and B be two nonempty subsets of $\mathbb{R}^n$ and $c \in \mathbb{R}$. The Minkowski addition and scalar multiplication are defined as follows:*

$$\begin{aligned} A + B &= \{a + b : a \in A \text{ and } b \in B\} \\ cA &= \{ca : a \in A\} \end{aligned}$$

Definition 2.0.12 *[33]Let $\tilde{A}^i$, $\tilde{B}^i \in IF_N(\mathbb{R}^n)$ and $c \in \mathbb{R} - \{0\}$. Minkowski addition and scalar multiplication of fuzzy numbers in $IF_N(\mathbb{R}^n)$ is defined level wise as follows:*

$$\begin{aligned} \tilde{A}^i + \tilde{B}^i &= \tilde{C}^i \Leftrightarrow C(\alpha) = A(\alpha) + B(\alpha) \text{ and } C^*(\beta) = A^*(\beta) + B^*(\beta), \\ c(\tilde{A}^i) &= \tilde{D}^i \Leftrightarrow D(\alpha) = cA(\alpha) \text{ and } D^*(\beta) = cA^*(\beta). \end{aligned}$$

Theorem 2.0.7 *[33] $IF_N(\mathbb{R}^n)$ is closed under Minkowski addition and scalar multiplication.*

Definition 2.0.13 *Let $\tilde{A}^i$, $\tilde{B}^i \in IF_N(\mathbb{R}^n)$. The Hukuhara difference of $\tilde{A}^i$ and $\tilde{B}^i$ is $\tilde{C}^i$, if it exists, such that*

$$\tilde{A}^i \ominus_H \tilde{B}^i = \tilde{C}^i \Longleftrightarrow \tilde{A}^i = \tilde{B}^i + \tilde{C}^i$$

Definition 2.0.14 *Let $\tilde{A}^i$, $\tilde{B}^i \in IF_N(\mathbb{R}^n)$. The generalized Hukuhara difference of $\tilde{A}^i$ and $\tilde{B}^i$ is $\tilde{C}^i$, if it exists, such that*

$$\tilde{A}^i \ominus_{gH} \tilde{B}^i = \tilde{C}^i \Longleftrightarrow \tilde{A}^i = \tilde{B}^i + \tilde{C}^i \text{ or } \tilde{B}^i = \tilde{A}^i + (-1)\tilde{C}^i$$

3. AN INTUITIONISTIC FUZZY METRIC AND ITS PROPERTIES

Theorem 3.0.1 *Let $\tilde{A}^i$, $\tilde{B}^i \in IF_N(\mathbb{R}^n)$. Let*

$$\begin{aligned} D_1(\tilde{A}^i, \tilde{B}^i) &= \sup\{d_H(A(\alpha), B(\alpha)) : \alpha \in [0,1]\} \\ D_2(\tilde{A}^i, \tilde{B}^i) &= \sup\{d_H(A(\beta), B(\beta)) : \beta \in [0,1]\} \end{aligned}$$

The function

$$D_\infty(\tilde{A}^i, \tilde{B}^i) = \max\{D_1(\tilde{A}^i, \tilde{B}^i), D_2(\tilde{A}^i, \tilde{B}^i)\}$$

defines a metric on $IF_N(\mathbb{R}^n)$. Hence $(IF_N(\mathbb{R}^n), D)$ is a metric space.

Proof Let us show that the metric axioms are satisfied by D_∞

M1.

$$\begin{aligned} D_\infty(\tilde{A}^i, \tilde{B}^i) &= 0 \Leftrightarrow D_1(\tilde{A}^i, \tilde{B}^i) = 0 \text{ and } D_2(\tilde{A}^i, \tilde{B}^i) = 0 \\ &\Leftrightarrow A(\alpha) = B(\alpha) \text{ and } A^*(\beta) = B^*(\beta) \\ &\Leftrightarrow \tilde{A}^i = \tilde{B}^i \end{aligned}$$

M2.

$$\begin{aligned} D_\infty(\tilde{A}^i, \tilde{B}^i) &= \max\{D_1(\tilde{A}^i, \tilde{B}^i), D_2(\tilde{B}^i, \tilde{A}^i)\} \\ &= \max\{D_1(\tilde{B}^i, \tilde{A}^i), D_2(\tilde{A}^i, \tilde{B}^i)\} \\ &= D_\infty(\tilde{B}^i, \tilde{A}^i) \end{aligned}$$

M3. Let $\tilde{A}^i$, $\tilde{B}^i$ and $\tilde{C}^i \in IF_N$. Since

$$\begin{aligned} D_1(\tilde{A}^i, \tilde{B}^i) &\leq D_1(\tilde{A}^i, \tilde{C}^i) + D_1(\tilde{C}^i, \tilde{B}^i) \\ D_2(\tilde{A}^i, \tilde{B}^i) &\leq D_2(\tilde{A}^i, \tilde{C}^i) + D_2(\tilde{C}^i, \tilde{B}^i) \end{aligned}$$

Then

$$\max\{D_1(\tilde{A}^i, \tilde{B}^i), D_2(\tilde{B}^i, \tilde{A}^i)\} \leq \max\{D_1(\tilde{A}^i, \tilde{C}^i) + D_1(\tilde{C}^i, \tilde{B}^i), D_2(\tilde{A}^i, \tilde{C}^i) + D_2(\tilde{C}^i, \tilde{B}^i)\}$$

Since for any reel numbers a and b

$$\max\{a, b\} = \frac{a + b + |a - b|}{2}$$

holds. So one can easily obtain that

$$\begin{aligned} \max\{D_1(\tilde{A}^i, \tilde{C}^i) + D_1(\tilde{C}^i, \tilde{B}^i), D_2(\tilde{A}^i, \tilde{C}^i) + D_2(\tilde{C}^i, \tilde{B}^i)\} &\leq \max\{D_1(\tilde{A}^i, \tilde{C}^i), D_2(\tilde{A}^i, \tilde{C}^i)\} \\ &+ \max\{D_1(\tilde{C}^i, \tilde{B}^i), D_2(C, B)\} \end{aligned}$$

Hence the triangle inequality

$$D_\infty(\tilde{A}^i, B) \leq D_\infty(\tilde{A}^i, \tilde{C}^i) + D_\infty(\tilde{C}^i, \tilde{B}^i)$$

is satisfied. □

Theorem 3.0.2 *Let $\tilde{A}^i$, $\tilde{B}^i$, $\tilde{C}^i$ and $\tilde{D}^i \in IF_N(\mathbb{R}^n)$ and $\lambda \in \mathbb{R}$. Then the followings hold:*

1.
$$D_\infty(\tilde{A}^i + \tilde{C}^i, \tilde{B}^i + \tilde{C}^i) = D_\infty(\tilde{A}^i, \tilde{B}^i)$$

2.
$$D_\infty(\lambda\tilde{A}^i, \lambda\tilde{B}^i) = |\lambda|\, D_\infty(\tilde{A}^i, \tilde{B}^i)$$

3.
$$D_\infty(\tilde{A}^i + \tilde{B}^i, \tilde{C}^i + \tilde{D}^i) \leq D_\infty(\tilde{A}^i, \tilde{C}^i) + D_\infty(\tilde{B}^i, \tilde{D}^i)$$

Proof

it is easy to see (1.) and (2.) are satisfied. Let us show (3.). By (3.) in Theorem 2.0.2 we have

$$\begin{aligned} D_1(\tilde{A}^i + \tilde{B}^i, \tilde{C}^i + \tilde{D}^i) &\leq D_1(\tilde{A}^i, \tilde{C}^i) + D_1(\tilde{B}^i, \tilde{D}^i) \\ D_2(\tilde{A}^i + \tilde{B}^i, \tilde{C}^i + \tilde{D}^i) &\leq D_2(\tilde{A}^i, \tilde{C}^i) + D_2(\tilde{B}^i, \tilde{D}^i) \end{aligned}$$

Since for any reel numbers a and b

$$\max\{a,b\} = \frac{a+b+|a-b|}{2}$$

holds then we can write that

$$\begin{aligned}\max\{D_1(\tilde{A}^i+\tilde{B}^i,\tilde{C}^i+\tilde{D}^i), D_2(\tilde{A}^i+\tilde{B}^i,\tilde{C}^i+\tilde{D}^i)\} &\leq \max\{D_1(\tilde{A}^i,\tilde{C}^i), D_2(\tilde{A}^i,\tilde{C}^i)\} \\ &+ \max\{D_1(\tilde{B}^i,\tilde{D}^i), D_2(\tilde{B}^i,\tilde{D}^i)\}\end{aligned}$$

Hence

$$D_\infty(\tilde{A}^i+\tilde{B}^i,\tilde{C}^i+\tilde{D}^i) \leq D_\infty(\tilde{A}^i,\tilde{C}^i) + D_\infty(\tilde{B}^i,\tilde{D}^i)$$

holds. □

Theorem 3.0.3 *$(IF_N(\mathbb{R}^n), D_\infty)$ is a complete metric space.*

Proof Let $(\tilde{A}_k^i)$ be a Cauchy sequence in $IF_N(\mathbb{R}^n)$. Let $A_k(\alpha)$ and $A_k^*(\beta)$ be the α and β cuts of $\tilde{A}_k^i$ for each $k \in \mathbb{N}$. Since $(\tilde{A}_k^i)$ is a Cauchy sequence then for each α and $\beta \in [0,1]$, $A_k(\alpha)$ and $A_k^*(\beta)$ are Cauchy sequences in $(K_C(\mathbb{R}^n), d_H)$ as well. Since $(K_C(\mathbb{R}^n), d_H)$ is a complete metric space then there exist $C(\alpha)$ and $C^*(\beta)$ in $K_C(\mathbb{R}^n)$ such that

$$\begin{aligned} d_H(A_k(\alpha), C(\alpha)) &\to 0 \\ d_H(A_k^*(\beta), C^*(\beta)) &\to 0 \end{aligned}$$

If the family of sets $\{A(\alpha) : \alpha \in [0,1]\}$ satisfies (1.)-(4.) in Theorem 2.0.5 and $\{A^*(\beta) : \beta \in [0,1]\}$ satisfies (5.)-(8.) in Theorem 2.0.5 then there exist an intuitionistic fuzzy number $\tilde{A}^i$ such that its α and β cuts are $A(\alpha) = C(\alpha)$ and $A^*(\beta) = C^*(\beta)$ by Theorem 2.0.6. Now let us prove this $\tilde{A}^i$ exists. By [22] $\{A(\alpha) : \alpha \in [0,1]\}$ satisfies (1.)-(4.) in Theorem 2.0.5. So let us show that $\{A^*(\beta) : \beta \in [0,1]\}$ satisfies (5.)-(8.) in Theorem 2.0.5.

5. Since for every $\beta \in [0,1]$, $C^*(\beta) \in K_C(\mathbb{R}^n)$, $C^*(\beta)$ is a compact and convex set.

6. Let $0 \leq \beta_1 \leq \beta_2 \leq 1$.

$$\rho(C^*(\beta_1), C^*(\beta_2)) \leq d_H^*(C^*(\beta_1), A_k^*(\beta_1)) + \rho(A_k^*(\beta_1), A_k^*(\beta_2)) + \rho(A_k^*(\beta_2), C^*(\beta_2))$$

Since $\beta_1 \leq \beta_2$ we can write that $A_k^*(\beta_1) \subseteq A_k^*(\beta_2)$. Hence the Hausdorff separation $d_H^*(A_k^*(\beta_1), A_k^*(\beta_2)) = 0$

And as $k \to \infty$ we have $\rho(C^*(\beta_1), A_k^*(\beta_1)) \to 0$ and $d_H^*(A_k^*(\beta_2), C^*(\beta_2)) \to 0$

So the Hausdorff separation $\rho(C^*(\beta_1), C^*(\beta_2)) = 0$ and this implies that $C^*(\beta_1) \subseteq C^*(\beta_2)$.

7. Let (β_n) be a non-increasing sequence converging to β in $[0,1]$. So by the result above $C^*(\beta) \subseteq C^*(\beta_n)$ for $n = 1, 2, 3, ...$, so

$$C^*(\beta) \subseteq \bigcap_{n=1}^{\infty} C^*(\beta_n)$$

Let $x \in \cap_{n=1}^{\infty} C^*(\beta_n)$ then for every $n \in \mathbb{N}$, $x \in C^*(\beta_n)$. Since $\{x\} \subseteq C^*(\beta_n)$, we can write that

$$\begin{aligned} \rho(\{x\}, C^*(\beta)) &\leq d_H^*(C^*(\beta_n), C^*(\beta)) \\ &\leq \rho(C^*(\beta_n), A_k^*(\beta_n)) + \rho(A_k^*(\beta_n), A_k^*(\beta)) + \rho(A_k^*(\beta), C^*(\beta)) \end{aligned}$$

Since $d_H(A_k^*(\beta), C^*(\beta)) \to 0$ we have $\rho(C^*(\beta_n), A_k^*(\beta_n)) \to 0$ and $\rho(A_k^*(\beta), C^*(\beta)) \to 0$. As $n \to \infty$ we have $\rho(A_k^*(\beta_n), A_k^*(\beta)) \to 0$. Thus $x \in C^*(\beta)$. So $\bigcap C^*(\beta_n) \subseteq C^*(\beta)$.

As a result

$$C^*(\beta) = \bigcap_{n=1}^{\infty} C^*(\beta_n)$$

8. Let (β_n) be a non-increasing sequence converging to 1 in $[0,1]$. Since for any $n \in \mathbb{N}$, $C^*(\beta_n) \subseteq C^*(1)$ then we can obtain that

$$kap\left(\bigcup_{n=1}^{\infty} C^*(\beta_n)\right) \subseteq C^*(1).$$

Let $x \in C^*(1)$. Then by the Hausdorff separation we can write that

$$\rho(\{x\}, C^*(\beta_n)) \leq \rho(\{x\}, C^*(1)) + \rho(C^*(1), C^*(\beta_n)).$$

Since $\{x\} \subseteq C^*(1)$ we obtain that $\rho(\{x\}, C^*(1)) = 0$. As $n \to \infty$,

$$\rho(C^*(1), C^*(\beta_n)) \to 0$$

is satisfied. Hence we obtain that $\rho(\{x\}, C^*(\beta_n)) \to 0$ and $\{x\} \subseteq C^*(\beta_n)$. So

$$C^*(\beta_n) \subseteq kap(\bigcup_{n=1}^{\infty} C^*(\beta_n))$$

and

$$C^*(1) \subseteq kap\left(\bigcup_{n=1}^{\infty} C^*(\beta_n)\right)$$

are satisfied. As a result, we obtain

$$C^*(1) = kap\left(\bigcup_{n=1}^{\infty} C^*(\beta_n)\right).$$

So, by Theorem 2.0.6 there exists an intuitionistic fuzzy number $\tilde{A}^i$ such that $A(\alpha) = C(\alpha)$ and $A^*(\beta) = C^*(\beta)$ Moreover,

$$\begin{aligned} d_H(A_k^*(\beta), A^*(\beta)) &\leq d_H(A_k^*(\beta), A_j^*(\beta)) + d_H(A_j^*(\beta), A^*(\beta)) \\ &\leq d_\infty(A_k^*(\beta), A_j^*(\beta)) + d_\infty(A_j^*(\beta), A^*(\beta)) \\ &\leq \varepsilon + d_\infty(A_j^*(\beta), A^*(\beta)) \end{aligned}$$

Taking the limit as $j \to \infty$ we obtain $d_H(A_k^*(\beta), A^*(\beta)) \leq \epsilon$ for all $k \geq N(\epsilon)$ uniformly in $\beta \in [0,1]$ so that $d_\infty(A_k^*(\beta), A^*(\beta)) \leq \epsilon$ for all $k \geq N(\epsilon)$.

Hence $\tilde{A}_k^i \to \tilde{A}^i$ in $IF_N(\mathbb{R}^n)$, which completes the proof. □

4. INTUITIONISTIC FUZZY NUMBER VALUED FUNCTIONS

Definition 4.0.1 *A mapping f from a domain $T \subseteq \mathbb{R}$ into $IF(\mathbb{R}^n)$ is called an intuitionistic fuzzy function (mapping).*

Definition 4.0.2 *An intuitionistic fuzzy function $f : [a,b] \subseteq \mathbb{R} \to IF_N(\mathbb{R}^n)$ is called continuous at $x_0 \in [a,b]$ if for every $\epsilon > 0$ there exists a $\delta > 0$ such that*

$$D_\infty(f(x), f(x_0)) < \epsilon$$

holds for all $x \in [a,b]$ with $|x - x_0| < \delta$.

Corollary 4.0.1 *Let $C([a,b], IF_N(\mathbb{R}^n))$ be the space of continuous functions from $[a,b]$ to $IF_N(\mathbb{R}^n)$. $C([a,b], IF_N(\mathbb{R}^n))$ is complete under the following metric:*

$$D_s(f,g) = \sup\{D_\infty(f(x), g(x)) : x \in [a,b]\}.$$

Proof Let $(f_n) \subseteq C([a,b], IF_N(\mathbb{R}^n))$ be a Cauchy sequence of functions. So for every $\epsilon > 0$ there exists $n_0 \in \mathbb{N}$ so that when $m, n > n_0$, we have

$$D_s(f_m, f_n) = \sup\{D_\infty(f_m(x), f_n(x)) : x \in [a,b]\} < \epsilon.$$

Hence for every $x \in [a,b]$

$$D_\infty(f_m(x), f_n(x)) < \epsilon$$

holds.. That is why, $(f_n(x))$, $IF_N(\mathbb{R})$ is a Cauchy sequence in $IF_N(\mathbb{R}^n)$ too. Since the space of intuitionistic numbers is complete with respect to D_∞,

$$f_n(x) \to f(x) \in IF_N(\mathbb{R}^n)$$

holds as $n \to \infty$. As the convergence under supremum metric is uniform and f_n is continuous for any $n \in \mathbb{N}$ then f is continuous, as well. That is why, $f \in C([a,b], IF_N(\mathbb{R}^n))$ and so $C([a,b], IF_N(\mathbb{R}))$ is complete with respect to the metric D_s. □

4.1. Hukuhara Differentiability

Definition 4.1.1 *[35] Let $f : (a,b) \to IF_N(\mathbb{R})$ be an intuitionistic fuzzy number valued function and $t_0, t_0+h \in (a,b)$. f is called Hukuhara differentiable at t_0 if there exists an element $f'_H(t_0) \in IF_N(\mathbb{R})$ such that for all $h>0$ the followings is satisfied*

$$\lim_{h\to 0^+} \frac{f(t_0+h) \ominus_H f(t_0)}{h} = \lim_{h\to 0^+} \frac{f(t_0) \ominus_H f(t_0-h)}{h} = f'_H(t_0$$

Theorem 4.1.1 *[35] Let $f : (a,b) \to IF(\mathbb{R})$ be an intuitionistic fuzzy function. Let $f(t,\alpha) = [f_1(t,\alpha), f_2(t,\alpha)]$ and $f(t,\beta) = [f_1(t,\beta), f_2(t,\beta)]$ be its α and β cuts, respectively. If $f : (a,b) \to IF(\mathbb{R})$ is Hukuhara differentiable then the functions $f_1(t,\alpha)$, $f_2(t,\alpha)$, $f_1^*(t,\beta)$ and $f_2^*(t,\beta)$ are differentiable in classical sense for each $\alpha,\beta \in [0,1]$ such that*

$$\begin{aligned} f'(t,\alpha) &= [f'_1(t,\alpha), f'_2(t,\alpha)] \\ f^{*\prime}(t,\beta) &= [f_1^{*\prime}(t,\beta), f_2^{*\prime}(t,\beta)] \end{aligned}$$

4.2. Aumann Integration

Definition 4.2.1 *[22] A selector of a set valued function $f : T \subseteq \mathbb{R} \to K_C(\mathbb{R}^n)$ is a single valued function $g : T \to \mathbb{R}^n$ such that for all $t \in T$, $g(t) \in f(t)$.*

We will denote the set of integrable selectors of f by $\mathbf{S}(f)$.

Definition 4.2.2 *[22] Let $f : [a,b] \to K_C(\mathbb{R}^n)$. Then the Aumann integral of f over $[a,b]$ is defined as*

$$\int_a^b f(t)dt = \{\int_a^b k(t)dt : k \in \mathbf{S}(f)\}$$

If $\mathbf{S}(f) \neq \emptyset$ then we say that f is Aumann integrable over $[a,b]$.

Definition 4.2.3 *An intuitionistic fuzzy function $f : T \subseteq \mathbb{R} \to IF(\mathbb{R}^n)$ is continuous at $t_0 \in T$, if for every $\varepsilon > 0$ there exists a $\delta > 0$ such that*

$$D_\infty(f(t), f(t_0)) < \varepsilon$$

for all $t \in T$ with $|t - t_0| < \delta$.

Definition 4.2.4 *$f : [a,b] \to IF(\mathbb{R}^n)$ is called integrably bounded if there exists an integrable real valued function $h : [0,1] \to \mathbb{R}$ such that*

$$D(f(t), 0) \leq h(t).$$

Definition 4.2.5 *Let $f : [a,b] \to IF(\mathbb{R}^n)$ be an intuitionistic fuzzy function. If for each α and $\beta \in [0,1]$, the α and β cuts of f are (Lebesgue) measurable then f is called strongly measurable.*

Definition 4.2.6 *Let $f : [a,b] \to IF(\mathbb{R}^n)$ and denote its α and β cuts by $f(t,\alpha)$ and $f^*(t,\beta)$ respectively. If there exists an intuitionistic fuzzy number $\tilde{A}^i \in IF(\mathbb{R}^n)$ such that for each α and $\beta \in [0,1]$*

$$A(\alpha) = \int_a^b f(t,\alpha)dt$$
$$A^*(\beta) = \int_a^b f^*(t,\beta)dt$$

then f is said to be Aumann integrable over $[a,b]$ and $\tilde{A}^i$, which is denoted by $\int_a^b f(t)dt$, is called its (intuitionistic) Aumann integral over $[a,b]$.

Theorem 4.2.1 *[22] If $f : [a,b] \to K_C(\mathbb{R}^n)$ is measurable and integrably bounded then it is Aumann integrable over $[a,b]$. Moreover, the integral of f is a compact and convex set in $K_C(\mathbb{R}^n)$.*

Theorem 4.2.2 *[22]Let f_k $(k = 1,2,....)$and $f : [a,b] \subseteq \mathbb{R} \to K_C(\mathbb{R}^n)$ be measurable and uniformly integrably bounded set valued functions. If for all $x \in [a,b]$, $f_k(x) \to f(x)$ as $k \to \infty$ then*

$$\int_a^b f_k(x)dx \to \int_a^b f(x)dx$$

Theorem 4.2.3 *Let $f : [a,b] \to IF_N(\mathbb{R}^n)$ and denote its α and β cut by $f(t,\alpha)$ and $f^*(t,\beta)$ respectively.*

If f is strongly measurable and integrably bounded, then it is Aumann integrable over $[a,b]$.

Proof

Let f be strongly measurable and integrably bounded then $f(t,\alpha)$ and $f^*(t,\beta)$ are integrable for each α and β in $[0,1]$.

Let $C_\alpha = \int_a^b f(t,\alpha)dt$ and $C_\beta = \int_a^b f(t,\beta)dt$. We need to show whether the family of sets $\{C_\alpha : \alpha \in [0,1]\}$ satisfies (1.)-(4.) in Theorem 2.0.5 and $\{C_\beta : \beta \in [0,1]\}$ satisfies (5.)-(8.) in Theorem 2.0.5. By [22], $\{C_\alpha : \alpha \in [0,1]\}$ satisfies (1.)-(4.) in Theorem 2.0.5. So let us show that $\{C_\beta : \beta \in [0,1]\}$ satisfies (5.)-(8.) in Theorem 2.0.5.

Since $f^*(t,\beta)$ is integrable for each $\beta \in [0,1]$, $C_\beta \neq \varnothing$ and since for each $0 \leq \beta_1 \leq \beta_2 \leq 1$ we have $f^*(t,\beta_1) \subseteq f^*(t,\beta_2)$. So we obtain $C_{\beta_1} \subseteq C_{\beta_2}$.

Let $(\beta_k) \subseteq [0,1]$ be a non-increasing sequence converging to β. Since f is an intuitionistic fuzzy number valued function, we obtain that $f^*(t,\beta_k) \to f^*(t,\beta)$. by Theorem 2.0.5. Moreover, since for all $\beta \in [0,1]$ and $t \in [a,b]$ we have $d_H(f(t,\beta),\{0\}) \leq d_H(f(t,1),\{0\})$, $f^*(t,\beta)$ is uniformly integrably bounded on $[a,b]$. So by Theorem 4.2.2

$$C_{\beta_k} \to C_\beta$$

in $(K_C(\mathbb{R}^n), d_H)$.

Let $(\beta_k) \subseteq [0,1]$ be a non-decreasing sequence converging to 1 then by the similar reasoning above we obtain

$$C_{\beta_k} \to C_1$$

Hence by Theorem 2.0.6, there exists an intuitionistic fuzzy number $\tilde{A}^i \in IF(\mathbb{R}^n)$ with $A(\alpha) = \int_a^b f(t,\alpha)dt$ and $A^*(\beta) = \int_a^b f^*(t,\beta)dt$. So f is Aumann integrable. □

Lemma 4.2.1 *If $f : [a,b] \to IF_N(\mathbb{R})$ is continuous then it is strongly measurable.*

Proof Let $\epsilon > 0$ be given. Since $f : [a,b] \to IF_N(\mathbb{R})$ is continuous at an arbitrary point $x_0 \in [a,b]$ then there exists a $\delta > 0$ such that for $x \in [a,b]$ and $|x - x_0| < \delta$ we have

$$D_\infty(f(x), f(x_0)) < \epsilon.$$

Since

$$D_\infty(f(x), f(x_0)) = \max\{D_1(f(x), f(x_0)), D_2(f(x), f(x_0))\} < \epsilon$$

for $x \in [a,b]$ and $|x - x_0| < \delta$ we have

$$d_H(f(x;\alpha), f(x_0;\alpha)) < \epsilon$$

and

$$d_H(f^*(x;\beta), f^*(x_0;\beta)) < \epsilon.$$

So $f(x;\alpha)$ and $f^*(x;\beta)$ are continuous an arbitrary point $x_0 \in [a,b]$. Since α and β cuts of intuitionistic fuzzy number valued functions are continuous they are measurable set valued functions [22]. Hence $f : [a,b] \to IF_N(\mathbb{R})$ is a strongly measurable intuitionistic fuzzy number valued function. □

Theorem 4.2.4 *If $f : [a,b] \to IF_N(\mathbb{R})$ is a continuous fuzzy number valued function then it is Aumann integrable.*

Proof Since f is continuous then it is strongly measurable by Lemma 4.2.1. Since

$$d_H(f(x;\alpha), 0) \le d_H(f(x;0), 0)$$

and

$$d_H(f^*(x;\beta), 0) \le d_H(f^*(x;1), 0)$$

then we have

$$D_\infty(f, 0) \le \max\{d_H(f(x;0), 0), d_H(f^*(x;1), 0)\}.$$

Let us define a function $h : [a,b] \to \mathbb{R}$ such that

$$h(x) = \max\{d_H(f(x;0), 0), d_H(f^*(x;1), 0)\}.$$

So for every $x \in [a,b]$

$$D_\infty(f, 0) \le h(x)$$

is satisfied. Since h is integrable f is integrably bounded.

Therefore, since $f : [a,b] \to IF_N(\mathbb{R})$ is strongly measurable and integrably bounded, f is Aumann integrable □

Theorem 4.2.5 *Let $f, g : [a,b] \to IF_N(\mathbb{R})$ and $\lambda \in \mathbb{R}$ be given. If f and g are strongly measurable and integrably bounded then the followings are satisfied.*

1. $f+g$ is Aumann integrable on $[a,b]$ and

$$\int_a^b [f(x)+g(x)]\,dx = \int_a^b f(x)dx + \int_a^b g(x)dx$$

holds.

2. $\lambda f$is Aumann integrable on $[a,b]$ and

$$\int_a^b \lambda f(x)dx = \lambda \int_a^b f(x)dx$$

holds.

3. For any $c \in (a,b)$,

$$\int_a^b f(x)dx = \int_a^c f(x)dx + \int_c^b f(x)dx$$

holds.

Proof

1. Let f and $g \in IF_N(\mathbb{R})$ such that their α and β cuts denoted by $f(x;\alpha) = [f_1(x;\alpha), f_2(x;\alpha)]$, $f^*(x;\beta) = [f_1^*(x;\beta), f_2^*(x;\beta)]$ and $g(x;\alpha) = [g_1(x;\alpha), g_2(x;\alpha)]$, $g^*(x;\beta) = [g_1^*(x;\beta), g_2^*(x;\beta)]$ respectively. Since f and g are are strongly measurable and integrably bounded then $f+g$ is also strongly measurable and integrably bounded. Hence $f+g$ is Aumann integrable. By the definition of Aumann integration we can obtain the followings.

$$\begin{aligned}
\left(\int_a^b (f(x)+g(x))dx\right)(\alpha) &= \int_a^b (f(x)+g(x))(\alpha)dx \\
&= \int_a^b (f(x;\alpha)+g(x;\alpha))dx \\
&= \int_a^b [f_1(x;\alpha)+g_1(x;\alpha), f_2(x;\alpha)+g_2(x;\alpha)]dx \\
&= \int_a^b [f_1(x;\alpha), f_2(x;\alpha)]dx + \int_a^b [g_1(x;\alpha), g_2(x;\alpha)]dx.
\end{aligned}$$

and

$$\begin{aligned}
\left(\int_a^b (f(x)+g(x))dx\right)(\beta) &= \int_a^b [f_1^*(x;\beta)+g_1^*(x;\beta), f_2^*(x;\beta)+g_2^*(x;\beta)]dx \\
&= \int_a^b [f_1^*(x;\beta), f_2^*(x;\beta)]dx + \int_a^b [g_1^*(x;\beta), g_2^*(x;\beta)]dx.
\end{aligned}$$

Hence

$$\int_a^b (f(x)+g(x))dx = \int_a^b f(x)dx + \int_a^b g(x)dx$$

is satisfied.

The proof of **2.** and **3.** can be done in a similar way. □

Theorem 4.2.6 *[22] If $f,g : [a,b] \to K_C(\mathbb{R}^n)$ are Aumann integrable, then $d_H(f,g) : [a,b] \to \mathbb{R}$ is integrable and*

$$d_H(\int_a^b f(t)dt, \int_a^b g(t)dt) \leq \int_a^b d_H(f(t),g(t))dt$$

Theorem 4.2.7 *If $f,g : [a,b] \to IF(\mathbb{R}^n)$ are Aumann integrable, then $D(f,g) : [a,b] \to \mathbb{R}$ is integrable and*

$$D_\infty(\int_a^b f(t)dt, \int_a^b g(t)dt) \leq \int_a^b D_\infty(f(t),g(t))dt$$

Proof We need to show that

$$\begin{aligned} D_1(\int_a^b f(t)dt, \int_a^b g(t)dt) &\leq \int_a^b D_1(f(t),g(t))dt \\ D_2(\int_a^b f(t)dt, \int_a^b g(t)dt) &\leq \int_a^b D_2(f(t),g(t))dt \end{aligned}$$

Since α and β cuts of an intuitionistic fuzzy number are non-empty compact and convex sets in $\mathbb{R}^n$,

$$D_\infty(\int_a^b f(t)dt, \int_a^b g(t)dt) \leq \int_a^b D_\infty(f(t),g(t))dt$$

holds by Theorem 4.2.6. □

Theorem 4.2.8 *Let $f : [a,b] \to IF(\mathbb{R})$ be a continuous function. Assume its α and β cuts by $f(t,\alpha) = [f_1(t,\alpha), f_2(t,\alpha)]$ and $f^*(t,\beta) = [f_1^*(t,\beta), f_2^*(t,\beta)]$ respectively. Then*

1. If $u(x) = \int_a^x f(t)dt$ is H-differentiable then $u'_H = f(x)$
2. If $u(x) = \int_x^b f(t)dt$ is H-differentiable then $u'_H = -f(x)$

Proof

1. Since f is a continuous function then it is Aumann integrable. So there exists $u \in IF(\mathbb{R})$ such that $u(x) = \int_a^x f(t)dt$. Then

$$\begin{aligned} u(x,\alpha) &= \int_a^x f(t,\alpha)dt \\ u^*(x,\beta) &= \int_a^x f^*(t,\alpha)dt. \end{aligned}$$

So

$$\begin{aligned}[u_1(x,\alpha), u_2(x,\alpha)] &= \int_a^x [f_1(t,\alpha), f_2(t,\alpha)]dt = [\int_a^x f_1(t,\alpha), \int_a^x f_2(t,\alpha)] \\ [u_1^*(x,\beta), u_2^*(x,\beta)] &= \int_a^x [f_1^*(t,\beta), f_2(t,\beta)]dt = [\int_a^x f_1^*(t,\beta), \int_a^x f_2(t,\beta)]dt\end{aligned}$$

Since $u(x)$ is H-differentiable then for each α and β in $[0,1]$, $u_1(x,\alpha)$, $u_2(x,\alpha)$, $u_1^*(x,\beta)$ and $u_2^*(x,\beta)$ are differentiable and by the fundamental theorem of calculus we obtain

$$\begin{aligned}[u_1'(x,\alpha), u_2'(x,\alpha)] &= [f_1(t,\alpha), f_2(t,\alpha)] \\ [(u_1^*)'(x,\beta), (u_2^*)'(x,\beta)] &= [f_1^*(t,\beta), f_2(t,\beta)]\end{aligned}$$

Hence, $u_H'(x) = f(x)$

2. This can be proved in a similar manner.

□

Theorem 4.2.9 *If $f : [a,b] \to IF(\mathbb{R})$ be an H-differentiable function on $[a,b]$ and $f_H'(t)$ is Aumann integrable then*

$$\int_a^b f_H'(t)dt = f(b) \ominus_H f(a)$$

holds.

Proof Assume α and β cuts of f are $f(t,\alpha) = [f_1(t,\alpha), f_2(t,\alpha)]$ and $f^*(t,\beta) = [f_1^*(t,\beta), f_2^*(t,\beta)]$, respectively. Since f is differentiable the following classical derivatives $f_1'(t,\alpha)$, $f_2'(t,\alpha)$, $(f_1^*)'(t,\beta)$ and $(f_2^*)'(t,\beta)]$ exist such that
$f'(t,\alpha) = [f_1'(t,\alpha), f_2'(t,\alpha)]$ and $(f^*)'(t,\beta) = [(f_1^*)'(t,\beta), (f_2^*)'(t,\beta)]$.

$$[\int_a^b f_H'(t)dt]^\alpha = f(b,\alpha) \ominus_H f(a,\alpha)$$

is proven in [22]. Similarly we can obtain that

$$\begin{aligned}[\int_a^b f_H'(t)dt]^\beta &= \int_a^b [(f_1^*)'(t,\beta), (f_2^*)'(t,\beta)]dt \\ &= [\int_a^b (f_1^*)'(t,\beta)dt, \int_a^b (f_2^*)'(t,\beta)dt] \\ &= [f_1^*(b,\beta) - f_1^*(a,\beta), f_2^*(b,\beta) - f_2^*(a,\beta)] \\ &= f^*(b,\beta) \ominus_H f^*(a,\beta)\end{aligned}$$

Since

$$f(b) = \int_a^b f_H'(t)dt + f(a)$$

holds if and only if

$$f(b,\alpha) = [\int_a^b f'_H(t)dt]^\alpha + f(a,\alpha) \text{ and } f^*(b,\beta) = [\int_a^b (f'_H)^*(t)dt]^\beta + f^*(a,\beta)$$

then we obtain

$$\int_a^b f'_H(t)dt = f(b) \ominus_H f(a)$$

□

5. SUMMARY AND RESULTS

In this paper, we have firstly defined a new distance function based on the well known Hausdorff metric in order to study the metric properties of intuitionistic fuzzy numbers by using α and β cuts. Then we have proved that this function satisfies the metric axioms and the space of intuitionistic fuzzy number valued functions is complete under the given metric. Besides, as a corollary we have proved that the space of continuous intuitionistic fuzzy number valued functions is complete with respect to the supremum metric D_s. And then, we have extended some fundamental theorems from fuzzy Aumann integration to intuitionistic fuzzy environment with the help of α and β cuts. Finally we have proved the relation between Hukuhara derivative and Aumann integral for intuitionistic fuzzy valued functions by using the fundamental theorem of calculus.

References

[1] Lotfi A. Z., "Fuzzy Sets," Information and Control, 8, (1965), pp. 338-353.

[2] Krassimir T. A., "Intuitionistic Fuzzy Sets," Fuzzy Sets and Systems, 20, 1, (1986), pp. 87–96.

[3] Joseph A. G. "L-Fuzzy Sets," Journal of Mathematical Analysis and Applications, 18, 1, (1967), 145-174.

[4] Jerry M. M. "Advances in Type-2 Fuzzy Sets and Systems," Information Sciences, 177, 1, (2007), pp. 84-110.

[5] Krassimir T. A., Intuitionistic Fuzzy Sets: Theory and Applications, Physica, Heidelberg, 1999.

[6] Laecio C. B., Rodney C. B, Pedro A. T., "Fuzzy Modelling in Population Dynamics," Ecol. Model, 128, (2000), pp. 27-33.

[7] Deng-Feng L., "Multiattribute Decision Making Models and Methods Using Intuitionistic Fuzzy Sets," Journal of Computer and System Sciences, 70, 1 (2005), pp. 73-85.

[8] Jun Y., "Multicriteria Fuzzy Decision-Making Method Based on a Novel Accuracy Function under Interval-Valued Intuitionistic Fuzzy Environment," Expert Systems with Applications, 36, 3, (2009), pp. 6899-6902.

[9] Li D., Cheng C., "New Similarity Measures of Intuitionistic Fuzzy Sets and Application to Pattern Recognitions," Pattern Recognition Letters, 23, 1-3, (2002), pp. 221-225.

[10] Supriya K. D., Ranjit B., Akhil R. R., "An Application of Intuitionistic Fuzzy Sets in Medical Diagnosis," Fuzzy Sets and Systems, 117, 2, (2001), pp. 209-213.

[11] Athar K., "Homeopathic Drug Selection Using Intuitionistic Fuzzy Sets," Homeopathy, 98, 1, (2009), pp. 35-39.

[12] Ming-Hung S., Ching-Hsue C., Jing-Rong C., "Using Intuitionistic Fuzzy Sets for Fault-tree Analysis on Printed Circuit Board Assembly," Microelectronics Reliability, 46, 12, (2006), pp. 2139-2148.

[13] Laecio C. B., Rodney C. B, Pedro A. T., "Fuzzy Modelling in Population Dynamics," Ecol. Model, 128, (2000), pp. 27-33.

[14] Oktay D., "Statistical Fuzzy Approximation to Fuzzy Differentiable Functions by Fuzzy Linear Operators," Hacettepe Journal of Mathematics and Statistics, 39, 4, (2010), pp. 497-514.

[15] Ömer A., Ömer O., "A Prey Predator Model with Fuzzy Initial Values," Hacettepe Journal of Mathematics and Statistics, 41, 3, (2012), pp. 387-395.

[16] Senol D., Lawrence. M. B., "Intuitionistic Textures Revisited," Hacettepe Journal of Mathematics and Statistics, 34, (2005), 115-130.

[17] Jin Han P., "Intuitionistic Fuzzy Metric Spaces", Chaos, Solitons & Fractals 22, 5, (2004), pp. 1039-1046.

[18] Qian L., Zeshui X., "Fundamental Properties of Intuitionistic Fuzzy Calculus," Knowledge-Based Systems, 76, (2015), pp. 1-16.

[19] M. Oberguggenberger, S. Pittschmann, "Differential Equations with Fuzzy Parameters," Math. Mod. Syst,, 5, (1999), 181-202.

[20] Ömer A., Tahir K., Ömer O., Burhan T., "An Algorithm for the Solution of Second Order Fuzzy Initial Value Problems," Expert Systems with Applications, 40, (2013), 953-957.

[21] Ömer A., Tahir K., Selami B., Burhan T., "Solving a Second Order Fuzzy Initial Value Problem Using the Heaviside Function," Turk. J. Math. Comput. Sci., 4, (2016), 16-25.

[22] Phil D., Peter E. K., Metric Spaces of Fuzzy Sets: Theory and Applications. World scientific, 1994.

[23] Masuo H., "Integration des Applications Mesurables dont la Valeur est un Compact Convexe," Funkcialaj Ekvacioj, 10, 3 (1967), pp. 205-223.

[24] Madan L. P., Dan A. R., "Differentials of Fuzzy Functions," Journal of Mathematical Analysis and Applications, 91, 2, (1983), 552-558.

[25] Osmo K., "Fuzzy Differential Equations," Fuzzy Sets and Systems, 24, 3, (1987), pp. 301-317.

[26] Eyke H., "An Approach to Modelling and Simulation of Uncertain Dynamical Systems," International Journal of Uncertainty, Fuzziness and Knowledge-Based Systems, 5, 02, (1997), pp. 117-137.

[27] Michio S., "Theory of Fuzzy Integrals and its Applications," Ph.D. Dissertation, Tokyo Institute of Technology, 1974.

[28] Dan R., Gregory A., "The Fuzzy Integral," Journal of Mathematical Analysis and Applications, 75, 2, (1980), pp. 562-570.

[29] Didier D., Henri P., "Towards Fuzzy Differential Calculus Part 1: Integration of Fuzzy Mappings." Fuzzy Sets and Systems, 8, 1, (1982), 1-17.

[30] Robert J. A., "Integrals of Set-Valued Functions," Journal of Mathematical Analysis and Applications, 12, 1, (1965), pp. 1-12.

[31] Jan V. T., "Convex Analysis: An Introductory Text," John Wiley&Sons, Chichester, UK, 1948.

[32] Carl P. S., Lawrence B., Mathematics for Economists, vol. 7, Norton, New York, 1994.

[33] Ömer A. and Selami B., "Initial Value Problems in Intuitionistic Fuzzy Environment," Proceedings of the the 5th International Fuzzy Systems Symposium, Ankara, Turkey, October 14-15, 2017.

[34] Ömer A., Selami B., "Intuitionistic Fuzzy Initial Value Problems - An Application," Hacettepe Journal of Mathematics and Statistics, (2017) Doi: 10.15672/HJMS.2018.598.

[35] Ömer A., Selami B., "System of Intuitionistic Fuzzy Differential Equations with Intuitionistic Fuzzy Initial Values," Notes on Intuitionistic Fuzzy Sets, 24, (2018), pp. 141-171.

MANAS Journal of Engineering
ISSN 1694-7398 | e-ISSN 1694-7398

Volume 6 (Issue 2) (2018) Pages 164-176

Learning Management System Implementation. Case Study on User Interface Configurations.

Okan Yakit*[1], Rita Ismailova[1]

[1] Kyrgyz Turkish Manas University, Department of Computer Engineering, Bishkek, Kyrgyzstan
okanyakit@gmail.com

Received: 19.11.2018; Accepted: 29.11.2018

***Abstract*:** *Using ICT, it is possible to build an educational process that will not only be independent of time and space, but also provide quick access to educational materials. In this case, educational material can be not only in a readable format, but also in the form of video materials. In the Kyrgyz Republic, the use of distance learning can be helpful to solve a number of problems. The focus of this study is the usability problems faced in Learning Management System, as well as to investigate factors influencing usage of the system. In the frame of the study, we have used several methods, including survey, the RAM usage analysis and loading time compression tests. Results suggested that the LMS usage could be widely adopted in the region. In addition, within the analysis of usage problems, decrease the loading time in Moodle by organizing the course resources, and hence improving the loading time and stopping users from abandoning the site was done.*

Keywords: *Distance education, learning management system, user interface, user satisfaction*

1. INTRODUCTION

We live in a world where technological innovations occur very quickly and digital technologies are becoming an integral part of everyday life. Technology not only provides an opportunity for rapid communication, but also for building systems that facilitate many aspects of our lives. These advantages of information and communication technologies (ICT) are used in entertainment, business and government. The use of ICT to improve the activities public sector organizations is called e-government. E-learning can be considered as one of the dimensions of e-government. With the help of ICT, education not only provides time and space independent education, but also provides quick access to learning materials [4]. For this reason, it is necessary to analyze the perceptions of both students and instructors in order to make a Learning Management System (LMS) a valuable part of the education system.
In the Kyrgyz Republic, the use of distance learning can be helpful to solve a number of problems. Many studies considering e-education in the country have shown that the use of LMS has a great potential not only for higher education but also for secondary education [13]. However, there is another problem with the use of LMS for education. For example, the rate of computer literacy among users is low [3]. Nevertheless, it has been emphasized that the use of internet technologies as a training tool is supported by young people in the country [9].

2. LITERATURE REVIEWS

Distance Learning by definition is the method of teaching and learning with other means than traditional teaching method of being physically present in the environment of teaching and learning. The methods to transfer information for distance learning may include but not limited to television, radio, magazines, mail, compacts discs, video tapes or internet.

2.1. Early Form of Distance Learning

The concept of LMS can be considered relatively new compared to the concept of Distance Education (DE) which's root dates back to late 1800's. Sir Isaac Pitman's Correspondence Collages was founded in 1840 England and his correspondence course study was one of the first forms DE [6]. The study materials were being sent by free mail delivery service. Within a few decades the method of correspondence was adopted by several other countries including Germany, Canada, Australia, the Soviet Union, Japan and the United States [6].

Vast number of studies has been done on Learning Management Systems, but majority of the studies focus on comparison of the system and importance of implementing the systems. Yet the number of studies done on usability is insufficient.

2.2. Learning Management Systems

The term "Learning Management System" refers to software applications for the documentation, archiving, administering and tracking the source study materials, reports and assignments [15]. It helps organizations and intuitions to create learning programs, track assignments, administer and evaluate tests and archive learning materials for later use in a virtual environment. Being open source, Moodle can be given as a popular example of such Learning Management Systems.

2.3. What is Moodle

Moodle, an acronym for Modular Object-Oriented Dynamic Learning Environment is a popular open source LMS designed for educators to create dynamic online courses [7]. With its multifunctional and interactive features Moodle is can be considered a superior alternative to traditional learning methods. A significant advantage of Moodle over its leading competitors is their foundation in social constructivist pedagogy embedded in its features to support student learning [8].

The high cost of distance learning is widely known, and as the institutions become more large-scale providers of distance learning the cost-effectiveness becomes more crucial [2]. The increasing cost of proprietary Learning Management Systems was a concern for most institutes (as cited in [14]). A system called 'MobiGlam' used by Koole et al. [5] to examine usability, learning and social interaction of students' mobile access to Moodle courses. From this example, one can see how mobile learning greatly enhances the possibilities of using Moodle as a part of an overall distance learning method.

2.4. Wideness of Moodle usage

Moodle is widely used among Learning Management Systems, with 106,176 registered websites in 228 Countries [7].

Moodle is used by a variety of institutions and individuals, including:

- Universities
- High schools
- Primary schools
- Government departments
- Healthcare organizations
- Military organizations
- Airlines
- Oil companies
- Homeschoolers
- Independent educators
- Special educators

However, considering Moodle usage in the Kyrgyz Republic, the LMS is used by higher educational institutions only. Thus, according to Nurakun Kyzy et al., Moodle is used mostly together with self-developed systems [12]. One of the main concerns in use of this LMS is the user interface of the system.

2.5. Problems faced by with Learning Management Systems

Learning Management Systems offers various tools and services for the end user such as documentation and tracking of the activities as stated before. However, to use these may cause new issues and challenges for the end user. As stated by Ssemugabi [18], majority of these challenges are associated with Learning Management Systems arise from technical limitations of computers and the internet, and not being able to get adjusted to the system because of low rate of ICT literacy.

As many researchers noted, these challenges can be categorized as [1, 16, 17];

- ICT illiteracy and feeling of discomfort while using ICT solutions
- Poor maintenance and Inefficient User Support Strategies
- Poor institution-wide regulations
- Selection of LMS and usability problems

Even though the learning management systems are widely used in higher education and corporate organizations, the number of researches done to examine the usability of such systems is insufficient. In applications, whose target audience is not necessarily consisting of high ITC literate individuals, usability is an essential party. According to the interview and further feedback from students, most of the LMS application designs are filled with redundant symbols and icons making the interface messy and hard to navigate. The overload of the information in webpages makes it difficult for low ICT literate individuals to focus their attention and navigate through the web page. These usability issues raised couple of questions:

- Is Moodle too complicated for novice users?
- Is there a usability problem with Moodle?
- Is the user satisfied while using the system?

3. METHODOLOGY

The main focus of this study is the usability problems faced in Learning Management System, as well as to investigate factors influencing usage of the system. Therefore, in the study, several methods have been used.
First, the 3.3.4+ version of Moodle was built. On the system, as a case study, 2 courses were launched. For the case study, we kept the default Moodle interface. Since the aim was to use the Moodle system as an additional component of selected courses, the lessons were conducted in a traditional way, with support in Moodle. For that, video content was prepared and uploaded to the system after each lesson. Additionally, reading materials, presentations and quizzed were placed.
To test the usability problems faced in LMS, we have stared with the user survey. The survey was conducted among students enrolled in courses, selected for the case study.
Next, the RAM usage analysis and loading time compression tests were conducted.

4. RESULTS AND GENERAL OVERVIEW

4.1. Student survey

A pilot study, carried out at the computer-engineering department of Kyrgyz-Turkish Manas University can be considered as an example of LMS implementation in the country. In the scope of this study, hybrid type of education was applied to one of the undergraduate courses provided by the department. The grade point average of the students showed an increase of 20%. However, since in the case study, only one course have been involved, yet further research is needed to identify all factors affecting the success of such courses.

Concerning details of the case study, as an LMS in this course, we have used Moodle. At the end of the course, a survey about the opinions of students about the system was conducted. According

to the survey results, 45% of the students said that the Moodle system was easy to use and 59% said that they would use the system in the future (Fig. 1).

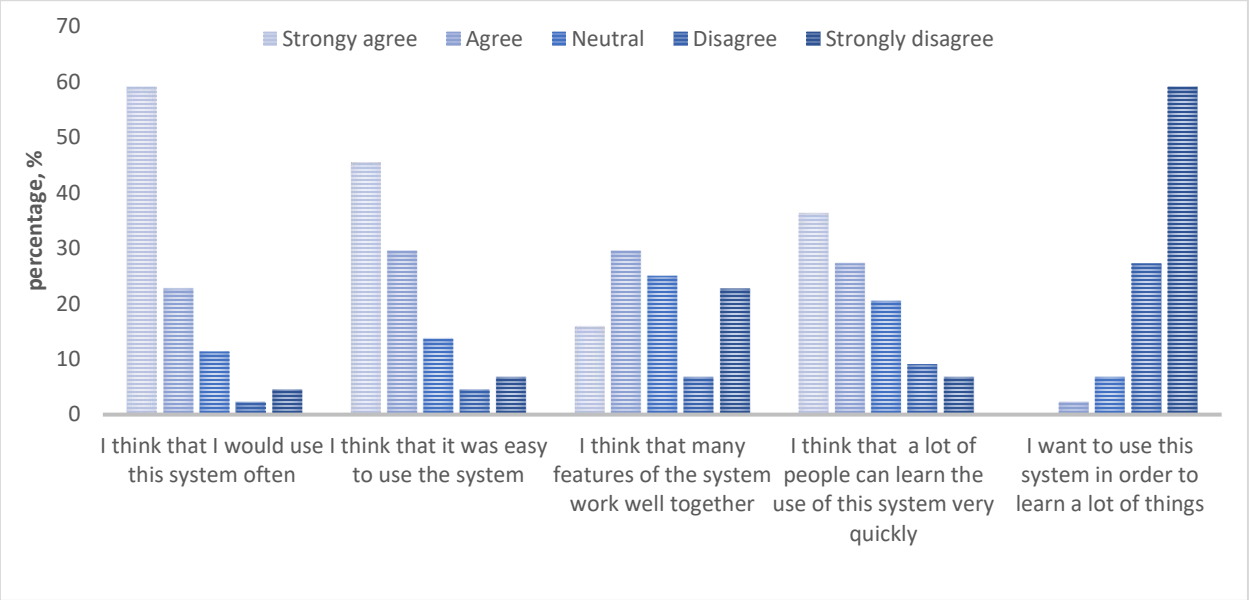

Figure 1. *Students' perception of Moodle system (positively defined questions).*

The second set of questions were negatively defined ones. According to the results, obtained in this section, 16% of users said that the technical support system could facilitate the use of the system (Fig. 2).

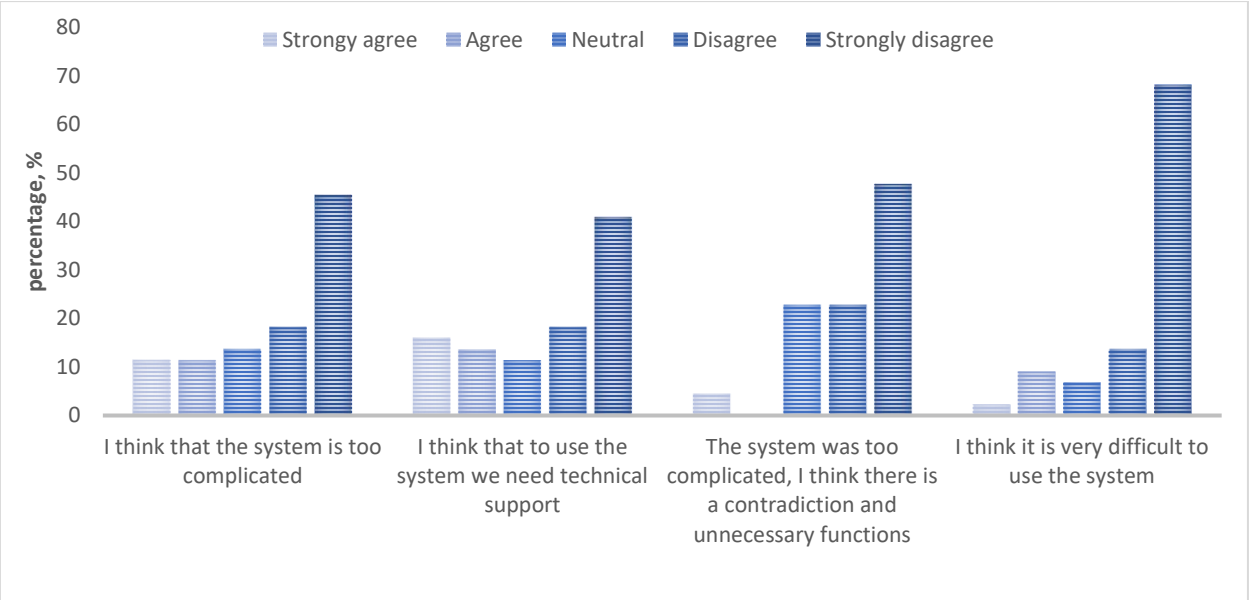

Figure 2. *Students' perception of Moodle system (negatively defined questions)*

As a direct derivation of the Fig. 3 we can assume that e-learning has a great potential in the Kyrgyz Republic as 68% of students states that it would be helpful if we had video lessons available for other disciplines; 75% indicated that they thought the video lessons were useful (Fig. 4).

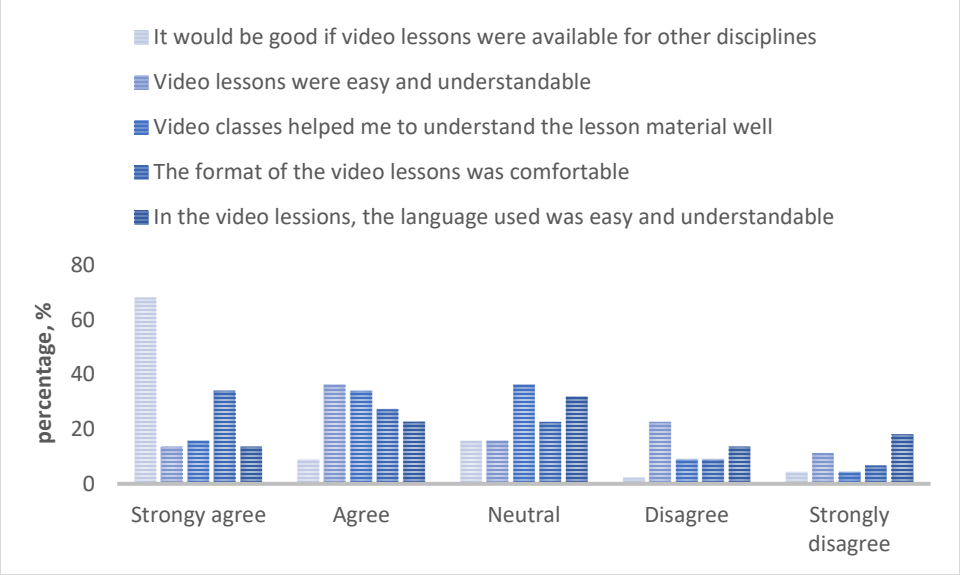

Figure 3. *Students' perception of video content (positively defined questions).*

For this set of question, we also added the negatively defined ones. Results of this section go in line with the positively defined ones.

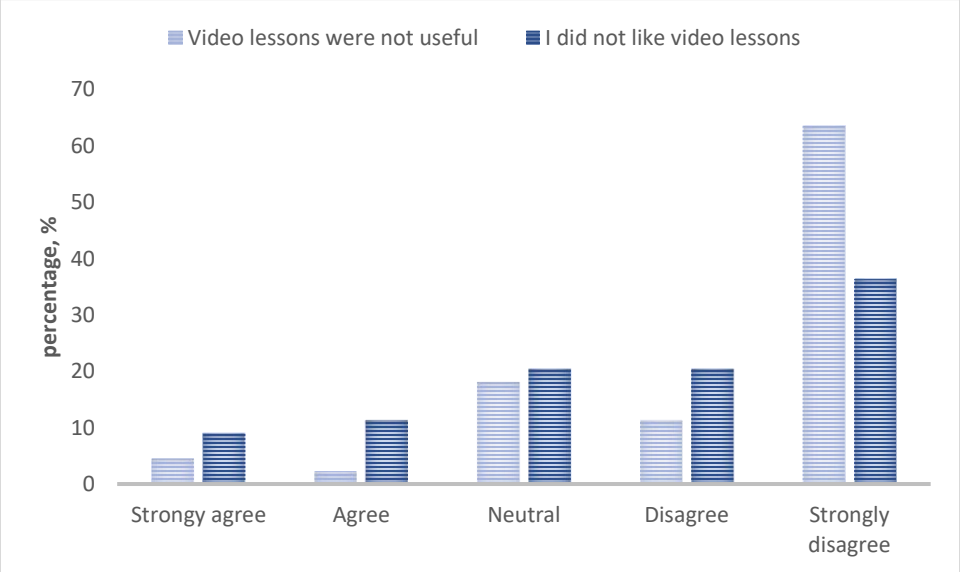

Figure 4. *Students' perception of video content (negatively defined questions).*

4.2. The Simplification of User Interface

To face these issues the simplification of the user interface seemed necessary. To simplify the user interface the layout of the page should be optimized to increase information hierarchy and decrease the cluttering. An example of the layout optimization can be seen in the figures below. Fig. 5 shows a bad example of layout design. In the design, used in Fig. 5, it is hard to navigate and hierarchy is not obvious while on the other hand in the Fig. 6 the information hierarchy is established and it is easier on the eye of the user. Simplification of the user interface makes it easier for novice users to adapt the system.

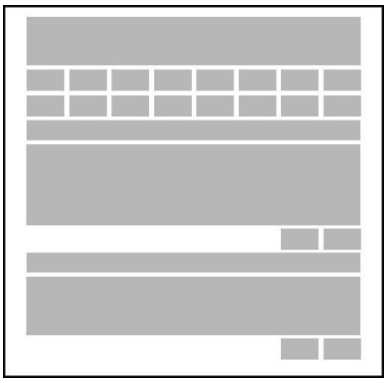

Figure 5. *An example of bad layout design*

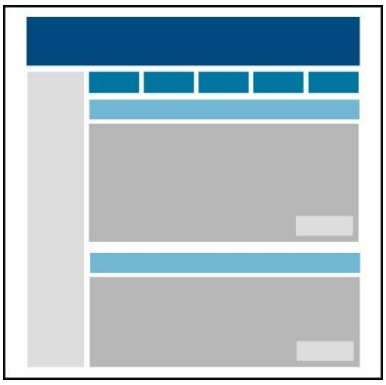

Figure 6. *An example of good layout design*

4.2.1. Decluttering and optimizing the pages

By default, Moodle system has 38 unique blocks for users to use for their needs, which 31 of them can be used on course pages. A fresh course page without any customization will only have ‘Navigation’ and ‘Settings’ blocks. Even though adding block near essential and provides lots of customization and functionality, these blocks may hinder the performance of the system hence the user experience will suffer. Each block will take up additional RAM while the page is generated.

To maximize the performance of the page one needs to keep the amount block to minimum. The ‘Comments’ and ‘RSS’ block showed to be most RAM consuming blocks with taking up 7.4MB RAM and 6.2MB RAM respectively. In the figure (Fig. 7) below one can see the amount of time to generate a page increases with each added block.

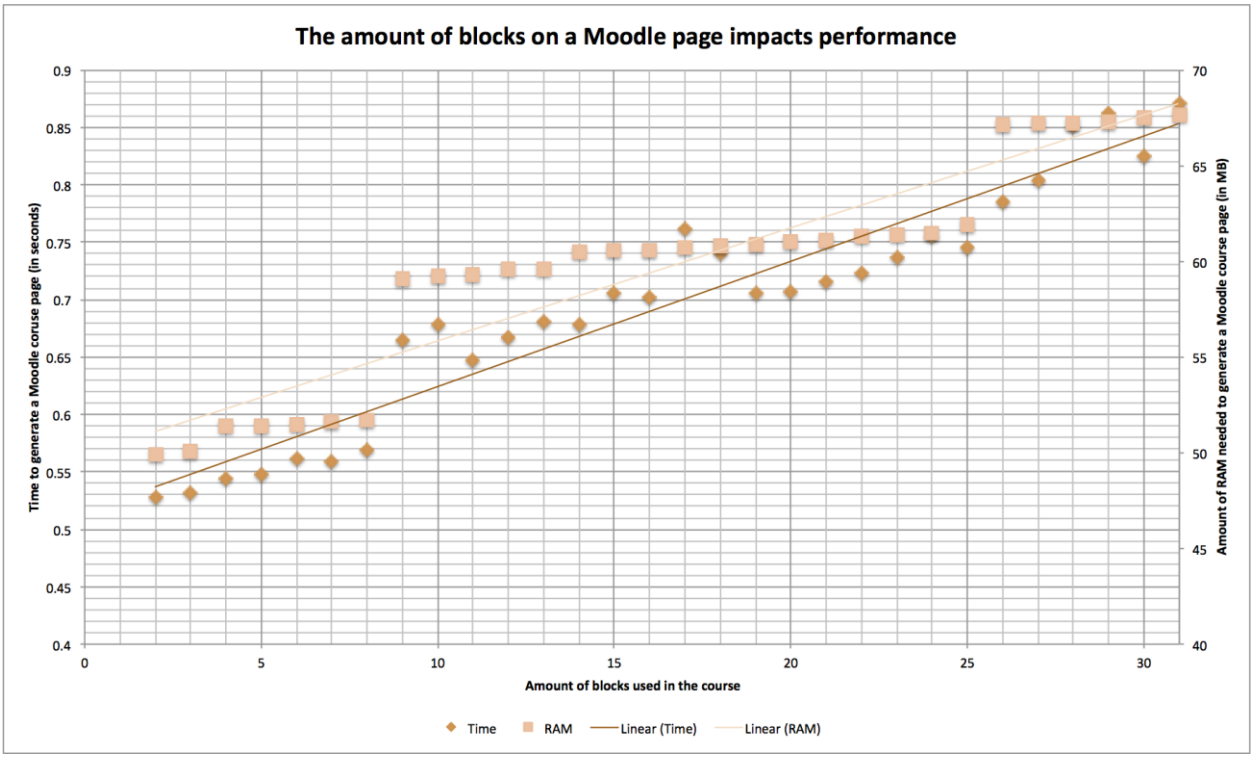

Figure 7. *Graph showing time needed to generate a page with added blocks. (from www.iteachwithmoodle.com).*

Using images during a course design makes the course easier to understand, navigate and much more appealing. But using too much image may also hinder the performance of the system. In the Fig. 8 and Fig. 9 below one can see the amount of database write and read calls made with each added amount of image.

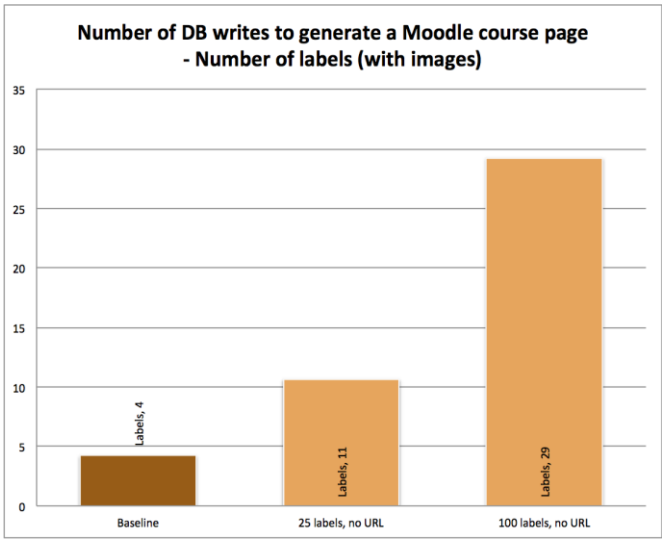

Figure 8. *Number of DB writes to Generate a Moodle Course Page - Number of Labels (from www.iteachwithmoodle.com)*

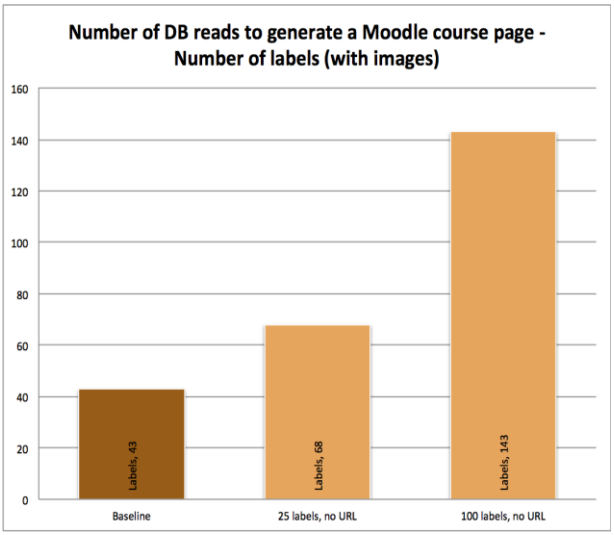

Figure 9. *Number of DB Reads to Generate a Moodle Course Page - Number of Labels. (from www.iteachwithmoodle.com)*

Considering the number of data base calls needed to generate a page with multiple images, inserting the images via URL instead of uploading directly to the Moodle system will decrease the number of needed calls hence improve the performance of the page.

4.2.2. Responsiveness

Responsive Web Design is an approach to web design in which a site is built to deliver an ideal viewing experience, easy reading and navigation with a minimum of resizing, panning, and scrolling across a wide range of devices like desktop, notebook, tablet, smart phones and other gadgets [11]. Since 61.5% of students stated they have smartphones and used it to access the pilot course, the responsiveness of the LMS is crucial.

Moodle is readily published as responsive web application but it can be further optimized to meet the necessary requirements to satisfy our needs to make it easier for novice users, such as decluttering the pages and increasing the visual hierarchy with use of colors and text points.

4.2.3. Heat Map

User interaction data is crucial for improving the user experience in web developing. To get a better understanding of user behavior one can use the help of heat maps. Compared to a traditional analytic a heat map focus on user behavior within the page not between the pages. A heat map tracks a user's cursor on the screen and presents the data as colors so it is easier for human understanding. It is a quick way to visualize data with the help of a heat map it is easier to see which parts of the page getting the most attention of the user so one can optimize the layout accordingly. An example for heat map of a webpage, taken from clicktale, is shown below in Fig. 10.

Figure 10. *A heat map example (from www.clicktale.com)*

An easy way to make use of heat maps in Moodle is by using the plugin called 'Heatmap' which is free to use. The plugin gives the user ability to add 'Heatmap' blocks to course pages separately and track the number of visitors to each activity of the course. The plugin keeps track of the data

and visualizes it in real-time and can be toggled on and off. The effect of the plugin is invisible to the 'student' users.

With the help of this plugin a teacher can improve the interaction in their courses by highlighting the less or more interacted activities.

4.2.4. Difference Between CSS & SCSS

The term CSS stands for Cascading Style Sheets and it describes how html elements are to be displayed on certain medium such as screen, paper, or in other media [19]. Moodle uses SCSS instead of CSS since SCSS shortens the code. In SCSS we can define variables as we can in php, which allows us to use the predefined variables over and over again. An example can be seen below;

```
body{
 width: 850px;
 color: #ffffff;
}
body content{
 width:648px;
 background:#cccccc;
}
```

Code snippet 1. *CSS example*

```
$color: #cccccc;
$width: 850px;

@mixin body{
 width: $width;
 color: $color;

 content{
  width: $width;
  background:$color;
 }
}
```

Code snippet 2. *SCSS variable example*

As it is seen in the example above the color and width has been defined and used as variables. This feature of SCSS allows for easier and more complex coding for the programmers. Another useful feature of SASS syntax is that it allows for nesting which makes the code easier to read;

```
nav {
 ul {
  margin: 5px;
  padding: 10px;
  list-style: none;
 }

 li { display: inline-block; }

 a {
  display: block;
  padding: 6px 12px;
  text-decoration: none;
 }
}
```

Code snippet 3. *SCSS Nesting feature*

CSS and SCSS can be further used to distinguish blocks of the webpage to make it easier to navigate and enhance the hierarchy.

5. CONCLUSION

A systems performance, visual appealing and user experience is crucial for its success especially when it comes to Learning Management Systems. As it has been stated before in this study using Learning Management Systems can be challenging for novice user due to high ITC-illiteracy rate. To make the adaptation processes to the system relatively easier for user one needs to take user experience in consideration. In this case to enhance the user experience of Moodle LMS, simplification of the user interface and decluttering has been done. The optimizations are made with consideration of the system performance.

5.1. Page Generating Time

As the page generating time increases the user experience is impacted negatively. According to a study done by Nah, a user's tolerable waiting time for information retrieval is approximately 2 [10]. As one can see in this study, it is possible to decrease the loading time in Moodle by organizing the course resources, using external images when possible, minimizing the number of blocks per page. By doing optimizations mentioned above, there will be less database calls, caching and RAM usage will be decreased hence improving the loading time and stopping users from abandoning the site.

5.2. Improvements on User Interface

With the necessary optimization now, the side panel on the right is always collapsible and completely removed while viewing courses to increase usable space for the content. In the Fig. 12 below you can see the representation of the course page layout from default boost theme of Moodle Learning Management System and in the Fig. 11 shows the representation of the optimized course page layout.

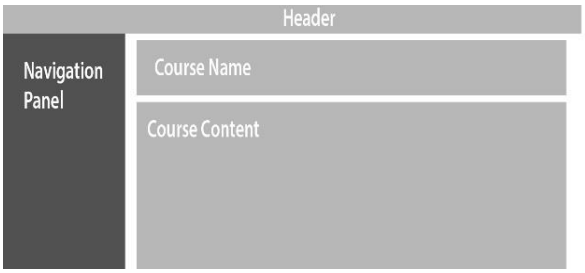

Figure 11. *Optimized layout*

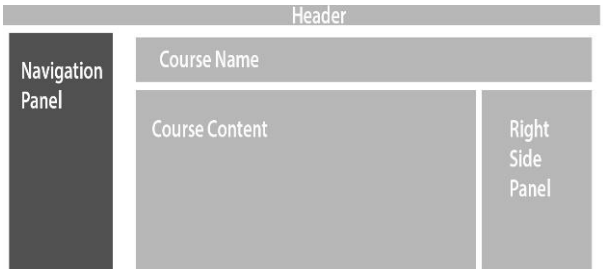

Figure 12. *Original boost layout*

After the optimization, the information clutter and distraction caused by the right-side panel is solved and in return, the available space for the course content has risen by 22.29%.

REFERENCES

[1] Conde M.Á., García-Peñalvo F.J., Rodríguez-Conde M.J., Alier M., Casany M.J., Piguillem J.. An evolving Learning Management System for new educational environments using 2.0 tools. Interactive Learning Environments, 22(2), (2014), 188-204.

[2] Chavan A., Pavri S. Open-source learning management with moodle. Linux Journal, (128), (2004), 2.

[3] Ismailova R., Muhametjanova G. "Cyber crime risk awareness in Kyrgyz Republic," Information Security Journal: A Global Perspective 25 (1-3), (2016), 32-38.

[4] Kakasevski G., Mihajlov M., Arsenovski S., Chungurski S. "Evaluating usability in learning management system moodle," In ITI, Vol. (2008), 30, 2008.

[5] Koole M., McQuilkin J. L., Ally M.. Mobile learning in distance education: Utility or futility? Journal of Distance Education, 24(2), (2010), 59-82.

[6] Matthews D. " The origins of distance education and its use in the United States," T.H.E. Journal, 27(2), (1999).

[7] Moodle Research Library. "About Moodle," Retrieved from https://docs.moodle.org/36/en/About_Moodle, (2011), access date November, 10, 2018

[8] Moodle Project. "About Moodle," Retrieved from https://docs.moodle.org/36/en/About_Moodle, (2018), access date November, 10, 2018

[9] Muhametjanova G., Ismailova R. Students' Level of Readiness to Use Social Media as Educational Tool in Kyrgyz Republic. Journal of Educational Multimedia and Hypermedia, in press

[10] Nah F.F.H. "A study on tolerable waiting time: how long are web users willing to wait?" Behaviour & Information Technology, 23(3), (2004), 153-163.

[11] Natda K. V. "Responsive web design," Eduvantage, 1(1), (2013).

[12] Nurakun Kyzy Z., Begimkulov Ch., Ismailova R., Dündar H. "Evaluation of Distance Education Applications in the Kyrgyz Republic Universities," International Online Journal of Educational Sciences 9 (3), (2017), 653-662.

[13] Nurakun Kyzy Z., Ismailova R., Dündar H." Learning management system implementation: a case study in the Kyrgyz Republic," Interactive Learning Environments 26 (8), (2018), 1010-1022.

[14] Pan G., Bonk C.J. "The emergence of open-source software in China," The International Review of Research in Open and Distributed Learning, 8 (1), (2007).

[15] Paulsen M.F. "Online education systems: Discussion and definition of terms." NKI Distance Education, 202, (2002).

[16] Ruiz J.G., Mintzer M.J., Leipzig R.M.. The impact of e-learning in medical education. Academic medicine, 81 (3), (2006). 207-212.

[17] Sife A., Lwoga E., Sanga C. New technologies for teaching and learning: Challenges for higher learning institutions in developing countries. International journal of education and development using ICT, 3 (2). (2007).

[18] Ssemugabi S. "Usability evaluation of a web-based e-learning application: a study of two evaluation method", Ph.D. dissertation, Information Systems Dept., Univ. of South Africa, (2009).

[19] w3school. "About W3Schools," Retrieved from https://www.w3schools.com/about/default.asp , (2018), access date November, 1, 2018

MANAS Journal of Engineering
ISSN 1694-7398 | e-ISSN 1694-7398

Volume 6 (Issue 2) (2018) Pages 193-202

Asymptotics of the Solution of the Parabolic Problem with a Stationary Phase and an Additive Free Member

Asan Omuraliev[1], Ella Abylaeva[1]

[1] Kyrgyz – Turkish Manas University, Faculty of Science, Department of Applied Mathematics and Informatics, Bishkek, Kyrgyzstan, asan.omuraliev@mail.ru; abylaeva.ella@gmail.com

Received: 02.10.2018; Accepted: 29.11.2018

Abstract: *In this paper we construct the asymptotics of the solution of the singularly perturbed parabolic problem with the stationary phase and the additive free term by using the regularization method for singularly perturbed problems. In this case, the asymptotic solution consists of regular and boundary layer terms. The boundary layer members are parabolic, power and rapidly oscillating boundary layer functions, and their products. These products are called angular boundary layer functions. Angular boundary layer functions have two components: the first is described by the product of a parabolic boundary layer function and a boundary layer function, which has a rapidly oscillating change.*

Keywords: *Asymptotics, singularly perturbed parabolic problem, stationary phase.*

1. INTRODUCTION

Singularly perturbed problems with rapidly oscillating free terms were studied in [1 - 3]. In [1], authors mostly focused on ordinary differential equations with a rapidly oscillating free term whose phase does not have stationary points. Using the regularization method for singularly perturbed problems [5], differential equations of parabolic type with a small parameter where fast-oscillating functions as a free member were studied in [2 - 3]. The asymptotic solutions constructed in [1 - 3] contain a boundary layer function having a rapidly oscillating character of change. In addition to such boundary-layer function, ordinary differential equations that contain an exponential boundary layer were studied in [1], parabolic equations with parabolic boundary layer were studied in [2], [3] and angular boundary layer were considered in [2], [6]. If the phase of the free term has stationary points, then boundary layers have an additional rise, which is due to a power character of a change. In this case, the asymptotic solution consists of regular and boundary layer terms. The boundary layer members are parabolic and power, rapidly oscillating boundary layer functions, and their products, which are called angular boundary layer functions [5]. In this paper we used the methods of [5], [6] to solve the parabolic problem.

2. ASYMPTOTIC CONSTRUCTION

2.1. Statement of the Problem

In this paper we study the following problem:

$$L_\varepsilon u\,(x,t,\varepsilon) \equiv \partial_t u - \varepsilon^2 a(x)\partial_x^2 u - b(x,t)u = \sum_{k=1}^{N} f_к(x,t)\exp\left(\frac{i\theta_к(t)}{\varepsilon}\right), (x,t)\in\Omega, \tag{1}$$

$$u(x,t,\varepsilon)|_{t=0} = u(x,t,\varepsilon)|_{x=0} = u(x,t,\varepsilon)|_{x=1} = 0$$

where $\varepsilon > 0$ – is a small parameter, $\Omega = \{(x, t): x \in (0,1),\ t \in (0,T]\}$.
The problem is solved under the following assumptions:

1. $a(x) > 0,\ a(x) \in C^\infty[0,1],\ b(x,t),\ f(x,t) \in C^\infty(\bar{\Omega})$,
2. $\forall\, x \in [0,1]$ function $a(x) > 0$
3. $\theta_k'(t) = 0$ – is the phase function.

2.2. Regularization of the Problem

For the regularization of the problem (1) we introduce regularizing independent variables using methods described in [4] and [6]:

$$\eta = \frac{t}{\varepsilon^2},\ r_k = \frac{i\,[\theta_k(t)-\theta_k(0)]}{\varepsilon}, \xi_\nu = \frac{\varphi_\nu(x)}{\varepsilon},\ i = \sqrt{-1}, \tag{2}$$

$$\zeta_\nu = \frac{\varphi_\nu(x)}{\varepsilon^2},\ \varphi_\nu(x) = (-1)^{\nu-1}\int_{\nu-1}^{x}\frac{ds}{\sqrt{a(s)}},\ \nu = 1,2\ ,$$

$$\sigma_k = \int_0^t exp(\frac{i\,[\theta_к(s)-\theta_к(0)]}{\varepsilon})ds \equiv p_к(t,\varepsilon), l = \overline{0,r}, j = \overline{0,k_l-1}$$

Instead of the desired function $u(x,t,\varepsilon)$ we study the extended function

$\breve{u}(M,\varepsilon), M=(x,t,r,\eta,\sigma,\xi,\zeta), \sigma=(\sigma_1,\sigma_2\dots\sigma_N),\ r=(r_1,r_2\dots r_N),\ \xi=(\xi_1,\xi_2), \zeta=(\zeta_1,\zeta_2)$ such that its constriction by regularizing variables coincides with the desired solution:

$$\breve{u}(M,\varepsilon)|_{\gamma=p(x,t,\varepsilon)} \equiv u(x,t,\varepsilon) \qquad \gamma=(r,\sigma,\eta,\xi,\zeta) \tag{3}$$

Taking into account (2) and (3), we find the derivatives:

$$\partial_t u(x,t,\varepsilon) \equiv (\partial_t \breve{u}(M,\varepsilon) + \frac{1}{\varepsilon^2}\partial_\eta \breve{u}(M,\varepsilon) + \sum_{k=1}^{N}[\frac{i\theta_k{}'(t)}{\varepsilon}\partial_{r_k}\breve{u}(M,\varepsilon) + exp(r_k)\,\partial_{\sigma_k}\breve{u}(M,\varepsilon))|_{\gamma=p(x,t,\varepsilon)},$$

$$\partial_x u(x,t,\varepsilon) \equiv \left((\partial_x \breve{u}\,(M,\varepsilon) + \sum_{\nu=1}^{2}\left\{\frac{\varphi_\nu'(x)}{\varepsilon}\partial_{\xi_\nu}\breve{u}(M,\varepsilon) + \frac{\varphi_\nu'(x)}{\varepsilon^2}\partial_{\zeta_\nu}\breve{u}(M,\varepsilon)\right\}\right)|_{\gamma=p(x,t,\varepsilon)},$$

$$\begin{aligned}\partial_x^2 u(x,t,\varepsilon) \equiv \Bigg(& (\partial_x^2 \breve{u}\,(M,\varepsilon) \\ & + \sum_{\nu=1}^{2}\left\{\left(\frac{\varphi_\nu'(x)}{\varepsilon}\right)^2\partial_{\xi_\nu}^2\breve{u}(M,\varepsilon) + \left(\frac{\varphi_\nu'(x)}{\varepsilon^2}\right)^2\partial_{\zeta_\nu}^2\breve{u}(M,\varepsilon) + \frac{1}{\varepsilon}D_{\xi,\nu}\breve{u}(M,\varepsilon)\right. \\ & \left.+\frac{1}{\varepsilon^2}D_{\zeta,\nu}\breve{u}(M,\varepsilon)\right\}\Bigg)|_{\gamma=p(x,t,\varepsilon)}\end{aligned} \tag{4}$$

$$D_{\xi,\nu} \equiv 2\varphi_\nu'(x)\partial_{x,\xi_\nu}^2 + \varphi_\nu''(x)\partial_{\xi_\nu},$$

$$D_{\zeta,\nu} \equiv 2\varphi_\nu'(x)\partial_{x,\zeta_\nu}^2 + \varphi_\nu''(x)\partial_{\zeta_\nu}.$$

On the basis of (1), (2), (3), (4) for the extended function $\breve{u}(M,\varepsilon)$ we set the problem as:

$$\begin{aligned}\widetilde{L_\varepsilon}\breve{u}(M,\varepsilon) &\equiv \frac{1}{\varepsilon^2}T_0\breve{u}(M,\varepsilon) + \sum_{k=1}^{N}\frac{i\theta'_k(t)}{\varepsilon}\partial_{r_k}\breve{u}(M,\varepsilon) + T_1\breve{u}(M,\varepsilon) \\ &= \sum_{k=1}^{N} f_k(x,t)\,exp\left(r_k + \frac{i\theta_k(0)}{\varepsilon}\right) + L_\zeta\breve{u}(M,\varepsilon) + \varepsilon L_\xi\breve{u}(M,\varepsilon) + \varepsilon^2 L_x\breve{u}(M,\varepsilon)\end{aligned}$$

$$\breve{u}(M,\varepsilon)|_{t=r_k=\eta=0} = \breve{u}(M,\varepsilon)|_{x=0,\xi_1=\zeta_1=0} = \breve{u}(M,\varepsilon)|_{x=1,\xi_2=\zeta_2=0} = 0, \tag{5}$$

$$T_1 \equiv \partial_\eta - \sum_{\nu=1}^{2}\partial_{\zeta_\nu}^2,$$

$$T_2 \equiv \partial_t - \sum_{\nu=1}^{2}\partial_{\xi_\nu}^2 - b(x,t) + \sum_{k=1}^{N}\exp(r_k)\,\partial_{\sigma_k},$$

$$L_\xi \equiv a(x)\sum_{v=1}^{2} D_{\xi,v},$$

$$L_\zeta \equiv a(x)\sum_{v=1}^{2} D_{\zeta,v},$$

$$L_x \equiv a(x)\partial_x^2.$$

The problem (5) is regular in ε as ε → 0:

$$\left(\widetilde{L_\varepsilon}\breve{u}(M,\varepsilon)\right)|_{q=q(x,t,\varepsilon)} \equiv L_\varepsilon \breve{u}(x,t,\varepsilon). \tag{6}$$

2.3. Solution of Iterative Problems

The solution of the problem (5) is determined in the form of a series

$$\breve{u}(M,\varepsilon) = \sum_{v=0}^{\infty} \varepsilon^v u_v(M). \tag{7}$$

For the coefficients of this series we obtain the following iterative problems:

$$T_1 u_0(M) = 0, \qquad T_1 u_1(M) = -i\sum_{k=1}^{N} \theta_k'(t)\,\partial_{r_k} u_0(M),$$

$$T_1 u_2(M) = -i\sum_{k=1}^{N} \theta_k'(t)\partial_{r_k} u_1(M) - T_2 u_0(M) + \sum_{k=1}^{N} f_к(x,t)\,exp\left(r_k + \frac{i\theta_к(0)}{\varepsilon}\right),$$

$$+L_\zeta u_0(M) \tag{8}$$

$$T_1 u_v(M) = -i\sum_{k=1}^{N} \theta_k'(t)\partial_{r_k} u_{v-1}(M) - T_2 u_{v-2}(M) + L_\zeta u_{v-2} + L_\xi u_{v-3}(M)$$

$$+ L_x u_{v-4}(M),$$

The solution of this problem contains parabolic boundary layer functions, internal power boundary layer functions which are connected with a rapidly oscillating free term a phase which are vanishes at $t = t_l, l = 0, 1, \ldots\ldots, n$ in addition, the asymptotics also contain angular boundary layer functions. We introduce a class of functions in which the iterative problems are solved:

$$G_0 \cong C^\infty(\bar{\Omega}), G_1 = \left\{u(M): u(M) = \oplus_{l=1}^{2} G_0 \otimes erfc\left(\frac{\xi_l}{2\sqrt{t}}\right)\right\},$$

$$G_2 = \{u(M): u(M) = \oplus_{k=1}^{N} G_0 \otimes exp(r_k)\},$$

$$G_3 = \left\{u(M): u(M) = \oplus_{k=1}^{N}\oplus_{l=1}^{2} Y_k^l(N_l) \otimes exp(r_k), \left\|Y_k^l(N_l)\right\| < c\,exp\left(-\frac{\varsigma_l^2}{8\eta}\right)\right\},$$

$$G_4 = \left\{u(M): u(M) = \oplus_{k=1}^{N} G_0 \left(\oplus_{l=1}^{2} G_0 \otimes erfc\left(\frac{\xi_l}{2\sqrt{t}}\right)\right)\sigma_k \right\}, N_l = (x, t, \eta, \varsigma_1, \varsigma_2)$$

From these spaces we construct a new space:

$$G = \oplus_{l=0}^{4} G_l.$$

The element $u(M) \epsilon G$ has the form:

$$\begin{aligned} u(M) = v(x,t) &+ \sum_{l=1}^{2} w^l(x,t) erfc\left(\frac{\xi_l}{2\sqrt{t}}\right) \\ &+ \sum_{k=1}^{N}\left[c_k(x,t) + \sum_{l=1}^{2} Y_k^l(N_l)\right] exp(r_k) \\ &+ \sum_{k=1}^{N}\left[z_k(x,t) + \sum_{l=1}^{2} q_k^l(x,t) erfc\left(\frac{\xi_l^2}{2\sqrt{t}}\right)\right]\sigma_k. \end{aligned} \tag{9}$$

2.4. Solvability of Intermediate Tasks

The iterative problems (9) in general form can be written as:

$$T_1 u(M) = H(M). \tag{10}$$

Theorem 1. Suppose that the conditions 1)-3) and $H(M) \epsilon G_3$ are satisfied. Then equation (10) is solvable in *G*.

Proof. Let the free term $H(M) \epsilon G_3$ be representable in the form:

$$H(M) = \sum_{k=1}^{N}\sum_{l=1}^{2} H_k^l(N_l), \quad \left\|H_k^l(N_l)\right\| < c\, exp\left(\frac{\varsigma_l^2}{8\eta}\right),$$

then, by directly substituting function $u(M) \epsilon\, G$ from (9) in (10) we see that this function is a solution of a given problem if and only if the function $Y_k^l(N_l)$ is a solution of equation:

$$\partial_\eta Y_k^l(N_l) = \partial_{\varsigma_l}^2 Y_k^l(N_l) + H_k^l(N_l), \; l = 1,2, \; k = 1,2,\ldots,N. \tag{11}$$

With the corresponding boundary conditions, this equation has a solution which has the estimate:

$$\left\|Y_k^l(N_l)\right\| < c\, exp\left(\frac{\varsigma_l^2}{8\eta}\right).$$

The theorem is proved.

Theorem 2. Suppose that the conditions of Theorem 1 are satisfied. Then, under the following additional conditions

1. $u(M)|_{t=\eta=0} = 0, u(M)|_{x=l-1,\xi_l=0,\varsigma_l=0} = 0, l = 1,2;$
2. $L_\varsigma u(M) = 0, L_\xi u(M) = 0;$
3. $i\sum_{k=1}^{N} \theta_k'(t) \partial_{r_k} u_v(M) + T_2 u_{v-1}(M) + h(M) \in G_3.$

equation (10) is uniquely solvable.

Proof. By Theorem 1 equation (10) has a solution that can be written in the form (9). If condition 1) is satisfied, we obtain:

$$\begin{gathered} v(x,t)|_{t=0} = -\sum_{k=1}^{N} c_k(x,0), w^l(x,t)|_{t=0} = \bar{w}^l(x), \\ Y_k^l(N_l)|_{t=\eta=0} = 0, q_k^l(x,t)|_{t=0}=\bar{q}_k^l(x), d_k^l(x,t)|_{t=0} = \bar{d}_k^l(x), \\ w^l(x,t)|_{x=l-1} = -c_k(l-1,t), q_k^l(x,t)|_{x=l-1} = -z_k(l-1,t), l = 1,2. \end{gathered} \tag{12}$$

Due to the fact that the function $erfc\left(\frac{\theta}{2\sqrt{t}}\right)$ is zero at $\theta = 0$ the values for $w^l(x,t)|_{t=0}, q_k^l(x,t)|_{t=0}$ are chosen arbitrarily.

We calculate:

$$\begin{aligned} & i\sum_{k=1}^{N}\theta_k'(t)\partial_{r_k}u_v(M) + T_2u_{v-1}(M) + h(M) \\ & = i\sum_{k=1}^{N}\theta_k'(t)\left[c_{k,v}(x,t) + \sum_{l=1}^{2}Y_{k,v}^l(N_l)\right]\exp(r_k) \\ & + [\partial_t v_{v-1}(x,t) - b(x,t)v_{v-1}(x,t)] \\ & + \sum_{l=1}^{2}[\partial_t w_{v-1}^l(x,t) - b(x,t)w_{v-1}^l(x,t)]erfc\left(\frac{\xi_l}{2\sqrt{t}}\right) \\ & + \sum_{k=1}^{N}\left[\partial_t c_{k,v-1}(x,t) - b(x,t)c_{k,v-1}(x,t)\right. \\ & \left. + \sum_{l=1}^{2}(\partial_t Y_{k,v-1}^l(N_l) - b(x,t)Y_{k,v-1}^l(N_l))\right]\exp(\tau_k) \\ & + \sum_{k=1}^{N}\left\{\partial_t z_{k,v-1}(x,t) - (x,t)z_{k,v-1}(x,t)\right. \\ & \left. + \sum_{l=1}^{2}[\partial_t q_{k,v-1}^l(x,t) - b(x,t)q_{k,v-1}^l(x,t)]erfc\left(\frac{\xi_l}{2\sqrt{t}}\right)\right\}\sigma_k \\ & + \sum_{k=1}^{N}\left[z_{k,v-1}(x,t) + \sum_{l=1}^{2}q_{k,v-1}^l(x,t)erfc\left(\frac{\xi_l}{2\sqrt{t}}\right)\right]exp(\tau_k) + h_0(x,t) \\ & + \sum_{l=1}^{2}h_1^l(x,t)\,erfc\left(\frac{\xi_l}{2\sqrt{t}}\right) \\ & + \sum_{k=1}^{N}\left[h_2^k(x,t) + \sum_{l=1}^{2}h_2^{l,k}(x,t)\right]exp(\tau_k) \\ & + \sum_{k=1}^{N}\left[h_3^k(x,t) + \sum_{l=1}^{2}h_3^{l,k}(x,t)erfc\left(\frac{\xi_l}{2\sqrt{t}}\right)\right]\sigma_k. \end{aligned} \tag{13}$$

The condition (3) of the theorem will be ensured, if we choose arbitrarily in (9) as the solutions of the following equations:

$$\begin{gathered}\partial_t v_{v-1}(x,t) - b(x,t)v_{v-1}(x,t) = -h_0(x,t),\\ \partial_t w^l_{v-1}(x,t) - b(x,t)w^l_{v-1}(x,t) = -h^l_1(x,t),\\ \partial_t Y^l_{k,v-1}(N_l) - b(x,t)Y^l_{k,v-1}(N_l) = -\left(h^{l,k}_2(x,t) + q^l_{k,v-1}(x,t)erfc\left(\frac{\varsigma_l}{2\sqrt{\eta}}\right)\right),\\ \partial_t z_{k,v-1}(x,t) - b(x,t)z_{k,v-1}(x,t) = -h^k_3(x,t),\\ \partial_t q^l_{k,v-1}(x,t) - b(x,t)q^l_{k,v-1}(x,t) = -h^{l,k}_3(x,t),\\ i\theta'_k(t)c_{k,v}(x,t) = -z_{k,v-1}(x,t) - \left[\partial_t c_{k,v-1}(x,t) - b(x,t)c_{k,v-1}(x,t)\right] - h^k_2(x,t).\end{gathered} \tag{14}$$

After the choice of arbitrariness, expression (13) is rewritten as

$$i\sum_{k=1}^{N}\theta'_k(t)\partial_{r_k}u_v(M) + T_2u_{v-1}(M) + h(M) = \sum_{k=1}^{N}\sum_{l=1}^{2}\left[i\theta'_k(t)Y^l_{k,v}(N_l)\right]\exp(\tau_k) \in G_3$$

In (14), transition is made from $\xi_l/2\sqrt{t}$ to variable $\varsigma_l/2\sqrt{\eta}$. The function $Y^l_k(N_l)$ is defined as the solution of equation (11) under the boundary conditions from (12) in the form:

$$\begin{aligned}Y^l_k(N_l) = {} & d^l_k(x,t)erfc\left(\frac{\varsigma_l}{2\sqrt{\eta}}\right)\\ & + \frac{1}{2\sqrt{\pi}}\int_0^{\eta}\int_0^{\infty}\frac{H^l_k(\cdot)}{\sqrt{\eta-\tau}}\left[exp\left(-\frac{(\varsigma_l-y)^2}{4(\eta-\tau)}\right) - exp\left(-\frac{(\varsigma_l+y)^2}{4(\eta-\tau)}\right)\right]dyd\tau.\end{aligned} \tag{15}$$

We substitute this function in the corresponding equation from (14), then with respect to $d^l_k(x,t)$ we obtain a differential equation. By solving it under the initial condition $d^l_k(x,t)|_{t=0} = \bar{d}^l_k(x)$, we find

$$d^l_k(x,t) = \bar{d}^l_k(x,t)B(x,t) + P^l_k(x,t), B(x,t) = \exp\left(\int_0^t b(x,s)ds\right),$$

where $P^l_k(x,t)$-is known function.

By substituting the obtained function into condition for $d^l_k(x,t)|_{x=l-1}$ from (12) we define the value of $\bar{d}^l_k(x)|_{x=l-1}$. The obtained value is used as an initial condition for a differential equation with respect to $\bar{d}^l_k(x)$, which is obtained after substitution $d^l_k(x,t)$ into the first condition of 2). With that we ensure fulfillment of this condition and uniqueness of the function $Y^l_k(N_l)$. Due to the fact that $\theta'_k(t_k) = 0$, the last equation from (14) is solvable if

$$z^l_{k,v-1}(x,0) = -h^k_2(x,0) - \left[\partial_t c_{k,v-1}(x,t) - b(x,t)c_{k,v-1}(x,t)\right]|_{t=0}.$$

The obtained ratio is used as the initial condition for the differential equation with respect to $z^l_{k,v-1}(x,t)$ from (14).

The equation with respect to $v_{v-1}(x,t)$ under the initial condition from (12) determines this function uniquely. Equations with respect to $w^l_{k,v-1}(x,t), q^l_{k,v-1}(x,t)$ under the corresponding condition from (12) have solutions in the form:

$$w_{k,v-1}^{l}(x,t) = \bar{w}_{k,v-1}^{l}(x)B(x,t) + H_{1,v-1}^{l}(x,t),$$
$$q_{k,v-1}^{l}(x,t) = \bar{q}_{k,v-1}^{l}(x)B(x,t) + H_{2,v-1}^{l}(x,t) \quad (16)$$

where $H_{1,v-1}^{l}(x,t), H_{2,v-1}^{l}(x,t)$- are known functions.

By substituting (16) into the conditions under $x = l-1$ from (12), we define values of $\bar{w}_{k,v-1}^{l}(x)|_{x=l-1}, \bar{q}_{k,v-1}^{l}(x)|_{x=l-1}$. These conditions are used for solving differential equations which are obtained from second condition of (2):

$$L_{\xi}\left(w_{k,v-1}^{l}(x,t)erfc\left(\frac{\xi_l}{2\sqrt{t}}\right)\right) = 0, L_{\xi}\left(q_{k,v-1}^{l}(x,t)erfc\left(\frac{\xi_l}{2\sqrt{t}}\right)\right) = 0.$$

Thus function $u(M)$ is determined uniquely. The theorem is proved.

2.5. Solution of iteration problems

Equation (8) is homogeneous for *k* = 0, therefore by Theorem 1, it has a solution in *G* in the form:

$$u_0(M) = v_0(x,t) + \sum_{l=1}^{2} w^{l}(x,t)erfc\left(\frac{\xi_l}{2\sqrt{t}}\right) + \sum_{k=1}^{N}\left\{\left(c_{k,0}(x,t) + \sum_{l=1}^{2} Y_{k,0}^{l}(N_l)\right)\mathrm{e}^{r_k} + \left[z_{k,0}(x,t) + \sum_{l=1}^{2} q_{k,0}^{l}(x,t)erfc\left(\frac{\xi_l}{2\sqrt{t}}\right)\right]\sigma_k\right\} \quad (17)$$

The function $Y_{k,0}^{l}(N_l)$ is solution of the equation $\partial_{\eta} Y_{k,0}^{l}(N_l) = \partial_{\varsigma_l}^{2} Y_{k,0}^{l}(N_l)$ which satisfies

$$Y_{k,0}^{l}(N_l)|_{t=\eta=0} = 0, Y_{k,0}^{l}(N_l)|_{x=l-1,\ \varsigma_l=0} = -c_{k,0}(l-1,t).$$

From the last problem we define

$$Y_{k,0}^{l}(N_l) = d_{k,0}^{l}(x,t)\ erfc\left(\frac{\varsigma_l}{2\sqrt{\eta}}\right), d_{k,0}^{l}(x,t)|_{x=l-1} = -c_{k,0}(l-1,t), \text{where } d_{k,0}^{l}(x,t)|_{t=0} = \bar{d}_{k,0}^{l}(x).$$

$\bar{d}_{k,0}^{l}(x)$ is arbitrary function. In the next step the equation (8) for *k = 1* takes the form:

$$T_1 u_1(M) = -i\sum_{k=1}^{N} \theta_k'(t)\left[c_{k,0}(x,t) + \sum_{l=1}^{2} Y_{k,0}^{l}(N_l)\right]\mathrm{e}^{r_k}.$$

According to the Theorem 1, this equation is solvable in U, if $c_{k,0}(x,t)$=0 and the function $Y_{k,0}^{l}(N_l)$ is solution of the differential equation $\partial_{\eta} Y_{k,0}^{l}(N_l) = \partial_{\varsigma_l}^{2} Y_{k,0}^{l}(N_l) + H_{k,0}^{l}(N_l)$ and its solution can be written in the form (14), where $H_k^{l}(0) = i\theta_k'(t)Y_{k,0}^{l}(N_l)$. By satisfying conditions 1) -3) of Theorem 1 we obtain (see (14)):

$$\partial_t v_0 - b(x,t)v_0(x,t) = 0, \partial_t w_0^{l}(x,t) - b(x,t)w_0^{l}(x,t) = 0,$$
$$\partial_t d_{k,0}^{l}(x,t) - b(x,t)d_{k,0}^{l}(x,t) = -q_{k,0}^{l}(x,t), \quad (18)$$

$$\partial_t z_{k,0}(x,t) - b(x,t) z_{k,0}(x,t) = 0,$$

$$\partial_t q^l_{k,0}(x,t) - b(x,t) q^l_{k,0}(x,t) = 0,$$

$$i\theta'_k(t) c_{k,1}(x,t) = -z_{k,0}(x,t) + f_k(x,t) \exp\left(\frac{i\theta_\kappa(0)}{\varepsilon}\right),$$

$$L_\varsigma\left(d^l_{k,0}(x,t) erfc\left(\frac{\varsigma_l}{2\sqrt{\eta}}\right)\right) = 0$$

When the equation is solved with respect to $d^l_{k,0}(x,t)$, in the $q^l_{k,0}(x,t) erfc\left(\frac{\xi_l}{2\sqrt{t}}\right)$ occurs a transition:

$$\frac{\xi_l}{2\sqrt{t}} = \frac{\varsigma_l}{2\sqrt{\eta}}.$$

The initial conditions for equations (18) are determined from (12). Functions $w^l_0(x,t), d^l_{k,0}(x,t), q^l_{k,0}(x,t)$ are expressed through arbitrary functions $\bar{w}^l_0(x), \bar{d}^l_{k,0}(x), \bar{q}^l_{k,0}(x)$. These arbitrary functions provide the condition

$$L_\xi u_k(m) = 0, L_\varsigma u_k(m) = 0$$

ensuring the solvability of the equation with respect to $c^l_{k,1}(x,t)$. Suppose that

$$Z_{k,0}(x,t)|_{t=0} = f_k(x,t) exp\left(\frac{i\theta_k(0)}{\varepsilon}\right).$$

This relation is used by the initial condition for determining $Z_{k,0}(x,t)$ by putting in to the equation (18).

Repeating this process, we can determine all the coefficients of $u_k(m)$ of the partial sum.

$$u_{\varepsilon n}(m) = \sum_{i=0}^{n} \varepsilon^i u_i(m).$$

In each iteration with respect to $v_i(x,t), w^l_i(x,t), d^l_{k,i}(x,t), z_{k,i}(x,t), q^l_{k,i}(x,t)$, we obtain inhomogeneous equations.

2.6. Assessment of the Remainder Term.

For the remainder term

$$R_{\varepsilon n}(x,t,\varepsilon) \equiv R_{\varepsilon n}(m,\varepsilon)|_{\gamma=\rho(x,t,\varepsilon)} = u(x,t,\varepsilon) - \sum_{i=0}^{n} \varepsilon^i u_i(m)|_{\gamma=\rho(x,t,\varepsilon)},$$

taking into account (3), (6), we obtain the equation

$$L_\varepsilon R_{\varepsilon n}(x,t,\varepsilon) = \varepsilon^{n+1} g_n(x,t,\varepsilon)$$

with homogeneous boundary conditions. Using the maximum principle, as in [7], we get the estimate

$$|R_{\varepsilon n}(x,t,\varepsilon)| < c\varepsilon^{n+1}. \tag{19}$$

Theorem 3. Suppose that conditions 1) -3) are satisfied. Then the constructed solution is an asymptotic solution of problem (1), i.e. $\forall n = 0,1,2,$ ... the estimate is fair (18).

3. CONCLUSION

It is shown that the asymptotic solution of the problem contains parabolic, power, rapidly oscillating, and angular boundary layer functions. Angular boundary layer functions have two components: the first is described by the product of a parabolic boundary layer function and a boundary layer function, which has a rapidly oscillating change.

REFERENCES

[1] Feschenko S., Shkil N. and Nikolaenko L., Asymptotic methods in the theory of linear differential equations. Kiev, *Naukova Dumka*, (1966).

[2] Omuraliev A.S., Sadykova D.A., Regularization of a singularly perturbed parabolic problem with a fast-oscillating right-hand side. *Khabarshy –Vestnik of the Kazak National Pedagogical University*, 20, (2007), 202-207.

[3] Omuraliev A.S., Sheishenova Sh.K., Asymptotics of the solution of a parabolic problem in the absence of the spectrum of the limit operator and with a rapidly oscillating right-hand side. *Investigated on the integral-differential equations*, 42, (2010), 122-128.

[4] Lomov S., Introduction to the general theory of singular perturbations. Moscow. *Nauka*, (1981).

[5] Butuzov V.F., Asymptotics of the solution of a difference equation with small steps in a rectangular area. *Computational Mathematics and Mathematical Physics*, 3 (3), (1972), 582-597.

[6] Omuraliev A., Regularization of a two-dimensional singularly perturbed parabolic problem. *Journal of Computational Mathematics and Mathematical Physics*, 8 (46), (2006), 1423-1432.

[7] Ladyzhenskaya O. A., Solonnikov V. A., Uraltseva N. N., Linear and quasilinear equations of parabolic type. Moscow. *Nauka*, (1967).

MANAS Journal of Engineering
ISSN 1694-7398 | e-ISSN 1694-7398

Volume 6 (Issue 2) (2018) Pages 177-192

Solutions of the Rational Difference Equations

$$x_{n+1}=\frac{x_{n-15}}{1+x_{n-3}x_{n-7}x_{n-11}}$$

Dağıstan Şimşek[*1,2], Peyil Esengul kyzy[1]

[1]Kyrgyz – Turkish Manas University, Department of Applied Mathematics and Informatics, Bishkek, Kyrgyzstan
[2]Konya Technical University, Faculty of Engineering and Natural Sciences, Konya, Turkey
dagistan.simsek@manas.edu.kg , dsimsek@selcuk.edu.tr

Received: 12.10.2018; Accepted: 13.12.2018

Abstract: *In this paper we study the solution behavior of the difference equation of the form*

$$x_{n+1}=\frac{x_{n-15}}{1+x_{n-3}x_{n-7}x_{n-11}},\ \ n=0,1,2,3,...,$$

is examined. The initial conditions of the equation are arbitrary positive real numbers. Also, we discuss and illustrate the stability of the solutions in the neighborhood of the critical points and the periodicity of the considered equations.

Keywords: *Difference equation, period 16 solution*

1. INTRODUCTION

In recent times, the study of the periodic nature of nonlinear difference equations attracts a lot of interest. For some latest results that focus, among other problems, on the periodic nature of scalar nonlinear difference equations see, [3-19, 21-27]. Such problems often find applications in various fields of applied and theoretical mathematics, engineering, medicine, etc. In particular, they can be used to study the structural properties of various classes of functions, the behavior of the rational and algebraic polynomials and their derivatives and etc. (see, for example, [1, 2, 20])

Çinar, studied the following problems with positive initial values

$$x_{n+1}=\frac{x_{n-1}}{1+ax_nx_{n-1}}$$

$$x_{n+1}=\frac{x_{n-1}}{-1+ax_nx_{n-1}}$$

$$x_{n+1}=\frac{ax_{n-1}}{1+bx_nx_{n-1}}$$

for $n=0,1,2,...$ in [4, 5, 6], respectively.

In [21] Steviç assumed that $\beta=1$ and solved the following problem

$$x_{n+1}=\frac{x_{n-1}}{1+x_n} \qquad \text{for} \quad n=0,1,2,...,$$

where $x_{-1},x_0\in(0,\infty)$. Also**,** this results was generalized to the equation of the form:

$$x_{n+1}=\frac{x_{n-1}}{g(x_n)} \qquad \text{for} \quad n=0,1,2,...,$$

where $x_{-1},x_0\in(0,\infty)$.

Şimşek et. al., studied the following problems

$$x_{n+1}=\frac{x_{n-3}}{1+x_{n-1}}$$

$$x_{n+1}=\frac{x_{n-5}}{1+x_{n-2}}$$

with positive initial values for $n=0,1,2,...$ in [19,20], respectively.

In this paper we investigated the nonlinear difference equation of the form

$$x_{n+1}=\frac{x_{n-15}}{1+x_{n-3}x_{n-7}x_{n-11}},\ n=0,1,2,3,\ldots, \tag{1}$$

where $x_{-15},x_{-14},x_{-13},x_{-12},x_{-11},x_{-10},x_{-9},x_{-8},x_{-7},x_{-6},x_{-5},x_{-4},x_{-3},x_{-2},x_{-1},x_0\in(0,\infty)$

2. MAIN RESULT

Let $\bar{x}$ be the unique positive equilibrum of equation (1). Then clearly

$$\bar{x}=\frac{\bar{x}}{1+\bar{x}\bar{x}\bar{x}}\Rightarrow \bar{x}+\bar{x}^4=\bar{x}\Rightarrow \bar{x}^4=0\Rightarrow \bar{x}=0.$$

We can obtain $\bar{x}=0$.

Theorem 1. Consider the difference equation (1). Then the following statements are true:

a) The sequences $(x_{16n-15}),(x_{16n-14}),(x_{16n-13}),(x_{16n-12}),(x_{16n-11}),(x_{16n-10}),(x_{16n-9}),(x_{16n-8}),(x_{16n-7}),(x_{16n-6}),(x_{16n-5}),(x_{16n-4}),(x_{16n-3}),(x_{16n-2}),(x_{16n-1}),(x_{16n})$ are decreasing and there exist $a_1,a_2,\ldots,a_{16}\geq 0$ such that

$$\lim_{n\to\infty}x_{16n-15}=a_1,\lim_{n\to\infty}x_{16n-14}=a_2,\lim_{n\to\infty}x_{16n-13}=a_3,\lim_{n\to\infty}x_{16n-12}=a_4,\lim_{n\to\infty}x_{16n-11}=a_5,\lim_{n\to\infty}x_{16n-10}=a_6$$
$$\lim_{n\to\infty}x_{16n-9}=a_7,\lim_{n\to\infty}x_{16n-8}=a_8,\lim_{n\to\infty}x_{16n-7}=a_9,\lim_{n\to\infty}x_{16n-6}=a_{10},\lim_{n\to\infty}x_{16n-5}=a_{11},\lim_{n\to\infty}x_{16n-4}=a_{12},$$
$$\lim_{n\to\infty}x_{16n-3}=a_{13},\lim_{n\to\infty}x_{16n-2}=a_{14},\lim_{n\to\infty}x_{16n-1}=a_{15},\lim_{n\to\infty}x_{16n}=a_{16}$$

b) $(a_1,a_2,\ldots,a_{16},a_1,a_2,\ldots,a_{16},\ldots)$ is a solution of equation (1) of period 16.

c) $\lim_{n\to\infty}x_{16n-15}.\lim_{n\to\infty}x_{16n-11}.\lim_{n\to\infty}x_{16n-7}.\lim_{n\to\infty}x_{16n-3}=0;$
$\lim_{n\to\infty}x_{16n-14}.\lim_{n\to\infty}x_{16n-10}.\lim_{n\to\infty}x_{16n-6}.\lim_{n\to\infty}x_{16n-2}=0;$
$\lim_{n\to\infty}x_{16n-13}.\lim_{n\to\infty}x_{16n-9}.\lim_{n\to\infty}x_{16n-5}.\lim_{n\to\infty}x_{16n-1}=0;$
$\lim_{n\to\infty}x_{16n-12}.\lim_{n\to\infty}x_{16n-8}.\lim_{n\to\infty}x_{16n-4}.\lim_{n\to\infty}x_{16n}=0.$

or $a_1.a_5.a_9.a_{13}=0$, $a_2.a_6.a_{10}.a_{14}=0$, $a_3.a_7.a_{11}.a_{15}=0$, $a_4.a_8.a_{12}.a_{16}=0$.

d) If there exist $n_0\in\mathbb{N}$ such that $x_{n+1}\leq x_{n-11}$ for all $n\geq n_0$, then $\lim_{n\to\infty}x_n=0$.

e) The following formulas hold:

$$x_{16n+1} = x_{-15}(1-\frac{x_{-3}x_{-7}x_{-11}}{1+x_{-3}x_{-7}x_{-11}}\sum_{j=0}^{n}\prod_{i=1}^{4j}\frac{1}{1+x_{4i-3}x_{4i-7}x_{4i-11}});$$

$$x_{16n+2} = x_{-14}(1-\frac{x_{-2}x_{-6}x_{-10}}{1+x_{-2}x_{-6}x_{-10}}\sum_{j=0}^{n}\prod_{i=1}^{4j}\frac{1}{1+x_{4i-2}x_{4i-6}x_{4i-10}});$$

$$x_{16n+3} = x_{-13}(1-\frac{x_{-1}x_{-5}x_{-9}}{1+x_{-1}x_{-5}x_{-9}}\sum_{j=0}^{n}\prod_{i=1}^{4j}\frac{1}{1+x_{4i-1}x_{4i-5}x_{4i-9}});$$

$$x_{16n+4} = x_{-12}(1-\frac{x_{0}x_{-4}x_{-8}}{1+x_{0}x_{-4}x_{-8}}\sum_{j=0}^{n}\prod_{i=1}^{4j}\frac{1}{1+x_{4i}x_{4i-4}x_{4i-8}});$$

$$x_{16n+5} = x_{-11}(1-\frac{x_{-3}x_{-7}x_{-15}}{1+x_{-3}x_{-7}x_{-11}}\sum_{j=0}^{n}\prod_{i=1}^{4j+1}\frac{1}{1+x_{4i-3}x_{4i-7}x_{4i-11}});$$

$$x_{16n+6} = x_{-10}(1-\frac{x_{-2}x_{-6}x_{-14}}{1+x_{-2}x_{-6}x_{-10}}\sum_{j=0}^{n}\prod_{i=1}^{4j+1}\frac{1}{1+x_{4i-2}x_{4i-6}x_{4i-10}});$$

$$x_{16n+7} = x_{-9}(1-\frac{x_{-1}x_{-5}x_{-13}}{1+x_{-1}x_{-5}x_{-9}}\sum_{j=0}^{n}\prod_{i=1}^{4j+1}\frac{1}{1+x_{4i-1}x_{4i-5}x_{4i-9}});$$

$$x_{16n+8} = x_{-8}(1-\frac{x_{0}x_{-4}x_{-12}}{1+x_{0}x_{-4}x_{-8}}\sum_{j=0}^{n}\prod_{i=1}^{4j+1}\frac{1}{1+x_{4i}x_{4i-4}x_{4i-8}});$$

$$x_{16n+9} = x_{-7}(1-\frac{x_{-3}x_{-11}x_{-15}}{1+x_{-3}x_{-7}x_{-11}}\sum_{j=0}^{n}\prod_{i=1}^{4j+1}\frac{1}{1+x_{4i-3}x_{4i-7}x_{4i-11}});$$

$$x_{16n+10} = x_{-6}(1-\frac{x_{-2}x_{-10}x_{-14}}{1+x_{-2}x_{-6}x_{-10}}\sum_{j=0}^{n}\prod_{i=1}^{4j+1}\frac{1}{1+x_{4i-2}x_{4i-6}x_{4i-10}});$$

$$x_{16n+11} = x_{-5}(1-\frac{x_{-1}x_{-9}x_{-13}}{1+x_{-1}x_{-5}x_{-9}}\sum_{j=0}^{n}\prod_{i=1}^{4j+1}\frac{1}{1+x_{4i-1}x_{4i-5}x_{4i-9}});$$

$$x_{16n+12} = x_{-4}(1-\frac{x_{0}x_{-8}x_{-12}}{1+x_{0}x_{-4}x_{-8}}\sum_{j=0}^{n}\prod_{i=1}^{4j+1}\frac{1}{1+x_{4i}x_{4i-4}x_{4i-8}});$$

$$x_{16n+13} = x_{-3}(1-\frac{x_{-7}x_{-11}x_{-15}}{1+x_{-3}x_{-7}x_{-11}}\sum_{j=0}^{n}\prod_{i=1}^{4j+1}\frac{1}{1+x_{4i-3}x_{4i-7}x_{4i-11}});$$

$$x_{16n+14} = x_{-2}(1-\frac{x_{-6}x_{-10}x_{-14}}{1+x_{-2}x_{-6}x_{-10}}\sum_{j=0}^{n}\prod_{i=1}^{4j+1}\frac{1}{1+x_{4i-2}x_{4i-6}x_{4i-10}});$$

$$x_{16n+15} = x_{-1}(1-\frac{x_{-5}x_{-9}x_{-13}}{1+x_{-1}x_{-5}x_{-9}}\sum_{j=0}^{n}\prod_{i=1}^{4j+1}\frac{1}{1+x_{4i-1}x_{4i-5}x_{4i-9}});$$

$$x_{16n+16} = x_{0}(1-\frac{x_{-4}x_{-8}x_{-12}}{1+x_{0}x_{-4}x_{-8}}\sum_{j=0}^{n}\prod_{i=1}^{4j+1}\frac{1}{1+x_{4i}x_{4i-4}x_{4i-8}}).$$

f) If $x_{16n+1} \to a_1 \neq 0$, $x_{16n+5} \to a_5 \neq 0$ and $x_{16n+9} \to a_9 \neq 0$ then $x_{16n+13} \to 0$ as $n \to \infty$.

If $x_{16n+2} \to a_2 \neq 0$, $x_{16n+6} \to a_6 \neq 0$ and $x_{16n+10} \to a_{10} \neq 0$ then $x_{16n+14} \to 0$ as $n \to \infty$. İf $x_{16n+3} \to a_3 \neq 0$, $x_{16n+7} \to a_7 \neq 0$ and $x_{16n+11} \to a_{11} \neq 0$ then $x_{16n+15} \to 0$ as $n \to \infty$.

İf $x_{16n+4} \to a_4 \neq 0$, $x_{16n+8} \to a_8 \neq 0$ and $x_{16n+12} \to a_{12} \neq 0$ then $x_{16n+16} \to 0$ as $n \to \infty$.

Proof. a) Firstly, we consider the equation (1). From this equation we obtain:

$$x_{n+1}(1+x_{n-3}x_{n-7}x_{n-11}) = x_{n-15}.$$

If $x_{n-11}, x_{n-7}, x_{n-3} \in (0,+\infty)$, then $(1+x_{n-3}x_{n-7}x_{n-11}) \in (1,+\infty)$. Since $x_{n-15} > x_{n+1}$ $n_0 \in \mathbb{N}$, we obtain

$$\lim_{n\to\infty} x_{16n-15} = a_1, \lim_{n\to\infty} x_{16n-14} = a_2, \lim_{n\to\infty} x_{16n-13} = a_3, \lim_{n\to\infty} x_{16n-12} = a_4, \lim_{n\to\infty} x_{16n-11} = a_5, \lim_{n\to\infty} x_{16n-10} = a_6$$
$$\lim_{n\to\infty} x_{16n-9} = a_7, \lim_{n\to\infty} x_{16n-8} = a_8, \lim_{n\to\infty} x_{16n-7} = a_9, \lim_{n\to\infty} x_{16n-6} = a_{10}, \lim_{n\to\infty} x_{16n-5} = a_{11}, \lim_{n\to\infty} x_{16n-4} = a_{12},$$
$$\lim_{n\to\infty} x_{16n-3} = a_{13}, \lim_{n\to\infty} x_{16n-2} = a_{14}, \lim_{n\to\infty} x_{16n-1} = a_{15}, \lim_{n\to\infty} x_{16n} = a_{16}.$$

b) $(a_1, a_2, ..., a_{16}, a_1, a_2, ..., a_{16}, ...)$ is a solution of equation (1) of period 16.

c) Taking into account the equation (1), we obtain:

$$x_{16n+1} = \frac{x_{16n-15}}{1+x_{16n-3}x_{16n-7}x_{16n-11}}.$$

Taking limit as $n \to \infty$ on both sides of the above equality, we get:

$$\lim_{n\to\infty} x_{16n+1} = \lim_{n\to\infty} \frac{x_{16n-15}}{1+x_{16n-3}x_{16n-7}x_{16n-11}}.$$

Then

$$\lim_{n\to\infty} x_{16n+1}.\lim_{n\to\infty} x_{16n-3}.\lim_{n\to\infty} x_{16n-7}.\lim_{n\to\infty} x_{16n-11} = 0 \text{ or } a_1.a_5.a_9.a_{13} = 0.$$

Similarly,

$$\lim_{n\to\infty} x_{16n+2}.\lim_{n\to\infty} x_{16n-10}.\lim_{n\to\infty} x_{16n-6}.\lim_{n\to\infty} x_{16n-2} = 0 \text{ or } a_2.a_6.a_{10}.a_{14} = 0.$$

$$\lim_{n\to\infty} x_{16n+3}.\lim_{n\to\infty} x_{16n-9}.\lim_{n\to\infty} x_{16n-5}.\lim_{n\to\infty} x_{16n-1} = 0 \text{ or } a_3.a_7.a_{11}.a_{15} = 0.$$

$$\lim_{n\to\infty} x_{16n+4}.\lim_{n\to\infty} x_{16n-8}.\lim_{n\to\infty} x_{16n-4}.\lim_{n\to\infty} x_{16n} = 0 \text{ or } a_4.a_8.a_{12}.a_{16} = 0.$$

d) If there exist $n_0 \in \mathbb{N}$ such that $x_{n-11} \geq x_{n+1}$ for all $n \geq n_0$, then

$a_2 \leq a_6 \leq a_{10} \leq a_{14} \leq a_2, a_3 \leq a_7 \leq a_{11} \leq a_{15} \leq a_3, a_4 \leq a_8 \leq a_{12} \leq a_{16} \leq a_4, a_5 \leq a_9 \leq a_{13} \leq a_1 \leq a_5$

Since $a_{16}^2 = 0,\ a_{15}^2 = 0,\ a_{14}^2 = 0,\ a_{13}^2 = 0,\ a_{12}^2 = 0,\ a_{11}^2 = 0,\ a_{10}^2 = 0,\ a_9^2 = 0,\ a_8^2 = 0,$

$a_7^2 = 0,\ a_6^2 = 0,\ a_5^2 = 0,\ a_4^2 = 0,\ a_3^2 = 0,\ a_2^2 = 0,\ a_1^2 = 0$ we obtain the result.

e) Subracting x_{n-15} from the left and right-hand sides of equation (1) we obtain:

$$x_{n+1} - x_{n-15} = \frac{1}{1 + x_{n-3}x_{n-7}x_{n-11}}(x_{n-3} - x_{n-19})$$

and the following formula holds:

$$n \geq 4 \text{ for } \begin{cases} x_{4n-15} - x_{4n-31} = (x_1 - x_{-11}) \prod_{i=1}^{n-4} \dfrac{1}{1 + x_{4i-3}x_{4i-7}x_{4i-11}} \\ x_{4n-14} - x_{4n-30} = (x_2 - x_{-10}) \prod_{i=1}^{n-4} \dfrac{1}{1 + x_{4i-2}x_{4i-6}x_{4i-10}} \\ x_{4n-13} - x_{4n-29} = (x_1 - x_{-11}) \prod_{i=1}^{n-4} \dfrac{1}{1 + x_{4i-1}x_{4i-5}x_{4i-9}} \\ x_{4n-12} - x_{4n-28} = (x_2 - x_{-10}) \prod_{i=1}^{n-4} \dfrac{1}{1 + x_{4i}x_{4i-4}x_{4i-8}} \end{cases} \tag{2}$$

Replacing n by $4j$ in (2) and summing from $j = 0$ to $j = n$ we obtain:

$$\left.\begin{aligned} x_{16n+1} - x_{-15} &= (x_1 - x_{-15}) \sum_{j=0}^{n} \prod_{i=1}^{4j} \frac{1}{1 + x_{4i-3}x_{4i-7}x_{4i-11}} \\ x_{16n+2} - x_{-14} &= (x_2 - x_{-14}) \sum_{j=0}^{n} \prod_{i=1}^{4j} \frac{1}{1 + x_{4i-2}x_{4i-6}x_{4i-10}} \\ x_{12n+3} - x_{-13} &= (x_1 - x_{-13}) \sum_{j=0}^{n} \prod_{i=1}^{4j} \frac{1}{1 + x_{4i-1}x_{4i-5}x_{4i-9}} \\ x_{12n+4} - x_{-12} &= (x_2 - x_{-12}) \sum_{j=0}^{n} \prod_{i=1}^{4j} \frac{1}{1 + x_{4i}x_{4i-4}x_{4i-8}} \end{aligned}\right\} (n = 0,1,2,\ldots,) \tag{3}$$

Also, replacing n by $4j+1$ in (2) and summing up elements from $j=0$ to $j=n$ we obtain:

$$\left.\begin{aligned}
x_{16n+5}-x_{-11}&=(x_1-x_{-15})\sum_{j=0}^{n}\prod_{i=1}^{4j+1}\frac{1}{1+x_{4i-3}x_{4i-7}x_{4i-11}}\\
x_{16n+6}-x_{-10}&=(x_2-x_{-14})\sum_{j=0}^{n}\prod_{i=1}^{4j+1}\frac{1}{1+x_{4i-2}x_{4i-6}x_{4i-10}}\\
x_{16n+7}-x_{-9}&=(x_1-x_{-13})\sum_{j=0}^{n}\prod_{i=1}^{4j+1}\frac{1}{1+x_{4i-1}x_{4i-5}x_{4i-9}}\\
x_{16n+8}-x_{-8}&=(x_2-x_{-12})\sum_{j=0}^{n}\prod_{i=1}^{4j+1}\frac{1}{1+x_{4i}x_{4i-4}x_{4i-8}}
\end{aligned}\right\}(n=0,1,2,\ldots,) \tag{4}$$

Also, replacing n by $4j+2$ in (2) and summing up elements from $j=0$ to $j=n$ we obtain:

$$\left.\begin{aligned}
x_{16n+9}-x_{-7}&=(x_1-x_{-15})\sum_{j=0}^{n}\prod_{i=1}^{4j+2}\frac{1}{1+x_{4i-3}x_{4i-7}x_{4i-11}}\\
x_{16n+10}-x_{-6}&=(x_2-x_{-14})\sum_{j=0}^{n}\prod_{i=1}^{4j+2}\frac{1}{1+x_{4i-2}x_{4i-6}x_{4i-10}}\\
x_{16n+11}-x_{-5}&=(x_1-x_{-13})\sum_{j=0}^{n}\prod_{i=1}^{4j+2}\frac{1}{1+x_{4i-1}x_{4i-5}x_{4i-9}}\\
x_{16n+12}-x_{-4}&=(x_2-x_{-12})\sum_{j=0}^{n}\prod_{i=1}^{4j+2}\frac{1}{1+x_{4i}x_{4i-4}x_{4i-8}}
\end{aligned}\right\}(n=0,1,2,\ldots,) \tag{5}$$

Replacing n by $4j+3$ in (2) in a similar way and summing up elements from $j=0$ to $j=n$ we obtain:

$$\left.\begin{aligned} x_{16n+13}-x_{-3}&=(x_1-x_{-15})\sum_{j=0}^{n}\prod_{i=1}^{4j+3}\frac{1}{1+x_{4i-3}x_{4i-7}x_{4i-11}}\\ x_{16n+14}-x_{-2}&=(x_2-x_{-14})\sum_{j=0}^{n}\prod_{i=1}^{4j+3}\frac{1}{1+x_{4i-2}x_{4i-6}x_{4i-10}}\\ x_{16n+15}-x_{-1}&=(x_3-x_{-13})\sum_{j=0}^{n}\prod_{i=1}^{4j+3}\frac{1}{1+x_{4i-1}x_{4i-5}x_{4i-9}}\\ x_{16n+16}-x_{0}&=(x_4-x_{-12})\sum_{j=0}^{n}\prod_{i=1}^{4j+3}\frac{1}{1+x_{4i}x_{4i-4}x_{4i-8}} \end{aligned}\right\}(n=0,1,2,\ldots,) \tag{6}$$

Thus, we attained the formulas below:

$$\begin{aligned} x_{16n+1}&=x_{-15}(1-\frac{x_{-3}x_{-7}x_{-11}}{1+x_{-3}x_{-7}x_{-11}}\sum_{j=0}^{n}\prod_{i=1}^{4j}\frac{1}{1+x_{4i-3}x_{4i-7}x_{4i-11}});\\ x_{16n+2}&=x_{-14}(1-\frac{x_{-2}x_{-6}x_{-10}}{1+x_{-2}x_{-6}x_{-10}}\sum_{j=0}^{n}\prod_{i=1}^{4j}\frac{1}{1+x_{4i-2}x_{4i-6}x_{4i-10}});\\ x_{16n+3}&=x_{-13}(1-\frac{x_{-1}x_{-5}x_{-9}}{1+x_{-1}x_{-5}x_{-9}}\sum_{j=0}^{n}\prod_{i=1}^{4j}\frac{1}{1+x_{4i-1}x_{4i-5}x_{4i-9}});\\ x_{16n+4}&=x_{-12}(1-\frac{x_{0}x_{-4}x_{-8}}{1+x_{0}x_{-4}x_{-8}}\sum_{j=0}^{n}\prod_{i=1}^{4j}\frac{1}{1+x_{4i}x_{4i-4}x_{4i-8}}); \end{aligned} \tag{7}$$

$$\begin{aligned} x_{16n+5}&=x_{-11}(1-\frac{x_{-3}x_{-7}x_{-15}}{1+x_{-3}x_{-7}x_{-11}}\sum_{j=0}^{n}\prod_{i=1}^{4j+1}\frac{1}{1+x_{4i-3}x_{4i-7}x_{4i-11}});\\ x_{16n+6}&=x_{-10}(1-\frac{x_{-2}x_{-6}x_{-14}}{1+x_{-2}x_{-6}x_{-10}}\sum_{j=0}^{n}\prod_{i=1}^{4j+1}\frac{1}{1+x_{4i-2}x_{4i-6}x_{4i-10}});\\ x_{16n+7}&=x_{-9}(1-\frac{x_{-1}x_{-5}x_{-13}}{1+x_{-1}x_{-5}x_{-9}}\sum_{j=0}^{n}\prod_{i=1}^{4j+1}\frac{1}{1+x_{4i-1}x_{4i-5}x_{4i-9}});\\ x_{16n+8}&=x_{-8}(1-\frac{x_{0}x_{-4}x_{-12}}{1+x_{0}x_{-4}x_{-8}}\sum_{j=0}^{n}\prod_{i=1}^{4j+1}\frac{1}{1+x_{4i}x_{4i-4}x_{4i-8}}); \end{aligned} \tag{8}$$

$$
\begin{aligned}
x_{16n+9} &= x_{-7}\left(1-\frac{x_{-3}x_{-11}x_{-15}}{1+x_{-3}x_{-7}x_{-11}}\sum_{j=0}^{n}\prod_{i=1}^{4j+2}\frac{1}{1+x_{4i-3}x_{4i-7}x_{4i-11}}\right);\\
x_{16n+10} &= x_{-6}\left(1-\frac{x_{-2}x_{-10}x_{-14}}{1+x_{-2}x_{-6}x_{-10}}\sum_{j=0}^{n}\prod_{i=1}^{4j+2}\frac{1}{1+x_{4i-2}x_{4i-6}x_{4i-10}}\right);\\
x_{16n+11} &= x_{-5}\left(1-\frac{x_{-1}x_{-9}x_{-13}}{1+x_{-1}x_{-5}x_{-9}}\sum_{j=0}^{n}\prod_{i=1}^{4j+2}\frac{1}{1+x_{4i-1}x_{4i-5}x_{4i-9}}\right);\\
x_{16n+12} &= x_{-4}\left(1-\frac{x_{0}x_{-8}x_{-12}}{1+x_{0}x_{-4}x_{-8}}\sum_{j=0}^{n}\prod_{i=1}^{4j+2}\frac{1}{1+x_{4i}x_{4i-4}x_{4i-8}}\right);\\
x_{16n+13} &= x_{-3}\left(1-\frac{x_{-7}x_{-11}x_{-15}}{1+x_{-3}x_{-7}x_{-11}}\sum_{j=0}^{n}\prod_{i=1}^{4j+3}\frac{1}{1+x_{4i-3}x_{4i-7}x_{4i-11}}\right);\\
x_{16n+14} &= x_{-2}\left(1-\frac{x_{-6}x_{-10}x_{-14}}{1+x_{-2}x_{-6}x_{-10}}\sum_{j=0}^{n}\prod_{i=1}^{4j+3}\frac{1}{1+x_{4i-2}x_{4i-6}x_{4i-10}}\right);\\
x_{16n+15} &= x_{-1}\left(1-\frac{x_{-5}x_{-9}x_{-13}}{1+x_{-1}x_{-5}x_{-9}}\sum_{j=0}^{n}\prod_{i=1}^{4j+3}\frac{1}{1+x_{4i-1}x_{4i-5}x_{4i-9}}\right);\\
x_{16n+16} &= x_{0}\left(1-\frac{x_{-4}x_{-8}x_{-12}}{1+x_{0}x_{-4}x_{-8}}\sum_{j=0}^{n}\prod_{i=1}^{4j+3}\frac{1}{1+x_{4i}x_{4i-4}x_{4i-8}}\right).
\end{aligned}
\tag{9}
\tag{10}
$$

f) Suppose that $a_1 = a_5 = a_9 = a_{13} = 0$. By **e)** we have:

$$\lim_{n\to\infty} x_{16n+1} = \lim_{n\to\infty} x_{-15}\left(1-\frac{x_{-3}x_{-7}x_{-11}}{1+x_{-3}x_{-7}x_{-11}}\sum_{j=0}^{n}\prod_{i=1}^{4j}\frac{1}{1+x_{4i-3}x_{4i-7}x_{4i-11}}\right)$$

$$a_1 = x_{-15}\left(1-\frac{x_{-3}x_{-7}x_{-11}}{1+x_{-3}x_{-7}x_{-11}}\sum_{j=0}^{\infty}\prod_{i=1}^{4j}\frac{1}{1+x_{4i-3}x_{4i-7}x_{4i-11}}\right)$$

$$a_1 = 0 \Rightarrow \frac{1+x_{-3}x_{-7}x_{-11}}{x_{-3}x_{-7}x_{-11}} = \sum_{j=0}^{\infty}\prod_{i=1}^{4j}\frac{1}{1+x_{4i-3}x_{4i-7}x_{4i-11}} \tag{11}$$

Similarly,

$$\lim_{n\to\infty} x_{16n+5} = \lim_{n\to\infty} x_{-11}\left(1-\frac{x_{-3}x_{-7}x_{-15}}{1+x_{-3}x_{-7}x_{-11}}\sum_{j=0}^{n}\prod_{i=1}^{4j+1}\frac{1}{1+x_{4i-3}x_{4i-7}x_{4i-11}}\right)$$

$$a_5 = x_{-11}\left(1-\frac{x_{-3}x_{-7}x_{-15}}{1+x_{-3}x_{-7}x_{-11}}\sum_{j=0}^{\infty}\prod_{i=1}^{4j+1}\frac{1}{1+x_{4i-3}x_{4i-7}x_{4i-11}}\right)$$

$$a_5 = 0 \Rightarrow \frac{1+x_{-3}x_{-7}x_{-11}}{x_{-3}x_{-7}x_{-15}} = \sum_{j=0}^{\infty}\prod_{i=1}^{4j+1}\frac{1}{1+x_{4i-3}x_{4i-7}x_{4i-11}} \tag{12}$$

From equations (11) and (12),

$$\frac{1+x_{-3}x_{-7}x_{-11}}{x_{-3}x_{-7}x_{-11}} = \sum_{j=0}^{\infty}\prod_{i=1}^{4j}\frac{1}{1+x_{4i-3}x_{4i-7}x_{4i-11}} > \frac{1+x_{-3}x_{-7}x_{-11}}{x_{-3}x_{-7}x_{-15}} = \sum_{j=0}^{\infty}\prod_{i=1}^{4j+1}\frac{1}{1+x_{4i-3}x_{4i-7}x_{4i-11}} \tag{13}$$

thus, $x_{-11} > x_{-15}$.

Similarly,

$$\lim_{n\to\infty} x_{16n+9} = \lim_{n\to\infty} x_{-7}\left(1-\frac{x_{-3}x_{-11}x_{-15}}{1+x_{-3}x_{-7}x_{-11}}\sum_{j=0}^{n}\prod_{i=1}^{4j+1}\frac{1}{1+x_{4i-3}x_{4i-7}x_{4i-11}}\right)$$

$$a_9 = x_{-7}\left(1-\frac{x_{-3}x_{-11}x_{-15}}{1+x_{-3}x_{-7}x_{-11}}\sum_{j=0}^{\infty}\prod_{i=1}^{4j+1}\frac{1}{1+x_{4i-3}x_{4i-7}x_{4i-11}}\right)$$

$$a_9 = 0 \Rightarrow \frac{1+x_{-3}x_{-7}x_{-11}}{x_{-3}x_{-11}x_{-15}} = \sum_{j=0}^{\infty}\prod_{i=1}^{4j+1}\frac{1}{1+x_{4i-3}x_{4i-7}x_{4i-11}} \tag{14}$$

From (12) and (14),

$$\frac{1+x_{-3}x_{-7}x_{-11}}{x_{-3}x_{-7}x_{-15}} = \sum_{j=0}^{\infty}\prod_{i=1}^{4j+1}\frac{1}{1+x_{4i-3}x_{4i-7}x_{4i-11}} > \frac{1+x_{-3}x_{-7}x_{-11}}{x_{-3}x_{-11}x_{-15}} = \sum_{j=0}^{\infty}\prod_{i=1}^{4j+1}\frac{1}{1+x_{4i-3}x_{4i-7}x_{4i-11}} \tag{15}$$

thus, $x_{-7} > x_{-11}$.

Similarly,

$$\lim_{n\to\infty} x_{16n+13} = \lim_{n\to\infty} x_{-3}\left(1-\frac{x_{-7}x_{-11}x_{-15}}{1+x_{-3}x_{-7}x_{-11}}\sum_{j=0}^{n}\prod_{i=1}^{4j+1}\frac{1}{1+x_{4i-3}x_{4i-7}x_{4i-11}}\right)$$

$$a_{13} = x_{-3}\left(1-\frac{x_{-7}x_{-11}x_{-15}}{1+x_{-3}x_{-7}x_{-11}}\sum_{j=0}^{\infty}\prod_{i=1}^{4j+1}\frac{1}{1+x_{4i-3}x_{4i-7}x_{4i-11}}\right)$$

$$a_{13} = 0 \Rightarrow \frac{1+x_{-3}x_{-7}x_{-11}}{x_{-7}x_{-11}x_{-15}} = \sum_{j=0}^{\infty}\prod_{i=1}^{4j+1}\frac{1}{1+x_{4i-3}x_{4i-7}x_{4i-11}} \tag{16}$$

From (14) and (16),

$$\frac{1+x_{-3}x_{-7}x_{-11}}{x_{-3}x_{-11}x_{-15}}=\sum_{j=0}^{\infty}\prod_{i=1}^{4j+1}\frac{1}{1+x_{4i-3}x_{4i-7}x_{4i-11}}>\frac{1+x_{-3}x_{-7}x_{-11}}{x_{-7}x_{-11}x_{-15}}=\sum_{j=0}^{\infty}\prod_{i=1}^{4j+1}\frac{1}{1+x_{4i-3}x_{4i-7}x_{4i-11}} \tag{17}$$

thus, $x_{-3}>x_{-7}$.

Hence we obtain $x_{-3}>x_{-7}>x_{-11}>x_{-15}$.

Suppose that $a_2=a_6=a_{10}=a_{14}=0$. The proofs of the following equations' correctness can be done similarly to the proofs of (13), (15), (17) and therefore, will be omitted here.

$$\frac{1+x_{-2}x_{-6}x_{-10}}{x_{-2}x_{-6}x_{-10}}=\sum_{j=0}^{\infty}\prod_{i=1}^{4j}\frac{1}{1+x_{4i-2}x_{4i-6}x_{4i-10}}>\frac{1+x_{-2}x_{-6}x_{-10}}{x_{-2}x_{-6}x_{-14}}=\sum_{j=0}^{\infty}\prod_{i=1}^{4j+1}\frac{1}{1+x_{4i-2}x_{4i-6}x_{4i-10}} \tag{18}$$

$$\frac{1+x_{-2}x_{-6}x_{-10}}{x_{-2}x_{-6}x_{-14}}=\sum_{j=0}^{\infty}\prod_{i=1}^{4j+1}\frac{1}{1+x_{4i-2}x_{4i-6}x_{4i-10}}>\frac{1+x_{-2}x_{-6}x_{-10}}{x_{-2}x_{-10}x_{-14}}=\sum_{j=0}^{\infty}\prod_{i=1}^{4j+1}\frac{1}{1+x_{4i-2}x_{4i-6}x_{4i-10}} \tag{19}$$

$$\frac{1+x_{-2}x_{-6}x_{-10}}{x_{-2}x_{-10}x_{-14}}=\sum_{j=0}^{\infty}\prod_{i=1}^{4j+1}\frac{1}{1+x_{4i-2}x_{4i-6}x_{4i-10}}>\frac{1+x_{-2}x_{-6}x_{-10}}{x_{-6}x_{-10}x_{-14}}=\sum_{j=0}^{\infty}\prod_{i=1}^{4j+1}\frac{1}{1+x_{4i-2}x_{4i-6}x_{4i-10}} \tag{20}$$

thus, $x_{-2}>x_{-6}>x_{-10}>x_{-14}$.

For the case where $a_3=a_7=a_{11}=a_{15}=0$, the proofs is similar to the proofs of the (13), (15), (17) and therefore, will be omitted here.

$$\frac{1+x_{-1}x_{-5}x_{-9}}{x_{-1}x_{-5}x_{-9}}=\sum_{j=0}^{\infty}\prod_{i=1}^{4j}\frac{1}{1+x_{4i-1}x_{4i-5}x_{4i-9}}>\frac{1+x_{-1}x_{-5}x_{-9}}{x_{-1}x_{-5}x_{-13}}=\sum_{j=0}^{\infty}\prod_{i=1}^{4j+1}\frac{1}{1+x_{4i-1}x_{4i-5}x_{4i-9}} \tag{21}$$

$$\frac{1+x_{-1}x_{-5}x_{-9}}{x_{-1}x_{-5}x_{-13}}=\sum_{j=0}^{\infty}\prod_{i=1}^{4j+1}\frac{1}{1+x_{4i-1}x_{4i-5}x_{4i-9}}>\frac{1+x_{-1}x_{-5}x_{-9}}{x_{-1}x_{-9}x_{-13}}=\sum_{j=0}^{\infty}\prod_{i=1}^{4j+1}\frac{1}{1+x_{4i-1}x_{4i-5}x_{4i-9}} \tag{22}$$

$$\frac{1+x_{-1}x_{-5}x_{-9}}{x_{-1}x_{-9}x_{-13}}=\sum_{j=0}^{\infty}\prod_{i=1}^{4j+1}\frac{1}{1+x_{4i-1}x_{4i-5}x_{4i-9}}>\frac{1+x_{-1}x_{-5}x_{-9}}{x_{-5}x_{-9}x_{-13}}=\sum_{j=0}^{\infty}\prod_{i=1}^{4j+1}\frac{1}{1+x_{4i-1}x_{4i-5}x_{4i-9}} \tag{23}$$

thus, $x_{-1}>x_{-5}>x_{-9}>x_{-13}$.

Suppose that $a_4=a_8=a_{12}=a_{16}=0$. As in the cases above, the proofs of the following equations is similar to the proofs of (13), (15), (17) and therefore, will be omitted here as well.

$$\frac{1+x_{0}x_{-4}x_{-8}}{x_{0}x_{-4}x_{-8}}=\sum_{j=0}^{\infty}\prod_{i=1}^{4j}\frac{1}{1+x_{4i}x_{4i-4}x_{4i-8}}>\frac{1+x_{0}x_{-4}x_{-8}}{x_{0}x_{-4}x_{-12}}=\sum_{j=0}^{\infty}\prod_{i=1}^{4j+1}\frac{1}{1+x_{4i}x_{4i-4}x_{4i-8}} \tag{24}$$

$$\frac{1+x_0x_{-4}x_{-8}}{x_0x_{-4}x_{-12}}=\sum_{j=0}^{\infty}\prod_{i=1}^{4j+1}\frac{1}{1+x_{4i}x_{4i-4}x_{4i-8}}>\frac{1+x_0x_{-4}x_{-8}}{x_0x_{-8}x_{-12}}=\sum_{j=0}^{\infty}\prod_{i=1}^{4j+1}\frac{1}{1+x_{4i}x_{4i-4}x_{4i-8}} \quad (25)$$

$$\frac{1+x_0x_{-4}x_{-8}}{x_0x_{-8}x_{-12}}=\sum_{j=0}^{\infty}\prod_{i=1}^{4j+1}\frac{1}{1+x_{4i}x_{4i-4}x_{4i-8}}>\frac{1+x_0x_{-4}x_{-8}}{x_{-4}x_{-8}x_{-12}}=\sum_{j=0}^{\infty}\prod_{i=1}^{4j+1}\frac{1}{1+x_{4i}x_{4i-4}x_{4i-8}} \quad (26)$$

thus, $x_0 > x_{-4} > x_{-8} > x_{-12}$.

Hence we obtain $x_0 > x_{-4} > x_{-8} > x_{-12}$, $x_{-1} > x_{-5} > x_{-9} > x_{-13}$, $x_{-2} > x_{-6} > x_{-10} > x_{-14}$, $x_{-3} > x_{-7} > x_{-11} > x_{-15}$. Thus, we face a contradiction which completes the proof of theorem.

3. EXAMPLES

Example 3.1: Consider the following equation $x_{n+1}=\frac{x_{n-15}}{1+x_{n-3}x_{n-7}x_{n-11}}$.

If the initial conditions are selected as:

$$x[-15]=2; x[-14]=3; x[-13]=4; x[-12]=5; x[-11]=6; x[-10]=7; x[-9]=8;$$
$$x[-8]=9; x[-7]=10; x[-6]=11; x[-5]=12; x[-4]=13; x[-3]=14; x[-2]=15;$$
$$x[-1]=16; x[0]=17;$$

the following solutions are obtained:

x(n) = {0.0023781212841854932,0.0025951557093425604,0.002602472348731295,
0.002512562814070352,4.5013380909901874,4.901271956390066,5.334490,
5.86752827140549,8.6966640806827,9.237538148524923,9.8189563365282,
10.42357512953368,12.807665010645849,13.422849340009103,14.080599812,
14.76265466816648,0.000047333739666817867,0.000042632384835581 93,
0.000035238568955208 63,0.000028184698278112 77,4.498965954184857,
4.898682432783714,5.331892555703612,5.784244170813406,…}

The graph of the solutions is given in Fig.1.

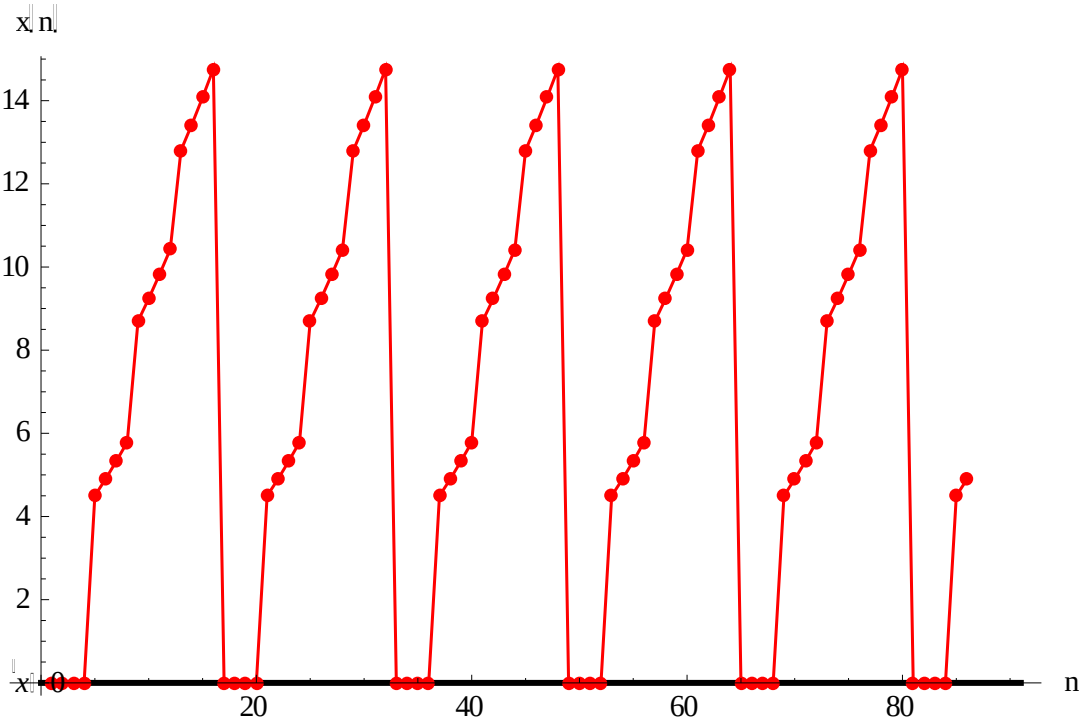

Figure 1. *x*(*n*) *graph of the solutions*.

Example 3.2: Consider the following equation $x_{n+1} = \dfrac{x_{n-15}}{1 + x_{n-3}x_{n-7}x_{n-11}}$.

If the initial conditions are selected as follows:

$$x[-15] = 0.999; x[-14] = 0.998; x[-13] = 0.997; x[-12] = 0.996; x[-11] = 0.995;$$
$$x[-10] = 0.994; x[-9] = 0.993; x[-8] = 0.992; x[-7] = 0.991; x[-6] = 0.99; x[-5] = 0.989;$$
$$x[-4] = 0.988; x[-3] = 0.987; x[-2] = .0986; x[-1] = 0.985; x[0] = 0.984;$$

the following solutions are obtained:

x(n)={0.5062774309150935,0.9097303920457783,0.5067741406697103,0.5070213125858963,
0.6654634543918772,0.9129296366989845,0.6648003025279128,0.6644687113750755,
0.74369846352699,0.9150659317837468,0.7425760891664093,0.7420150386695299,
0.7892471743846864,0.05602335091853418,0.7878887127855291,0.7872096248661782,
0.36407076922682924,0.8690573002926931,0.3648605575249685,0.365254820148283,…}

The graph of the solutions is given in Fig.2.

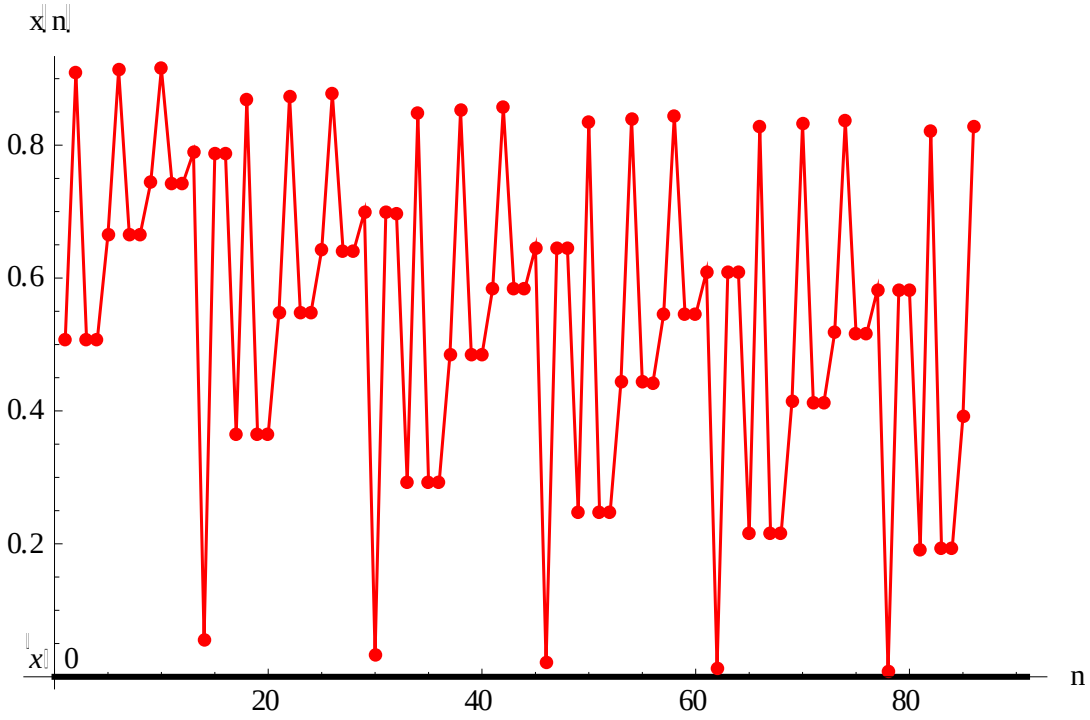

Figure 2. *x*(*n*) *graph of the solutions.*

REFERENCES:

[1] Abdullayev F.G., Ozkartepe N.P., On the ımprovement of the rate of convergence of the generalızed Bıeberbach polynomıals ın regıons wıth zero angles, *Ukr.Math. J.*, 64 (5), (2012), 653-671.

[2] Abdullayev F.G., Ozkartepe N.P., Unıform Convergence of the p-Bıeberbach Polynomıals in Domaıns wıth Zero Angles, *Science China Math*, 58 (5), (2015), 1063-1078.

[3] Amleh A. M., Grove E. A., Ladas G., Georgiou D. A., On the recursive sequence $x_{n+1} = \alpha + \frac{x_{n-1}}{x_n}$, *J. Math. Anal. Appl.*, 233 (2), (1999), 790-798.

[4] Çinar C., On the positive solutions of the difference equation $x_{n+1} = \frac{x_{n-1}}{1 + a x_n x_{n-1}}$, *Appl. Math. Comp.*, 158 (3), (2004), 809–812.

[5] Çinar C., On the positive solutions of the difference equation $x_{n+1} = \frac{x_{n-1}}{-1 + a x_n x_{n-1}}$, *Appl. Math. Comp.*, 158 (3), (2004), 793–797.

[6] Çinar C., On the positive solutions of the difference equation $x_{n+1}=\frac{ax_{n-1}}{1+bx_nx_{n-1}}$, *Appl. Math. Comp*., 156 (3), (2004), 587–590.

[7] Elabbasy E. M., El-Metwally H., Elsayed E. M., On the difference equation $x_{n+1}=ax_n-\frac{bx_n}{cx_n-dx_{n-1}}$, *Advances in Difference Equation*, (2006), 1-10.

[8] Elabbasy E. M., El-Metwally H., Elsayed E. M., Qualitative behavior of higher order difference equation, *Soochow Journal of Mathematics*, 33 (4), (2007), 861-873.

[9] Elabbasy E. M., El-Metwally H., Elsayed E. M., Global attractivity and periodic character of a fractional difference equation of order three,*Yokohama Mathematical Journal*, 53, (2007), 89-100.

[10] Elabbasy E. M., El-Metwally H., Elsayed E. M., On the difference equation $x_{n+1}=\frac{\alpha x_{n-k}}{\beta+\gamma\prod_{i=0}^{k}x_{n-i}}$, *J. Conc. Appl. Math*., 5 (2), (2007), 101-113.

[11] Elabbasy E. M. and Elsayed E. M., On the Global Attractivity of Difference Equation of Higher Order,*Carpathian Journal of Mathematics*, 24 (2), (2008), 45–53.

[12] Elsayed E. M., On the Solution of Recursive Sequence of Order Two, *Fasciculi Mathematici*, 40, (2008), 5–13.

[13] Elsayed E. M., Dynamics of a Recursive Sequence of Higher Order, *Communications on Applied Nonlinear Analysis*, 16 (2), (2009), 37–50.

[14] Elsayed E. M., Solution and atractivity for a rational recursive sequence, *Discrete Dynamics in Nature and Society*, (2011),17.

[15] Elsayed E. M., On the solution of some difference equation, *Europan Journal of Pure and Applied Mathematics*, 4 (3), (2011), 287–303.

[16] Elsayed E. M., On the Dynamics of a higher order rational recursive sequence, *Communications in Mathematical Analysis*, 12 (1), (2012), 117–133.

[17] Elsayed E. M., Solution of rational difference system of order two, *Mathematical and Computer Modelling*, 55, (2012), 378–384.

[18] Gibbons C. H., Kulenović M. R. S. and Ladas G., *On the recursive sequence* $x_{n+1}=\frac{\alpha+\beta x_{n-1}}{\chi+x_n}$, *Math. Sci. Res. Hot-Line*, 4 (2), (2000), 1-11.

[19] Kulenović M.R.S., Ladas G.,Sizer W.S., On the recursive sequence $x_{n+1}=\frac{\alpha x_n+\beta x_{n-1}}{\chi x_n+\delta x_{n-1}}$ *Math. Sci. Res. Hot-Line*, 2, 5, (1998), 1-16.

[20] Özkartepe N.P., Abdullayev F.G., Interference of the weight and contour for algebraic polynomials in the weighted Lebesgue spaces I , *Ukr. Math, 68 (10), (2017),*1574–1590.

[21] Steviç S., On the recursive sequence $x_{n+1}=\frac{x_{n-1}}{g(x_n)}$, *Taiwan. J. Math.*, 6 (3), (2002), 405-414.

[22] Şimşek D., Çınar C. and Yalçınkaya İ., On the recursive sequence $x_{n+1}=\frac{x_{n-3}}{1+x_{n-1}}$, *Int. J. Contemp. Math. Sci.*, 1 (9-12), (2006), 475-480.

[23] Şimşek D., Çınar C., Karataş R., Yalçınkaya İ., On the recursive sequence $x_{n+1}=\frac{x_{n-5}}{1+x_{n-2}}$, *Int. J. Pure Appl. Math.*, 27, 4, (2006), 501-507.

[24] Şimşek D., Çınar C., Karataş R., Yalçınkaya İ., On the recursive sequence $x_{n+1}=\frac{x_{n-5}}{1+x_{n-1}x_{n-3}}$ *Int. J. Pure Appl. Math.*, 28, 1, (2006), 117-124.

[25] Şimşek D., Çınar C., Yalçınkaya İ., On The Recursive Sequence *x(n+1) = x[n-(5k+9)] / 1+x(n-4)x(n-9) x[n-(5k+4)], Taiwan.Journal of Mathematics*, Vol. 12, 5, (2008), 1087-1098.

[26] Şimşek D., Doğan A., On a Class of Recursive Sequence, *Manas Journal of Engineering*, 2, 1, (2014), 16-22.

[27] Şimşek D., Eröz M., Solutions of the Rational Difference Equations $x_{n+1}=\frac{x_{n-3}}{1+x_nx_{n-1}x_{n-2}}$, *Manas Journal of Engineering*, 4, 1, (2016), 12-20.